3TIER by Vaisala

Due Diligence Analysis

PROJECT

Rush Creek I : Colorado, USA

using 200 Vestas V110-2.0 wind turbines at 80 m

FOR

Xcel Energy

DATE

10 May, 2016

CONTACT

ph: +1 206.325.1573
fax: +1 206.325.1618

info@3tier.com
www.3tier.com

2001 6th Avenue, Suite 2100
Seattle, WA 98121-2534

Disclaimer

This report has been prepared for the use of the client named in the report for the specific purpose identified in the report. Any other party should not rely upon this report for any other purpose. This report is not to be used, circulated, quoted or referred to, in whole or in part, for any other purpose without the prior written consent of Vaisala, Inc. The conclusions, observations and recommendations contained herein attributed to Vaisala, Inc. constitute the opinions of Vaisala, Inc. For a complete understanding of the conclusions and opinions, this report should be read in its entirety. To the extent that statements, information and opinions provided by the client or others have been used in the preparation of this report, Vaisala, Inc. has relied upon the same to be accurate. While we believe the use of such information provided by others is reasonable for the purposes of this report, no assurances are intended and no representations or warranties are made. Vaisala, Inc. makes no certification and gives no assurances except as explicitly set forth in this report.

Contents

1 EXECUTIVE SUMMARY

3TIER has conducted a wind resource assessment of the Rush Creek I project, located in Colorado, USA. This project consists of 200 Vestas V110-2.0 wind turbines at 80 m, for a total capacity of 400.0 MW. The project is located southwest of the town of Limon in a mixture of farmland and shrub-steppe terrain.

A summary of the major results is provided here. Table 1 provides configuration details of the project as well as primary wind speed, generation, uncertainty results, and probability of exceedance levels associated with the P50 project estimate. The long-term reference period used in this analysis extends over 36 years (January, 1980 – December, 2015). The wind resource assessment yields a gross project-average long-term wind speed estimate, at hub height, of **8.27 m/s**. The long-term mean gross generation estimate is **1909.7 GWh**, with a corresponding gross capacity factor of 54.5 %. Loss factors are considered, leading to a net energy estimate of **1498.4 GWh**, with a corresponding net capacity factor of 42.7 %.

A map of the hub height long-term mean wind speed values across the Rush Creek I project area is displayed in Wind Speed Maps.

Project Size	400.0 MW
Number of Turbines	200
Turbine Type	V110-2.0
Hub Height	80 m
Project-Average Wind Speed	8.27 m/s
Project-Average Density	0.997 kg/m^3
Gross Generation	1909.7 GWh
Net Generation	1498.4 GWh
Gross Capacity Factor	54.5 %
Net Capacity Factor	42.7 %
Aggregate Loss Factor	78.5 %
Standard Error of 20-year Estimate	7.3 %
Net-P10 20-year Generation	1637.8 GWh
Net-P25 20-year Generation	1571.7 GWh
Net-P75 20-year Generation	1425.0 GWh
Net-P90 20-year Generation	1358.9 GWh
Net-P10 20-year Capacity Factor	46.7 %
Net-P25 20-year Capacity Factor	44.8 %
Net-P75 20-year Capacity Factor	40.6 %
Net-P90 20-year Capacity Factor	38.8 %

Table 1: Project Overview

1.1 Wind Speed Maps

This section contains a map of MOS-corrected long-term mean wind speed values at hub height (80 m) across the Rush Creek I project area.

1.1.1 80 m Hub Height

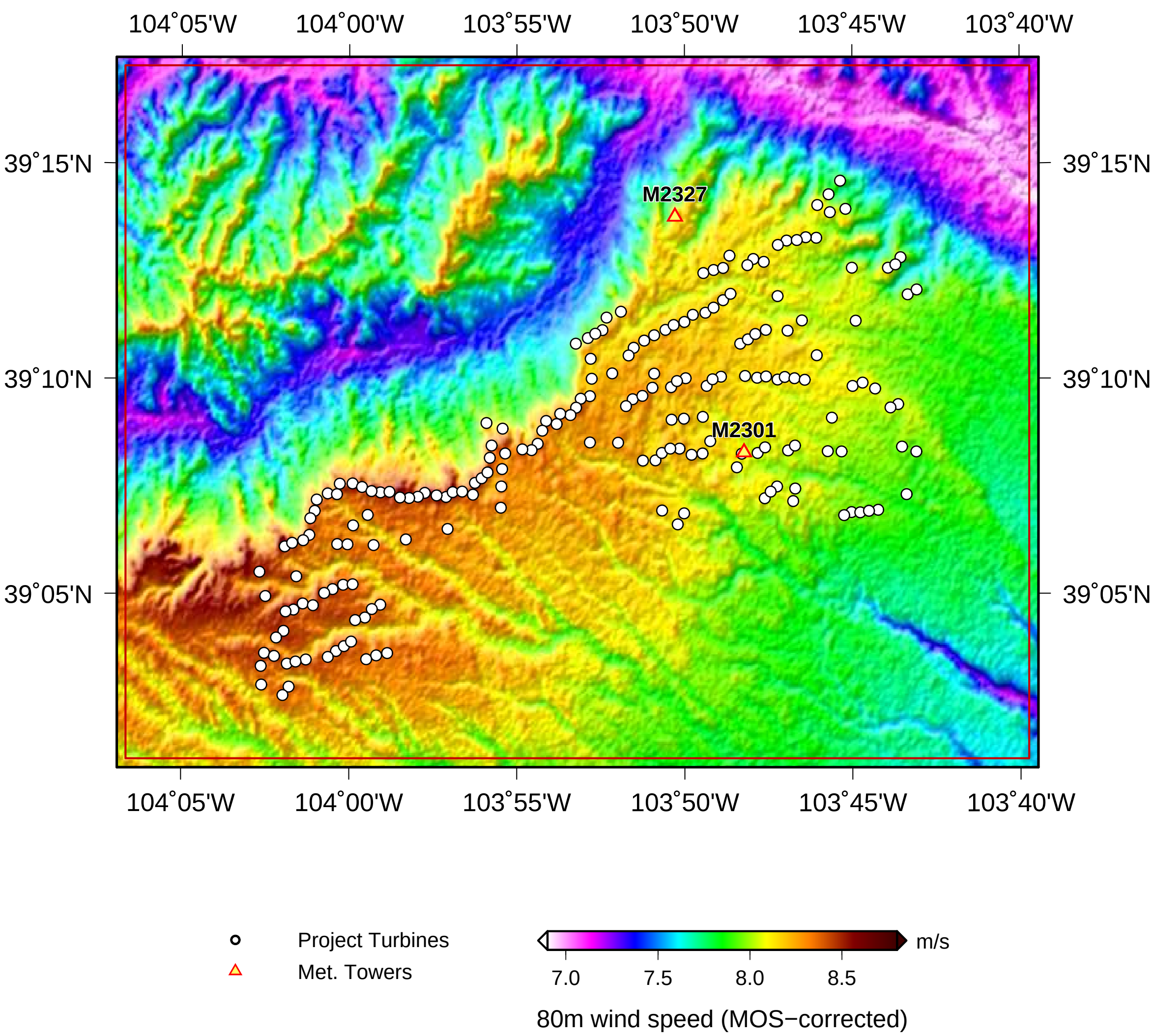

Figure 1: 36-year (January, 1980 – December, 2015) mean wind speed at 80 m.

2 METHODOLOGY

Wind resource assessments are conducted using 3TIER's modeling platform that combines on-site observations with mesoscale and microscale weather simulation models. The output from the modeling system is a four-dimensional data set of modeled historical weather for each meteorological (met) tower and wind turbine location. Model output is statistically calibrated using observed data from met towers. The resulting data sets are the basis for analysis of the wind resource.

The core of this modeling system is the Weather Research and Forecasting (WRF) Numerical Weather Prediction (NWP) model, developed in a partnership between U.S. federal agencies and universities. WRF is suitable for a broad spectrum of applications including air quality plume modeling, wind resource assessment, and climate modeling. WRF provides a flexible and computationally efficient framework that allows the worldwide academic, government, and private research communities to contribute advancements in physics, numerical methods, and data assimilation.

The WRF model uses reanalysis data for initial and boundary conditions. A reanalysis data set is a coarse resolution, observational-based data set that exists for the past several decades. WRF relies on the reanalysis data set to provide an accurate representation of the large-scale (hundreds of kilometers) historic flow patterns throughout the atmosphere (e.g. the location of high and low pressure centers, the position of the jet stream, etc). In addition, WRF requires as input high-resolution topographic and land-use data in order to accurately represent surface conditions. Land surface characteristics are derived from the 10 arc second (approximately $300\,m$) resolution European Space Agency (ESA) GlobCover data set [2]. Topographic data are sourced from the Shuttle Radar Topography Mission (SRTM) data set at 3 arc-second (approximately $90\,m$) resolution [4]. With these primary inputs, WRF then solves the dynamical and physical equations that describe the processes of the atmosphere. A nested grid configuration is used to simulate the fine-resolution, local-scale flow conditions given the large-scale state of the atmosphere (as described by the reanalysis data).

The Time-Varying Microscale (TVM) Model enables high-resolution mapping (tens of meters to a few hundred meters) of meteorological fields without the computational cost of running a high-resolution NWP model, such as the WRF model. TVM uses several techniques to analyze microscale winds. Kinematic terrain effects are applied to the wind field allowing TVM to resolve the effects of microscale terrain features, effects that are unresolved by a mesoscale NWP model [7]. A Froude number adjustment is applied [1], which incorporates terrain blocking effects on the wind flow (i.e., determine whether the wind flows over or around specific terrain features). A log-profile surface roughness adjustment is also calculated to adjust the near-surface wind fields for the effects of roughness features that could not be resolved on the coarser WRF model grid. These effects are computed at each time step in the study period and are based not only on wind speed and elevation, but also on other quantities, including wind direction and the thermodynamic properties of the lower atmosphere. This enables a sophisticated time-varying spatial analysis at high-resolution.

On-site observational data are incorporated into the analysis to validate and correct the raw model data from WRF and TVM using a process of Model Output Statistics (MOS) correction. MOS uses multi-linear regression equations to remove bias and adjust the variance of the raw model output to improve the match with observational data at met tower locations. The MOS equation for each met tower is fit to the observational period of record. The MOS equation is then applied over the entire data set, correcting the historical period during which direct observational data are unavailable. MOS corrections are distributed across the model domain using a weighting scheme that depends on horizontal and vertical distance from the met tower.

A detailed analysis of the data set from each met tower ensures the integrity of the observational data before MOS-correction. Data are reviewed to ensure that:

- The functions to convert anemometer output to wind speed are appropriate, assuming raw data logger files and conversion functions are provided.
- Periods of icing affecting the accuracy of wind speed and direction measurement are excluded.
- Sensor data affected by the tower structures may be properly accounted for.
- Periods of anemometer dragging and/or malfunction are excluded.

During wind project development, met tower sensors are usually placed lower than the hub height of the proposed wind turbines. The analysis process must extrapolate the sensor data to hub height using a wind shear coefficient. Wind shear is a meteorological phenomenon in which wind speed values generally increase with height above ground level (AGL); the surrounding ground cover, trees, and topographic features such as hills and valleys can significantly affect the measured wind shear. The analysis calculates the shear coefficient from the observed data and then applies the coefficient to highest observed wind speed data to estimate wind speed values at hub height.

Long-term time series at each proposed turbine location are extracted from the MOS-corrected data set. These hourly time series are then combined with the manufacturer's specified power curve to compute gross capacity factor values. Applying site-specific loss factor estimates to the mean P50 gross capacity factor yields the P50 net capacity factor. Uncertainty of the measured data and modeling data is then estimated to calculate the final net capacity factors at various probabilities of exceedance.

2.1 Wind Resource Assessment Steps

To determine the energy production potential of the proposed Rush Creek I wind project, the following procedure was implemented:

1. For the ECMWF ERA-I [3], NCAR/NCEP [5], and MERRA [8] reanalysis data sets, simulate 36 years at $4.5\,km$ resolution using WRF to understand the long-term temporal variability of weather over the project site.
2. Validate time series data collected from each met tower.
3. Perform correlation analysis between observations and $4.5\,km$ models to determine primary reanalysis data set for NWP modeling.
4. Simulate 1 year at $500\,m$ resolution using WRF to understand the spatial variability of the wind resource at the site.
5. Run TVM to downscale $500\,m$ WRF simulation to $90\,m$ spatial resolution.
6. Perform ensemble analysis to integrate effects of each long term data set including consistency checks to determine usefulness of entire 36 year period for each data set
7. Run MOS to eliminate temporal bias and mitigate spatial bias of WRF/TVM model output. Compute MOS corrections at each met tower. Combine the high-resolution spatial model data with the ensemble adjusted coarser resolution long-term data, creating the final MOS-corrected $90\,m$ resolution long term data set.
8. Calculate the expected (P50) gross capacity factor using modeled long-term time series at each turbine location in combination with the appropriate power curve.
9. Perform numerical wake and turbulence modeling.
10. Apply wake deficit as well as other site-specific loss factor estimates to the gross capacity factor, yielding the expected (P50) net capacity factor.
11. Calculate probability of exceedance levels for the net capacity factor data based on year-to-year wind resource variation, measurement uncertainty, and modeling uncertainty.

The following sections provide detail regarding the process outlined above as applied to the Rush Creek I wind project.

3 OBSERVATIONAL DATA

Xcel Energy provided observational data from the following towers at the proposed Rush Creek I site:

- Tower M2301
- Tower M2327

The location of each tower and the proposed turbine locations are shown in Wind Speed Maps, and a summary of each tower is presented in Table 2. 3TIER performed a site visit of the Rush Creek I wind project, and the data were inspected for quality control purposes following the visit. Site visit information and quality control of the observed data for each tower are described in detail within the following sections.

	M2301	**M2327**
Latitude	39.13808°	39.22934°
Longitude	-103.80388°	-103.83809°
Time Series Start	2010-Jun-11	2009-Oct-21
Time Series End	2014-May-02	2014-May-02
Observed 20 m Wind Speed	6.75	7.05
Observed 40 m Wind Speed	7.53	7.71
Observed 60 m Wind Speed	7.89	8.14
Average Shear	0.15	0.13
Hub Height 80 m Wind Speed	8.24	8.46
Long-term 80 m Wind Speed	8.16	8.24
Long-term 80 m Adjustment Factor	99.1 %	97.5 %
Mean Turbulence Intensity (TI) 80 m	7.3 %	5.8 %
Characteristic TI 80 m	10.8 %	9.2 %

Table 2: On-site met tower summary. Hub height wind speeds are extrapolated unless there is a sensor at the hub height. Wind speed values shown above are in units of m/s. Mean and characteristic turbulence intensity are at $15\,m/s$.

3.1 Tower M2301

The M2301 Tower is located at $39.13808° N$, $103.80388° W$. The location of the tower and the turbine locations are shown in Wind Speed Maps. The tower is located in cultivated farmland in the eastern cluster of project turbines. The tower has instrumentation up to $60\,m$, with anemometers at three heights and wind vanes at two heights. A summary of instruments installed on the tower is shown in Table 3. An image of the terrain surrounding the M2301 Tower is shown in Figure 2.

Instrument	Height (m)	Boom Orientation	Recovery Rate
Anemometer	60	233°	84.3 %
Anemometer	60	53°	80.3 %
Anemometer	40	235°	63.9 %
Anemometer	40	55°	71.7 %
Anemometer	20	237°	84.7 %
Anemometer	20	57°	78.0 %
Wind Vane	58	233°	88.0 %
Wind Vane	19	237°	88.0 %

Table 3: M2301 Tower instrumentation.

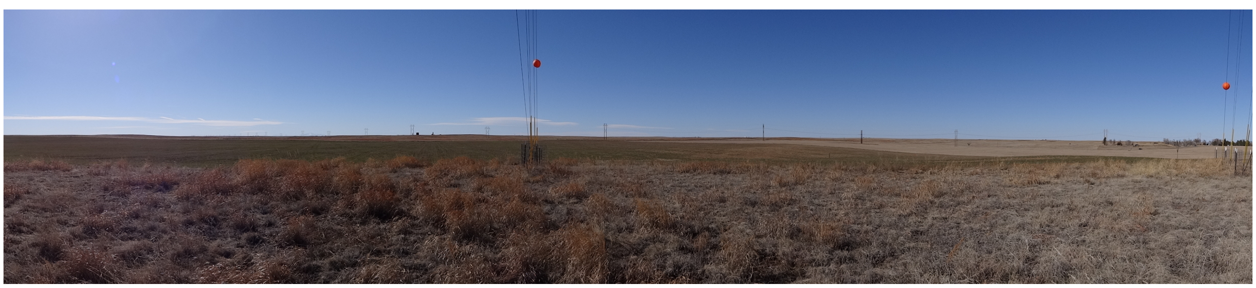

Figure 2: Panoramic view from the base of the M2301 Tower.

3.1.1 Quality Control

The observed data at the M2301 Tower were quality controlled to check for instrument malfunction and tower shadow. The tower was installed on April 27, 2010, although the tower did not begin collecting data until June 11, 2010. Raw data were processed using provided calibrated anemometer transfer functions. Offsets of $55°$ and $40°$ were applied to the $58\,m$ and $19\,m$ wind vane data, respectively, to correct for expected tower shadow regions. Due to guy wire distortion, data from direction sectors $138°$ - $153°$ and $314°$ - $332°$ were removed from the analysis for the $40\,m$ anemometer oriented at $233°$. Due to guy wire distortion, data from direction sectors $127°$ - $137°$ and $328°$ - $340°$ were removed from the analysis for the $40\,m$ anemometer oriented at $55°$. The logger had periods of failure from June 23 - 27, 2011; July 4 - 24, 2011; September 2 - 5, 2011 and September 17 - November 12, 2011. The $40\,m$ anemometer oriented at $233°$ failed from February 23 - August 8, 2013. The pressure sensor failed from June 11, 2010 - August 22, 2011. On August 8, 2013, the logger, temperature sensor, pressure sensor and $40\,m$ anemometer oriented at $233°$ were all replaced. The tower experienced intermittent periods of icing during the winter months resulting in approximately 4% data loss. The overall selectively averaged $60\,m$ wind speed data recovery rate was 89.2%.

3.1.2 Shear Extrapolation

Observed anemometer data from M2301 were used for extrapolating top sensor level wind speed data to 80 m hub height level. A 12-by-24 table, see Figure 3 below, was developed based on observed data from the anemometers at all of the available sensor levels. These shear exponent values were then applied to the observed data using the power law extrapolation method to calculate wind speed values at 80 m.

Hour of Day (Local)	Jan	Feb	Mar	Apr	May	Jun	Jly	Aug	Sep	Oct	Nov	Dec	Avg
0	0.17	0.18	0.19	0.21	0.18	0.23	0.24	0.26	0.23	0.18	0.16	0.15	0.20
1	0.16	0.18	0.18	0.20	0.17	0.22	0.23	0.24	0.21	0.18	0.16	0.15	0.19
2	0.15	0.17	0.17	0.19	0.16	0.21	0.22	0.23	0.20	0.17	0.16	0.15	0.18
3	0.15	0.17	0.17	0.19	0.16	0.21	0.20	0.21	0.19	0.16	0.16	0.16	0.18
4	0.15	0.16	0.17	0.19	0.15	0.20	0.19	0.21	0.18	0.15	0.16	0.16	0.17
5	0.16	0.16	0.17	0.19	0.14	0.18	0.18	0.19	0.18	0.14	0.16	0.16	0.17
6	0.16	0.16	0.16	0.16	0.12	0.14	0.15	0.17	0.17	0.13	0.16	0.15	0.15
7	0.16	0.16	0.14	0.12	0.08	0.09	0.10	0.12	0.13	0.12	0.16	0.15	0.13
8	0.16	0.15	0.10	0.07	0.06	0.06	0.06	0.08	0.09	0.09	0.14	0.14	0.10
9	0.13	0.12	0.07	0.05	0.05	0.05	0.05	0.06	0.06	0.06	0.10	0.11	0.08
10	0.09	0.10	0.06	0.05	0.05	0.05	0.05	0.06	0.06	0.06	0.07	0.08	0.06
11	0.07	0.08	0.05	0.05	0.05	0.05	0.05	0.06	0.06	0.06	0.05	0.06	0.06
12	0.06	0.08	0.06	0.05	0.05	0.05	0.05	0.06	0.06	0.06	0.05	0.06	0.06
13	0.07	0.08	0.06	0.05	0.06	0.05	0.05	0.06	0.06	0.06	0.06	0.06	0.06
14	0.08	0.09	0.06	0.06	0.06	0.06	0.06	0.06	0.06	0.07	0.07	0.09	0.07
15	0.11	0.11	0.07	0.06	0.07	0.07	0.07	0.07	0.08	0.09	0.11	0.12	0.09
16	0.17	0.14	0.10	0.08	0.08	0.08	0.08	0.09	0.11	0.13	0.17	0.17	0.12
17	0.20	0.18	0.15	0.12	0.11	0.11	0.11	0.14	0.17	0.19	0.22	0.20	0.16
18	0.21	0.21	0.21	0.17	0.16	0.15	0.15	0.20	0.24	0.23	0.23	0.20	0.20
19	0.19	0.21	0.24	0.20	0.21	0.20	0.20	0.26	0.29	0.24	0.22	0.18	0.22
20	0.18	0.20	0.24	0.22	0.24	0.24	0.24	0.29	0.31	0.23	0.20	0.17	0.23
21	0.17	0.19	0.22	0.21	0.23	0.26	0.25	0.30	0.29	0.22	0.17	0.16	0.22
22	0.17	0.18	0.21	0.21	0.21	0.25	0.25	0.29	0.27	0.21	0.16	0.16	0.21
23	0.17	0.17	0.19	0.21	0.19	0.24	0.25	0.28	0.25	0.19	0.16	0.15	0.21
Avg	0.15	0.15	0.14	0.14	0.13	0.14	0.14	0.17	0.16	0.14	0.14	0.14	0.15

Figure 3: Shear exponent values for the M2301 Tower.

3.2 Tower M2327

The M2327 Tower is located at $39.22934^{\circ}\,N$, $103.83809^{\circ}\,W$. The location of the tower and the turbine locations are shown in Wind Speed Maps. The decommissioned tower was located just outside the northern edge of the project area in shrub steppe terrain. The tower has instrumentation up to $60\,m$, with anemometers at three heights and wind vanes at two heights. A summary of instruments installed on the tower is shown in Table 4. An image of the terrain surrounding the M2327 Tower is shown in Figure 4.

Instrument	Height (m)	Boom Orientation	Recovery Rate
Anemometer	60	250°	52.9 %
Anemometer	60	69°	49.7 %
Anemometer	40	247°	49.0 %
Anemometer	40	66°	46.7 %
Anemometer	20	244°	52.5 %
Anemometer	20	63°	46.5 %
Wind Vane	59	250°	52.9 %
Wind Vane	19	244°	52.9 %

Table 4: M2327 Tower instrumentation.

Figure 4: Panoramic view from the base of the M2327 Tower.

3.2.1 Quality Control

The observed data at the M2327 Tower were quality controlled to check for instrument malfunction and tower shadow. Data for the tower were provided beginning on October 21, 2009. There were numerous logger and processing issue with the data until November 3, 2010. Therefore, data before November 3, 2010 were not used for the analysis. Offsets of 55° were applied to both wind vanes to correct for expected tower shadow regions. Logger failures occurred from June 8 - August 23, 2011 and December 31, 2012 - August 9, 2013. The $40\,m$ anemometer oriented at 250° failed from March 3 - May 2, 2014. The pressure failed from November 3, 2010 - June 7, 2011. Maintenance was performed on August 9, 2013 to replace the logger, both $60\,m$ anemometers, the $20\,m$ anemometer oriented at 63° along with the temperature and pressure sensors. The tower experienced intermittent periods of icing during the winter months resulting in approximately 4% data loss. The overall selectively averaged $60\,m$ wind speed data recovery rate was 69.5%. The tower was decommissioned in early May 2014.

3.2.2 Shear Extrapolation

Observed anemometer data from M2327 were used for extrapolating top sensor level wind speed data to 80 m hub height level. A 12-by-24 table, see Figure 5 below, was developed based on observed data from the anemometers at all of the available sensor levels. These shear exponent values were then applied to the observed data using the power law extrapolation method to calculate wind speed values at 80 m.

Hour of Day (Local)	Jan	Feb	Mar	Apr	May	Jun	Jly	Aug	Sep	Oct	Nov	Dec	Avg
0	0.17	0.17	0.20	0.18	0.17	0.19	0.20	0.23	0.18	0.16	0.15	0.15	0.18
1	0.18	0.17	0.20	0.18	0.17	0.18	0.20	0.22	0.17	0.16	0.16	0.16	0.18
2	0.18	0.16	0.20	0.17	0.16	0.17	0.19	0.21	0.17	0.17	0.15	0.16	0.18
3	0.17	0.16	0.21	0.17	0.16	0.17	0.18	0.19	0.18	0.16	0.15	0.16	0.17
4	0.17	0.17	0.20	0.16	0.15	0.17	0.17	0.18	0.17	0.15	0.14	0.16	0.17
5	0.16	0.18	0.20	0.16	0.13	0.16	0.16	0.17	0.16	0.14	0.14	0.15	0.16
6	0.14	0.17	0.18	0.14	0.11	0.12	0.13	0.14	0.14	0.12	0.14	0.14	0.14
7	0.13	0.15	0.14	0.10	0.07	0.08	0.08	0.09	0.11	0.10	0.14	0.13	0.11
8	0.11	0.13	0.10	0.07	0.05	0.05	0.05	0.06	0.07	0.07	0.12	0.13	0.08
9	0.10	0.11	0.07	0.05	0.04	0.04	0.04	0.04	0.05	0.05	0.09	0.11	0.07
10	0.08	0.09	0.05	0.05	0.05	0.04	0.04	0.04	0.04	0.05	0.06	0.08	0.06
11	0.07	0.08	0.05	0.05	0.05	0.04	0.04	0.04	0.04	0.05	0.05	0.06	0.05
12	0.06	0.07	0.05	0.05	0.05	0.04	0.04	0.04	0.04	0.05	0.04	0.06	0.05
13	0.06	0.07	0.05	0.05	0.05	0.04	0.04	0.04	0.05	0.05	0.05	0.06	0.05
14	0.07	0.08	0.05	0.05	0.05	0.05	0.04	0.04	0.05	0.05	0.06	0.08	0.06
15	0.10	0.10	0.06	0.06	0.05	0.05	0.04	0.05	0.06	0.07	0.09	0.10	0.07
16	0.14	0.13	0.08	0.07	0.06	0.06	0.05	0.07	0.08	0.10	0.13	0.14	0.09
17	0.17	0.16	0.12	0.10	0.09	0.08	0.08	0.10	0.13	0.14	0.16	0.16	0.12
18	0.17	0.18	0.17	0.14	0.13	0.11	0.12	0.15	0.18	0.16	0.17	0.16	0.15
19	0.16	0.18	0.20	0.17	0.17	0.16	0.16	0.20	0.21	0.17	0.17	0.16	0.17
20	0.16	0.17	0.21	0.18	0.19	0.19	0.20	0.23	0.21	0.16	0.16	0.16	0.18
21	0.16	0.17	0.21	0.18	0.19	0.20	0.21	0.24	0.20	0.15	0.16	0.15	0.19
22	0.17	0.17	0.20	0.18	0.18	0.20	0.21	0.23	0.20	0.15	0.16	0.14	0.18
23	0.17	0.17	0.20	0.18	0.17	0.20	0.21	0.23	0.19	0.15	0.15	0.14	0.18
Avg	0.14	0.14	0.14	0.12	0.11	0.12	0.12	0.13	0.13	0.12	0.12	0.13	0.13

Figure 5: Shear exponent values for the M2327 Tower.

4 LONG-TERM REFERENCE

In order to put the short-term observational data into the climatological context, 3TIER performed a review of several long term climate data sources. 3TIER primarily relies on global reanalysis data sets for understanding long-term climate variability. The reanalysis data sets are derived from thousands of global observations, including ground based weather stations, ocean surface buoys, satellites, and weather balloons.

3TIER analyzed three major reanalysis data sets that are each produced independently by various institutions. Each data set offers an independent view of the climate, and 3TIER will consider each in determining the most appropriate data set. The statistics relating each met tower to the reanalysis data sets reviewed are shown below in Table 5, including the daily-mean explained variance, long-term climate adjustment, and considered start year statistics. Figure 6 shows the annual-mean wind speed values extracted from each reanalysis data set across the period of record. Each time series shown in Figure 6 has been MOS-corrected using the observed data at Tower M2301.

Tower	Data Set	Explained Variance (R^2)	Climate Adjustment	Start Year
M2301	MERRA	71.1%	98.9%	1982
M2301	NCEP/NCAR	54.5%	99.3%	1980
M2301	ECMWF ERA-I	74.7%	99.0%	1980
M2327	MERRA	71.5%	97.5%	1996
M2327	NCEP/NCAR	52.2%	99.3%	1985
M2327	ECMWF ERA-I	74.9%	98.0%	1980

Table 5: Daily explained variance and long-term climate adjustment values for the considered reanalysis data sets.

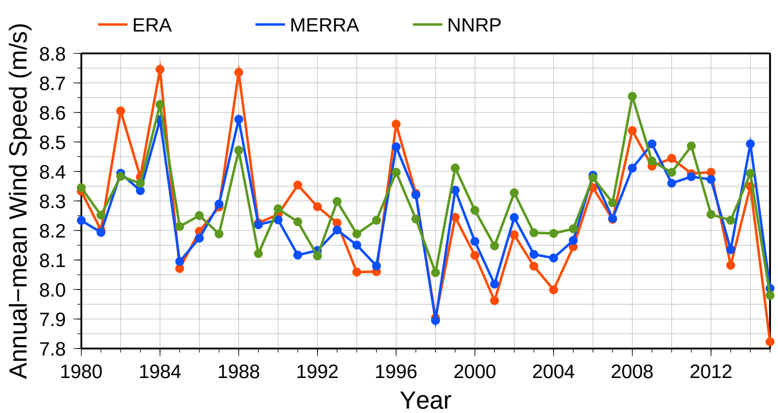

Figure 6: Time series of annual-mean wind speed data for each considered reanalysis data set.

5 GROSS GENERATION

5.1 Wind Resource Variability

This section provides an analysis of the MOS-corrected model-simulated project-average wind resource at hub height. To generate the project-average wind resource time series, MOS-corrected wind resource time series data are extracted at each turbine location at the appropriate height ($80\,m$) and then averaged across all 200 turbine locations.

Based on the results of 3TIER's Energy Risk Framework, the last 36 years (January, 1980 – December, 2015) of data have been utilized for estimating the expected future generation at Rush Creek I. The long-term mean project-average wind speed at hub height is $\mathbf{8.27\,m/s}$. A map of the 36-year average wind speed values at $80\,m$ is displayed in Figure 1. Gross wind speed values and average density values at each of the 200 turbine locations are provided in Appendix Turbine Means. The project-average density value at hub height is $0.997\,kg/m^3$.

The distribution of hourly MOS-corrected project-average wind speed values is shown below in Figure 7. The distribution is based on the 36 years of modeled data. The annual wind rose is shown in Figure 8. Figure 9 displays the time series of gross project-average annual-mean wind speed values. Tables 10 and 11 shown on the following pages contain tabular-formatted month-hour and monthly-mean wind speed values, respectively. Table 10, often referred to as a '12x24' table, shows the average diurnal profile of wind speed values for each month of the calendar year. Table 11 shows the monthly-mean wind speed value for each month of the 36-year analysis period. Annual-mean wind speed values are also displayed in the right-most column of data in Table 11. Additional analysis of the long-term variability is available in Project-average Long-term Wind Resource Assessment.

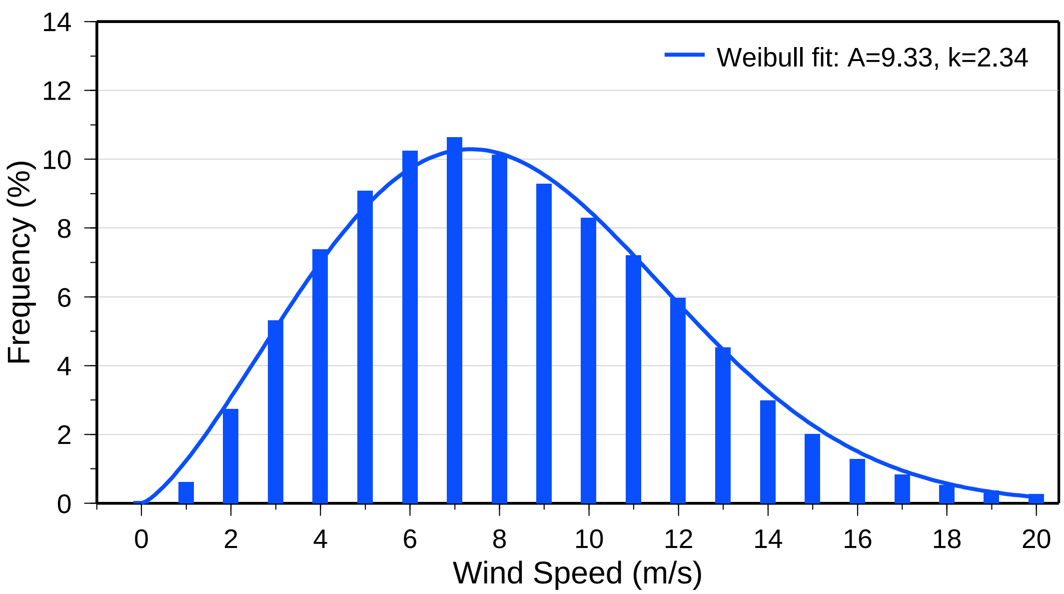

Figure 7: Hourly distribution of simulated project-average wind speed using $1\,m/s$ bins. ($0\,m/s$ bin contains only values ≤ 0.5.) Weibull distribution is also shown with the scale (A) and shape (k) parameters listed in the legend.

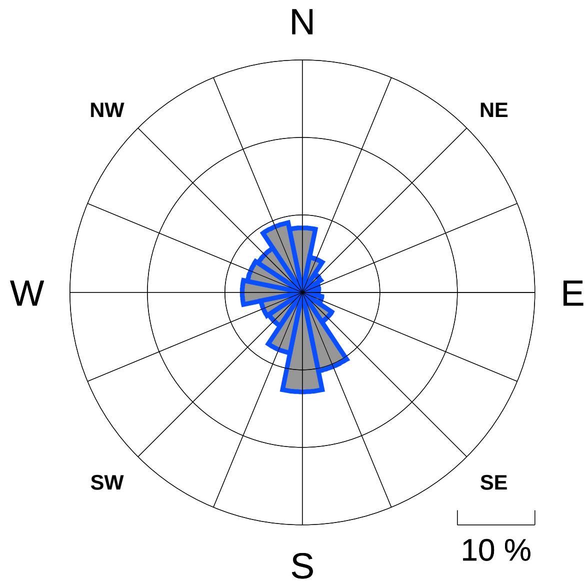

Figure 8: Annual wind rose of the hourly-mean project-average wind direction time series. Directional bins are 22.5° wide, and the radial contour interval is 10%.

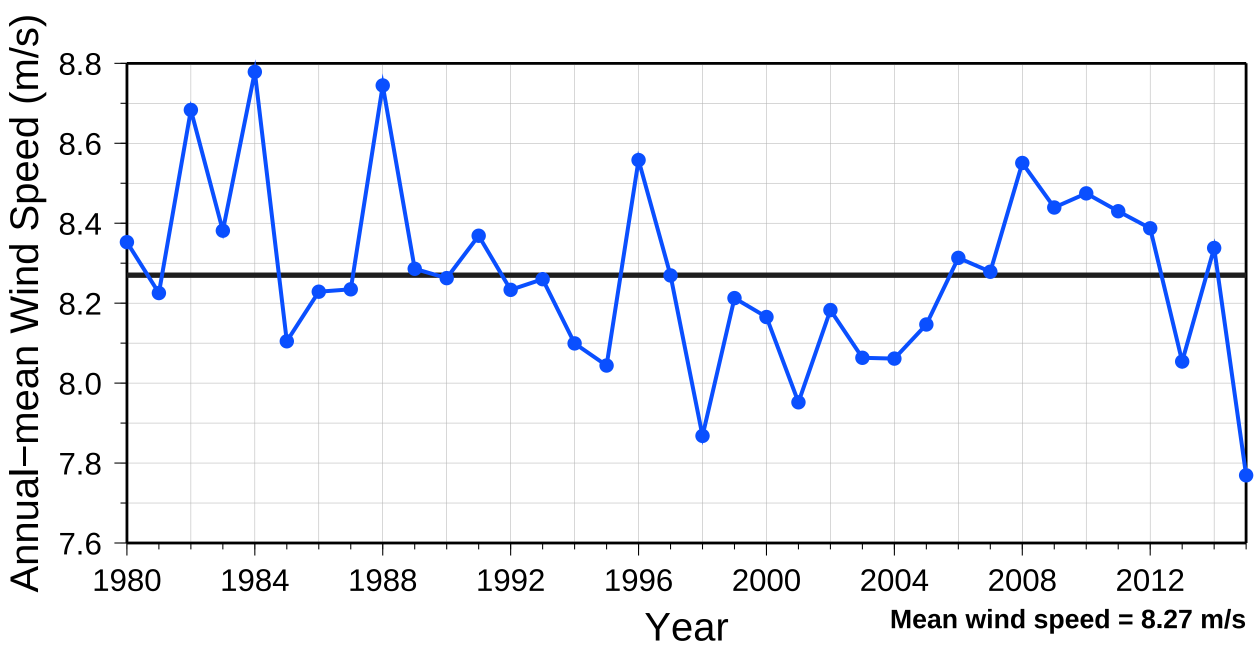

Figure 9: Time series of annual-mean project-average wind speed. Black line denotes the long-term mean.

Hour of Day (MST)	Jan	Feb	Mar	Apr	May	Jun	Jly	Aug	Sep	Oct	Nov	Dec	Avg
0	9.27	9.17	9.73	9.98	9.46	9.22	8.49	8.09	8.35	8.31	8.54	8.75	8.95
1	9.39	9.28	9.66	9.80	9.04	8.94	8.30	8.02	8.36	8.47	8.50	8.61	8.86
2	8.99	9.16	9.47	9.56	8.74	8.92	8.32	7.95	8.40	8.44	8.56	8.59	8.75
3	8.96	9.12	9.33	9.38	8.53	8.49	7.96	7.87	8.38	8.43	8.72	8.66	8.65
4	8.63	8.83	9.15	9.18	8.33	8.14	7.62	7.69	8.47	8.37	8.74	8.69	8.48
5	8.77	8.65	9.01	9.15	7.99	7.85	7.49	7.49	8.24	8.15	8.59	8.57	8.33
6	8.70	8.55	8.81	9.11	7.66	7.41	7.30	7.15	7.81	7.90	8.39	8.47	8.10
7	8.56	8.43	8.46	8.55	7.06	6.81	6.24	6.23	7.22	7.76	8.40	8.40	7.67
8	8.46	8.29	7.99	8.52	7.41	7.03	6.25	5.86	6.43	7.01	7.88	8.61	7.47
9	7.97	8.07	7.84	8.68	7.49	6.89	6.17	6.00	6.39	6.75	7.26	8.26	7.31
10	7.67	8.08	8.00	8.70	7.54	6.95	6.25	6.00	6.29	6.96	7.25	7.85	7.29
11	7.74	7.96	8.23	8.75	7.74	7.09	6.19	5.95	6.17	7.06	7.57	8.08	7.37
12	7.65	7.85	8.51	8.97	8.00	7.08	5.93	5.89	6.21	7.30	7.58	8.01	7.41
13	7.44	7.76	8.58	8.87	8.40	7.33	6.21	6.00	6.52	7.71	7.72	7.85	7.53
14	7.50	7.87	8.73	9.03	8.54	7.74	6.87	6.20	6.66	8.13	8.14	7.91	7.78
15	7.51	7.84	8.85	9.26	9.04	8.50	7.19	6.66	7.04	8.35	8.45	7.95	8.05
16	7.69	7.77	9.08	9.49	9.25	9.37	7.48	6.96	7.53	8.66	8.78	8.09	8.34
17	8.19	7.80	9.17	9.61	9.41	9.18	7.67	7.50	7.91	8.65	9.19	8.75	8.59
18	8.49	8.21	9.45	9.46	9.12	9.26	8.27	7.85	8.34	8.88	9.01	8.81	8.76
19	8.55	8.60	9.69	9.71	9.23	9.63	8.92	8.28	8.96	8.58	8.88	8.87	8.99
20	8.47	8.73	9.74	9.90	9.38	9.74	9.53	8.77	9.04	8.29	8.68	8.91	9.10
21	8.66	8.57	9.49	9.76	9.33	9.38	9.03	8.54	9.11	8.40	8.60	8.93	8.99
22	9.00	8.61	9.48	9.91	9.19	9.01	8.58	8.35	8.91	8.57	8.58	8.80	8.92
23	9.26	8.86	9.49	9.96	9.20	8.95	8.52	8.14	8.48	8.33	8.30	8.79	8.85
Avg	8.40	8.42	9.00	9.30	8.55	8.29	7.53	7.23	7.72	8.06	8.35	8.47	8.27

Wind Speed (m/s): 5.5 6.0 6.5 7.0 7.5 8.0 8.5 9.0 9.5 10.0

Figure 10: Hourly-mean values of simulated project-average wind speed. Vertical axis is local time.

Year	Jan	Feb	Mar	Apr	May	Jun	Jly	Aug	Sep	Oct	Nov	Dec	Avg
1980	9.20	7.93	9.92	8.86	8.75	8.89	7.46	7.87	7.87	7.54	7.49	8.42	8.35
1981	7.46	8.98	8.81	8.70	9.10	8.33	7.99	6.77	7.53	8.10	8.43	8.56	8.23
1982	9.99	8.04	9.60	10.16	7.80	8.46	7.93	6.88	8.10	9.17	8.42	9.60	8.68
1983	8.56	8.19	8.90	9.15	8.83	7.50	7.97	6.87	8.12	7.89	9.56	9.04	8.38
1984	7.98	10.05	9.31	10.83	8.58	8.47	8.00	7.38	7.77	8.34	9.37	9.39	8.78
1985	7.63	7.91	9.75	8.76	8.08	7.94	7.08	7.47	8.20	7.94	8.56	7.96	8.10
1986	8.75	8.49	8.55	9.92	8.38	8.32	7.41	7.69	8.34	7.85	8.27	6.85	8.23
1987	9.34	7.99	10.52	9.05	8.09	7.87	8.28	7.20	6.35	7.24	8.10	8.73	8.23
1988	9.63	8.50	9.97	9.16	10.65	8.37	7.79	7.79	8.28	7.56	8.78	8.42	8.74
1989	8.53	7.47	9.27	8.53	9.02	8.25	8.38	7.80	7.95	8.12	8.35	7.68	8.29
1990	9.34	8.41	7.88	8.59	8.90	9.30	7.39	7.17	7.45	8.05	8.50	8.21	8.26
1991	7.76	8.08	10.31	8.77	9.82	9.26	7.04	7.16	7.99	7.67	8.48	8.08	8.37
1992	9.26	8.30	7.97	8.47	8.45	7.76	7.30	7.19	8.06	8.03	8.41	9.60	8.23
1993	8.32	8.07	9.08	9.18	7.84	8.50	8.46	7.11	7.62	7.50	8.32	9.12	8.26
1994	8.19	8.76	8.44	8.41	8.46	7.87	7.43	7.25	7.69	7.96	9.22	7.60	8.10
1995	8.12	8.04	8.93	8.34	8.86	8.23	7.46	6.83	7.29	8.71	8.03	7.69	8.04
1996	9.43	8.20	9.19	9.72	8.66	7.68	7.23	7.29	7.84	8.55	8.63	10.22	8.56
1997	8.52	8.65	9.01	8.68	7.96	8.37	8.03	6.49	7.02	9.25	8.22	9.03	8.27
1998	7.61	7.97	8.63	8.39	8.27	8.71	6.85	6.88	7.78	7.87	8.05	7.46	7.87
1999	8.51	9.56	9.31	9.57	8.87	8.46	7.41	6.60	6.89	7.69	7.32	8.47	8.21
2000	7.66	8.88	8.40	9.65	8.69	8.52	7.35	6.57	7.93	7.90	7.87	8.64	8.17
2001	8.13	8.21	7.47	9.69	8.17	7.77	7.01	7.28	7.40	8.15	7.92	8.26	7.95
2002	8.51	9.26	8.85	9.04	8.42	8.30	7.96	7.82	8.02	7.69	7.37	7.06	8.18
2003	7.59	7.26	8.74	9.97	7.85	7.61	7.33	7.46	7.49	7.87	8.62	8.93	8.06
2004	7.44	8.54	8.66	8.67	8.44	7.82	6.70	7.17	8.57	8.65	8.22	7.93	8.06
2005	7.96	7.22	8.49	9.98	8.05	8.20	8.09	6.58	7.77	7.93	9.43	8.07	8.15
2006	9.20	8.77	9.55	9.65	7.76	8.17	7.39	7.25	7.28	7.86	8.05	8.86	8.31
2007	7.98	8.47	8.51	8.95	7.91	9.02	7.56	7.27	8.38	8.81	7.56	8.99	8.28
2008	9.08	8.68	8.32	9.90	9.61	7.69	7.73	7.59	7.59	8.61	8.35	9.45	8.55
2009	8.87	8.88	9.75	9.95	7.96	7.53	7.32	7.61	8.06	8.70	7.85	8.81	8.44
2010	7.10	7.01	9.53	10.54	10.01	8.64	7.67	7.78	8.34	8.08	8.93	8.02	8.47
2011	7.75	9.76	9.07	10.06	9.28	8.86	7.30	7.16	7.17	7.99	8.90	8.02	8.43
2012	8.67	9.18	9.37	9.53	8.31	9.44	7.35	7.98	7.10	7.70	7.67	8.42	8.39
2013	7.90	8.49	8.71	8.98	7.76	8.51	7.69	6.84	7.99	8.06	8.06	7.74	8.05
2014	8.44	8.55	9.28	10.37	8.56	8.80	7.05	6.60	7.62	7.66	8.98	8.24	8.34
2015	7.82	8.28	7.81	8.74	7.55	6.95	6.77	7.45	7.00	7.53	8.21	9.30	7.77
Avg	8.40	8.42	9.00	9.30	8.55	8.29	7.53	7.23	7.72	8.06	8.35	8.47	8.27

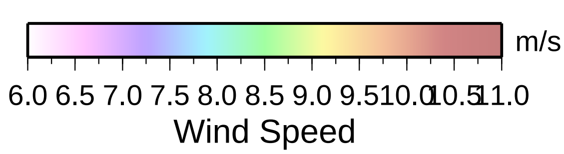

Figure 11: Monthly-mean values of simulated project-average wind speed.

5.2 Gross Generation Variability

Following WRF/TVM modeling and MOS correction, 36 years of hourly wind speed, wind direction, temperature, and pressure time series data were extracted for each proposed turbine location at hub height. The simulated temperature and pressure data are used to normalize simulated wind speed data to the power curve's reference density with the equation

$$V_{norm} = V\left((\frac{\rho}{\rho_0})^{1/3}\right)$$

where V_{norm} is normalized hourly wind speed at hub height, V is simulated hourly wind speed at hub height, ρ is density calculated from simulated hourly temperature and pressure at hub height using the Ideal Gas Law, and ρ_0 is the reference density of the power curve.

The turbine power curve is then applied to the normalized wind speed data using piecewise linear interpolation between the power curve points supplied by the manufacturer. Turbine specific cut-in and cut-out limits on wind speed are also applied. This allows the manufacturer's power curve to be applied to the wind speed time series to calculate gross expected energy for all proposed turbine locations for each hour over the past 36 years.

Computing the nameplate capacity factor at each turbine and then averaging across all 200 turbines yields the project-wide gross capacity factor value. A turbine-by-turbine gross energy estimate is calculated by multiplying the nameplate capacity factor at each turbine by the turbine-specific nameplate capacity, and by 8766 hours. Averaging these across all 200 turbines yields the project-average gross energy estimate.

Based on the results of 3TIER's Energy Risk Framework, the last 36 years (January, 1980 – December, 2015) of data have been utilized for estimating the expected future generation at Rush Creek I. The 36-year long-term mean gross energy estimate at the proposed Rush Creek I project is $\mathbf{1909.7\,GWh}$. Figure 12 below shows the time series of gross project-average annual-mean energy values. Gross energy values at each of the 200 turbine locations are provided in Appendix Turbine Means. Additional analysis of the long-term variability is available in Project-average Long-term Gross Power Capacity Assessment.

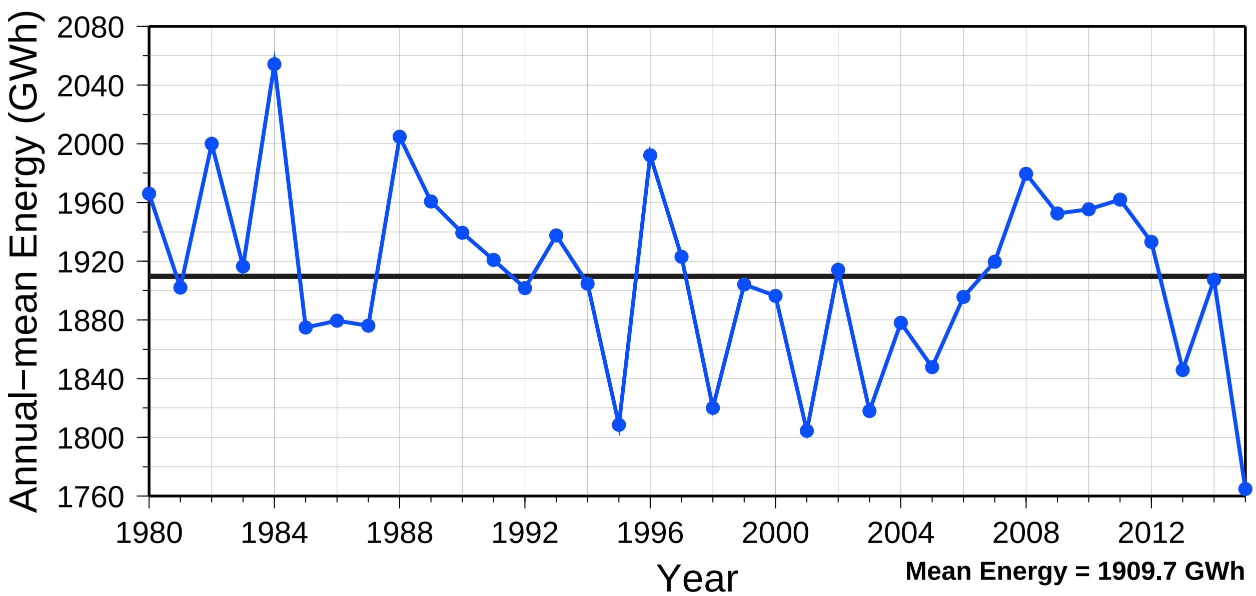

Figure 12: Time series of annual-mean project-average gross energy. Black line denotes the long-term mean.

5.3 Power Curves

It is expected that Vestas V110-2.0 wind turbines at a hub height of 80 m will be erected at the site. The Vestas V110-2.0 power curve is shown in Figure 13 and Table 6. The reference density for each power curve is shown in the caption of each respective Figure and Table below.

5.3.1 Vestas V110-2.0

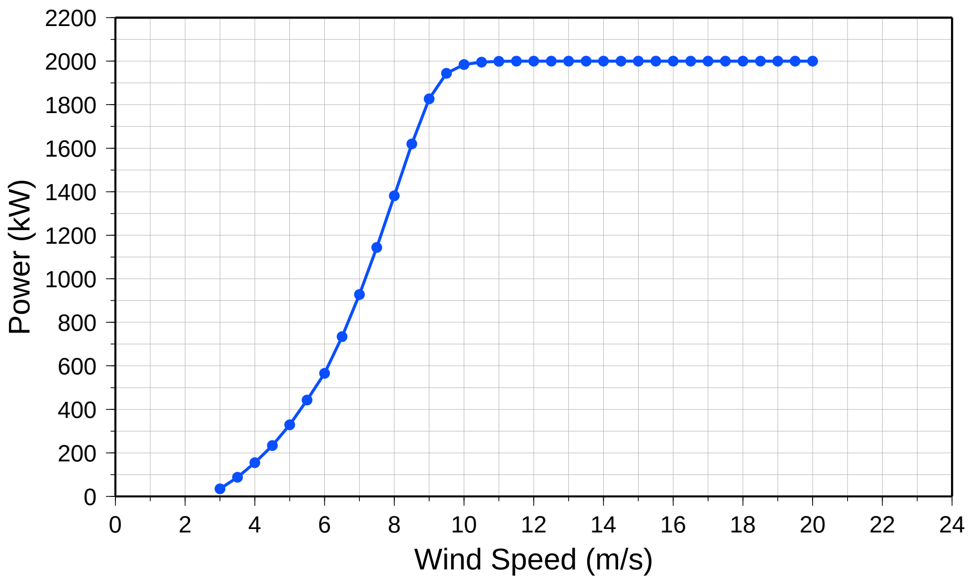

Figure 13: Power curve values for a Vestas V110-2.0 turbine with a reference density of 1.225 kg/m^3.

Wind Speed ($\frac{m}{s}$)	Power (kW)	Wind Speed ($\frac{m}{s}$)	Power (kW)	Wind Speed ($\frac{m}{s}$)	Power (kW)
3.0	35.0	9.0	1827.0	15.0	2000.0
3.5	88.0	9.5	1944.0	15.5	2000.0
4.0	155.0	10.0	1985.0	16.0	2000.0
4.5	234.0	10.5	1996.0	16.5	2000.0
5.0	329.0	11.0	1999.0	17.0	2000.0
5.5	443.0	11.5	2000.0	17.5	2000.0
6.0	566.0	12.0	2000.0	18.0	2000.0
6.5	734.0	12.5	2000.0	18.5	2000.0
7.0	928.0	13.0	2000.0	19.0	2000.0
7.5	1144.0	13.5	2000.0	19.5	2000.0
8.0	1381.0	14.0	2000.0	20.0	2000.0
8.5	1620.0	14.5	2000.0		

Table 6: Power curve values for a Vestas V110-2.0 turbine with a reference density of 1.225 kg/m^3.

6 LOSS FACTORS

To convert from expected gross generation to expected net generation, the following loss factor categories are considered: availability, curtailment, wake deficit, electrical efficiency, turbine efficiency, and environmental. Details for each loss factor are discussed below.

6.1 Availability

Availability losses include losses driven by turbine and transmission shutdowns caused by planned and unexpected faults.

6.1.1 Turbine Availability

3TIER has observed that turbine availability at newly constructed wind farms achieve 96.0% or higher availability when averaged over an entire calendar year. Therefore, the turbine availability loss factor is estimated to be **96.0%**.

6.1.2 Grid Availability

The ability of the electric grid to receive and transmit wind power to load centers varies by year, season and location. Issues with grid availability are very dynamic and may actually be worsened as wind penetration levels increase. Grid availability is expected to be high across the United States. 3TIER has assumed a regional grid availability loss factor of **99.5%** for the Rush Creek I wind energy project.

6.1.3 Balance of Plant Availability

The balance of the plant availability is based on a total of 24 hours of outage time per year per turbine for transformer inspections and maintenance. Therefore, the balance of plant availability loss factor is estimated to be **99.7%**.

6.2 Curtailment

Curtailment losses are based on forced wind plant shutdowns resulting from environmental conditions that can adversely effect the turbines. These curtailments include wind driven sector management, high wind hysteresis, extreme icing events, and extreme temperatures.

6.2.1 Sector Management

Standard minimum turbine spacing of three rotor diameters perpendicular to the dominant wind direction and five rotor diameters parallel to the dominant wind direction was tested against the layout. Turbine spacing perpendicular to the prevailing wind direction is less than three rotor diameters for a significant number of turbines. Due to the tight spacing, a sector management curtailment loss factor may apply, and the layout should be verified by the turbine manufacturer to ensure sector management is properly considered. A quantitative sector management loss calculation may be performed, once details of a sector loss algorithm (if required) are provided by the turbine manufacturer.

6.2.2 High Wind Hysteresis

High wind speed hysteresis loss potentially occurs after a turbine has shut down because of a high wind speed cut-out event. Before the turbine can re-start, the wind speed must slow down to the hysteresis cut-in wind speed. If wind speed values reduce to below the cut-out wind speed, but remain above the hysteresis cut-in wind speed, then hysteresis loss will occur. Based on 36 years of modeled hourly wind speed data, cut-out wind speed events are expected to periodically occur. The hysteresis loss factor associated with cut-out events is estimated to be **98.9%**.

6.2.3 Extreme Temperature

The Vestas V110-2.0 has an assumed operating temperature between $-20°C$ and $40°C$ without an additional cold weather package. 36 years of MOS-corrected temperature data were analyzed to determine the production losses due to the temperature constraints. Based on the potential power production during periods with temperatures outside the operating limits, and a total wind farm shutdown during these times, the extreme temperature loss factor is estimated to be **99.8%** due to extreme temperatures below $-20°C$.

6.2.4 Icing Shutdown

Observational data were inspected for significant icing events that may lead an operator to shutdown the wind farm. The observational data suggest a curtailment associated with icing events of **99.0%**.

6.3 Wake Deficit

3TIER's wake model is used to determine the expected wake deficit for the turbine layout. The magnitude of the losses at any given time is a combination of the gross wind field and ambient turbulence intensity across the park, the turbine layout, and physical characteristics of the installed turbines. 3TIER analyzes wakes using a proprietary time-varying wake model that analyzes the wake at every individual time within the simulated record, rather than relying on bulk statistical descriptions of the wind field. Wakes for each turbine are computed individually and interact in a physically consistent way, eliminating the need for posterior models to combine wakes from multiple turbines or add in deep-array effects. The single turbine wake model is based on concepts originally presented by Larsen et al. (1996). [6] 3TIER's internal research has shown that the low bias associated with other Larsen-derived wake models [9] is a result of poorly handled wake addition rather than the underlying model. The full system has been calibrated using production numbers from permanently installed turbines under a wide range of environmental conditions, including a broad span of turbulence intensities and stability regimes. The outputs from the model are wake-induced velocity deficit and turbulence intensity at all turbine locations, and can include additional reference locations.

6.3.1 Internal Wakes

Internal wakes represent wakes caused by turbines within the project. The effect of wake deficit on energy output for the layout leads to an internal wake loss factor of **93.4%**.

6.3.2 External Wakes

External wakes represent additional wakes caused by turbines from surrounding wind farms. Cedar Point and Limon (Phases 1, 2 and 3) Wind Farms are over 12 km to the northeast of the nearest Rush Creek I wind turbine. 3TIER considered the distances between and positions of project turbines and surrounding turbines within the context of the local wind rose and determined the surrounding wind farms to be inconsequential.

6.3.3 Future Wakes

Future wakes represent wakes caused by turbines that will be built in the future, not related to this project. NextEra's Golden West Wind Farm will be constructed to the west and southwest of Rush Creek I with the nearest turbines being approximately 9 km away. 3TIER considered the distances between and positions of the project turbines and proposed Golden West turbines within the context of the local wind rose and determined this future project to be inconsequential. 3TIER discovered records of Determination of No Hazard to Air Navigation filed with the FAA for turbine locations for two additional areas of possible development much closer to the Rush Creek I project than Golden West. These records were filed in 2013 and 2014 with one group of turbines associated with the presumed canceled Big Sandy Creek Wind project. Another group of turbines is associated with PowerWorks LLC and is also assumed to be canceled. With no known feasible future project with wake impacts to Rush Creek I, the future wakes loss factor is assumed to be **100%**.

6.3.4 Total Wakes

The total wake loss factor, including the project (i.e. internal) turbines, is **93.4%**. Waked generation values for each individual turbine are shown in Appendix Turbine Means.

6.4 Electrical Efficiency

Electrical efficiency considers losses associated with the electrical systems connecting the turbines to the metering point. These systems include the on-site collection system, the substation power transformer, and the transmission line depending on the meter location. 3TIER assumes the wind farm will be metered on the low side of the substation power transformer. Given this assumption, the electrical system efficiency is expected to be **98.0%**.

6.4.1 Collection System Efficiency

The collection system efficiency covers the efficiency of all components from the turbines to the pooling substation, including the medium voltage transformer efficiency that steps up the turbine voltage to the collection system voltage.

6.4.2 Substation Power Transformer Efficiency

The substation power transformer converts the voltage of the collection system to the voltage of the high voltage transmission line. This analysis ends at the low side of the substation transformer and does not consider substation power transformer losses. The client is undertaking a study to determine the full substation loss.

6.4.3 High Voltage Transmission Line Efficiency

Transmission line efficiency is dependent on the cable type, voltage, load, and the distance from the pooling substation to the plant metering point. The client has indicated that the export power will be delivered to a substation that is approximately 90 miles away which would incur additional high voltage transmission line losses. The client is undertaking a study to determine these added losses. 3TIER has not included an assumption for additional high voltage transmission line losses in this analysis.

6.4.4 Consumptive Power

Consumptive power considers the fact that a wind farm consumes electrical power when generation levels are very low. This is primarily due to power required to keep generators and transformers active and ready for operations. When the plant is operating, consumptive power is inherent to the turbine power curve and electrical efficiency assumptions. The client has specified that the wind farm will have a bidirectional meter and has requested that consumptive power of the wind farm be accounted for as an additional loss factor. 3TIER has assumed a loss factor of **99.5%** for consumptive power.

6.5 Turbine Efficiency

Turbine efficiency is based on the ability of the turbines to perform at a level relative to the manufacturer's suggested performance rating. This can be affected by many factors, including the manufacturer's warranted performance level, the turbulence, and inflow angle.

6.5.1 Turbine Performance

3TIER's experience with operating wind farms suggests a loss factor should be applied for turbine performance. This loss factor is related to turbines not performing at the manufacturer's rated power curve. The Vestas V110-2.0 is a relatively new turbine. Within the United States, there are 5 projects currently under construction with this model and a limited number of operating turbines. This turbine model is based on the Vestas V100-2.0, with a longer blade and new gear box. According to a database of installed turbines created by the American Wind Energy Association, there are 2,288 V100-2.0 turbines installed in the United States. Based on the lack operational history for the Vestas V110-2.0, 3TIER suggests that a turbine performance loss factor of **98.0%** be applied to account for the risk that the turbines do not perform exactly at the manufacturer's rated power curve.

6.5.2 Turbulence Intensity

Research has linked turbine under performance to stable atmospheric conditions. These conditions are often identified by low turbulence intensity. In addition, periods of low or high turbulence intensity can affect the specified power curve by creating a statistical averaging effect. The statistical averaging effect is assessed by comparing the average of the instantaneous wind speeds using a theoretical zero turbulence power curve against the manufacturer's power curve at given turbulence level. 3TIER analyzes the potential for both of these effects using the measured turbulence intensity and has calculated a loss factor of **96.8%**.

6.5.3 Inflow Angle

Reduced efficiency associated with extreme inflow angles is expected to be negligible; therefore, an inflow angle loss factor of **100.0%** is applied.

6.6 Environmental

Potential environmental losses include turbine under-performance caused by turbine blade soiling and degradation, extreme weather conditions such as icing and thunderstorms, and changes to the surrounding environment such as tree growth.

6.6.1 Blade Soiling

In locations where the ground is dry and the soil is loose, turbine blades can build up substantial amounts of soil, leading to a power curve derating. 3TIER has analyzed projects in similar terrain and has calculated a standard loss factor for cultivated farmland and shrub steppe conditions. A loss factor of **98.5%** is applied for blade soiling.

6.6.2 Blade Degradation

Blade degradation, unlike blade soiling, is permanent damage caused to the turbine blades by material in hitting the blades. This can include corrosive material, such as sodium chloride (sea salt), and larger diameter soil and dirt particles. 3TIER has analyzed projects in similar terrain and has calculated a standard loss factor for cultivated farmland and shrub steppe conditions. A loss factor of **99.5%** is applied for blade degradation. While this elevated risk of hail applies to the general region, the probability of hail damage at the project or at an individual turbine location is relatively small. No additional loss factor has been applied for blade degradation due to hail.

6.6.3 Soft Icing

Soft icing occurs when ice builds up on the turbine blades and affects the ability of the turbine to operate optimally. Soft icing is often found as shoulder events to hard ice in which loads are exceeded and turbine shutdown occurs. A loss factor of **99.5%** is applied for soft icing.

6.6.4 Other Environmental Losses

3TIER has considered the effects from additional environmental losses. Average lightning density for the project is expected to be moderate relative to the state of Colorado as a whole. Local lightning density is expected to be lower than high risk lightning areas in the Midwestern and Southeastern United States. Additional losses such thunderstorms and tree growth, are expected to be negligible.

6.7 Aggregate Loss Factor

Table 7 below shows the individual loss factors for all considered categories and the aggregate loss factor. The product of all considered losses is **78.5%**. The expected gross P50 generation is $1909.7\,GWh$; therefore, the net P50 generation is the product of 78.5% and $1909.7\,GWh$, which equals $\mathbf{1498.4\,GWh}$. Table 8 displays the monthly-mean net values as a percent of the expected annual-mean generation value (GWh).

Loss Factor	Percent Loss
Project Availability	
Turbine Availability	96.0 %
Balance Of Plant Availability	99.7 %
Grid Availability	99.5 %
Curtailment	
Sector Management	–
High Wind Hysteresis	98.9 %
Icing	99.0 %
Extreme Temperature	99.8 %
Wake Deficit	
Total Wakes	93.4 %
Electrical Efficiency	
Total Electrical Efficiency	98.0 %
Consumptive Power	99.5 %
Turbine Efficiency	
Turbine Performance	98.0 %
Turbulence Intensity	96.8 %
Inflow Angle	100.0 %
Environmental	
Blade Soiling	98.5 %
Blade Degradation	99.5 %
Soft Icing	99.5 %
Aggregate Loss Factor	**78.5 %**

Table 7: Summary of loss factors. Sector management loss has not been considered, but a calculation could be made with additional data from the turbine manufacturer.

Month	GWh (%)
January	8.6 %
February	7.9 %
March	9.4 %
April	9.6 %
May	9.0 %
June	8.4 %
July	7.4 %
August	7.0 %
September	7.7 %
October	8.2 %
November	8.2 %
December	8.6 %

Table 8: Monthly-mean net values as a percent of the total annual-mean generation.

7 UNCERTAINTY ANALYSIS

To calculate uncertainty and estimates of probabilities of exceedance, 3TIER has utilized its Energy Risk Framework. This framework is based on theoretical propagation of error theory and models hundreds of sources of uncertainty and their relationships throughout the modeling process. Each source of uncertainty is treated in a separate model that interacts with the framework through overlying covariance models. The analysis considers the following sources of uncertainty: measurement, vertical extrapolation, MOS correction, climate variability, spatial modeling, and power modeling.

7.1 Uncertainty Methodology

7.1.1 Measurement Uncertainty

Measurement uncertainty captures the uncertainties related to the on-site measured data utilized in the energy assessment. It is a measure of the confidence that the recorded data, which are presumed to represent the truth, actually do represent the truth. Individual components of measurement uncertainty include the following: anemometer uncertainty, benefits of utilizing redundant sensors, measurement height uncertainty, and the statistical propagation of these uncertainties through the wind shear and extrapolation calculations to estimate hub height wind speed values. Uncertainty is separately estimated for each measurement sensor, and the sensor uncertainties are aggregated together to represent the total measurement uncertainty at hub height level for each met tower. Measurement uncertainty estimates at each met tower are considered to be independent when predicting measurement uncertainty at each turbine location.

7.1.2 Vertical Extrapolation Uncertainty

If on-site measurements are not directly recorded at hub height, an uncertainty exists that the true vertical wind speed profile may differ from the assumed power law profile. A vertical extrapolation uncertainty is required to account for this uncertainty. Remote sensing and/or hub height measurements can reduce and potentially eliminate this uncertainty.

Vertical extrapolation uncertainty is estimated at each met tower individually and, met tower estimates are combined assuming partial dependency on the mast and turbine heights when estimating vertical extrapolation uncertainty at the turbine locations. For example, if met towers are located in meteorologically similar environments, risk is increased that common errors are present in the vertical extrapolation process.

7.1.3 MOS Correction Uncertainty

A MOS Correction uncertainty is applied at each met tower that accounts for the probability that the statistical correction applied to the long term climate signal will accurately capture the true historic climate variability. The uncertainty associated with 3TIER's MOS correction algorithm decreases as the training period increases. The uncertainty depends on the length of data available at the met tower and the quality of the relationship between the met tower and the long term data set.

MOS correction uncertainty is estimated at each met tower, and then individual uncertainties are combined to predict the uncertainty at each turbine location assuming partial dependence between each met tower. This dependence is a function of the concurrency of measurements between the met towers, since the uncertainty of this relationship will depend on common errors in the climate signal used as the reference.

7.1.4 Climate Variability Uncertainty

Climate variability uncertainty is comprised of the following individual component uncertainties: historic climate, future climate, climate change, and climate signal consistency. Historic and future climate uncertainties represent the uncertainty associated with the natural variability of the climate and whether the climate reference period or future prediction period will capture the true climate. These uncertainties are a function of the inter-annual variability and auto-correlation of the climate signal. Climate change and climate signal consistency uncertainties represent the probability of error of the future prediction because the climate of the future may not be accurately represented by the climate of the past. These uncertainties are higher if the past few years show potential trends that may point towards a changing pattern.

Climate variability uncertainty is considered common across all met towers and is modeled with complete dependence in the uncertainty framework.

7.1.5 Spatial Modeling Uncertainty

Spatial modeling uncertainty is estimated by calibrating a spatial model for each met tower that applies the MOS correction derived at that met tower to all the turbine locations. The individual spatial models are combined at each turbine location using weights that are a function of the total uncertainty at each met tower considering dependence and independence of each component uncertainty. Spatial uncertainties are a function of the geographic covariance between each met tower and turbine location. 3TIER applies two spatial modeling uncertainties: micro spatial uncertainty and macro spatial uncertainty. Micro spatial uncertainty represents the uncertainty associated with the grid resolution of the spatial model and whether the model is capturing micro scale effects. Macro spatial uncertainty represents the risk that a spatial model calibration at the location of a met tower is applicable at distances away from that met tower.

This complex uncertainty is a function of all the prior uncertainties and relative proximity and complexity of each geospatial relationship. The dependence on prior uncertainties is driven by the weighting scheme of each met tower, which has uncertainty dependence. Spatial covariance is also considered when aggregating each individual turbine uncertainty into a project average uncertainty.

7.1.6 Power Modeling Uncertainty

Power modeling uncertainty considers each step in converting wind speed estimates into energy estimates. In this step, wind speed uncertainties are expanded by the wind speed to energy relationship and then the following is considered: representativeness of the modeled frequency distribution when applying the specified power curve, wakes, availabilities, electrical losses, and all other losses considered in the loss evaluation process. Power modeling uncertainties are considered to be dependent between each turbine location.

7.2 Uncertainty Framework Results

The largest contributors of uncertainty for the Rush Creek I project originates in spatial modeling and vertical extrapolation. The average weighted turbine to tower distance is approximately $11.1\,km$, which is high for a quality pre-construction due diligence analysis. The installation of additional, well-instrumented met towers at locations that reduce the average weighted turbine to tower distance may further reduce the spatial modeling uncertainty. The vertical extrapolation uncertainty is elevated because the turbine hub height is $20\,m$ above the top measured met tower height. Collecting wind speed measurements at or near hub height will further reduce the vertical extrapolation uncertainty. This can be achieved by installing additional met towers with hub height measurements, or by utilizing a wind profiler device such as a Triton SODAR (Sonic Detection and Ranging) or LIDAR (Light Detection and Ranging). 3TIER can provide further recommendations regarding potential met tower locations, sensor configurations and wind profiler options to reduce the spatial modeling and vertical extrapolation uncertainties. Other uncertainty categories are at acceptable or typical levels.

7.2.1 Met Tower Uncertainty

Uncertainty values for each met tower are presented as a function of wind speed below in Table 9.

	M2301	M2327
Measurement	1.2	1.1
Vertical Extrapolation	1.4	1.4
MOS Correction	0.3	0.7
Climate Variability	1.2	1.2
Combined Uncertainty	**2.3**	**2.3**

Table 9: Standard error of wind speed estimation at each met tower (%)

7.2.2 Combined Project Uncertainties

The total project uncertainties, represented as a percent of the P50 estimate are presented in Table 10 as a function of energy.

	1-year	10-year	20-year
Measurement	1.0	1.0	1.0
Vertical Extrapolation	1.7	1.7	1.7
MOS Correction	0.5	0.5	0.5
Climate Variability	3.7	1.6	1.4
Spatial Modeling	5.1	5.1	5.1
Power Modeling	4.5	4.5	4.5
Total Uncertainty	**8.0**	**7.3**	**7.3**

Table 10: Standard error of wind energy estimation (%)

8 PROBABILITY OF EXCEEDANCES

Based on the estimated total project uncertainties, Tables 11 and 12 present the probability of exceedance levels associated with the P50 project estimate. Table 11 provides results in terms of GWh, while Table 12 shows results in terms of project-average capacity factor (%). Table 13 shows the net P50, P75, and P90 values for each calendar month.

	1-year	10-year	20-year
Gross-P50	1909.7	1909.7	1909.7
Net-P50	1498.4	1498.4	1498.4
Net-P10	1652.3	1638.6	1637.8
Net-P25	1579.4	1572.2	1571.7
Net-P65	1452.1	1456.2	1456.4
Net-P75	1417.3	1424.5	1425.0
Net-P90	1344.4	1358.1	1358.9
Net-P95	1300.8	1318.4	1319.4
Net-P99	1218.9	1243.8	1245.3

Table 11: Probability of Exceedance Values (GWh)

	1-year	10-year	20-year
Gross-P50	54.5	54.5	54.5
Net-P50	42.7	42.7	42.7
Net-P10	47.1	46.7	46.7
Net-P25	45.0	44.8	44.8
Net-P65	41.4	41.5	41.5
Net-P75	40.4	40.6	40.6
Net-P90	38.3	38.7	38.8
Net-P95	37.1	37.6	37.6
Net-P99	34.8	35.5	35.5

Table 12: Probability of Exceedance Values (%)

	Net P50	20-year Net P75	20-year Net P90
January	129.5	122.8	116.6
February	118.8	113.0	107.8
March	140.6	134.8	129.4
April	143.3	137.4	132.0
May	134.2	127.5	121.4
June	125.3	118.7	112.8
July	111.6	104.8	98.8
August	105.0	98.3	92.3
September	114.7	108.0	102.0
October	122.9	116.4	110.5
November	123.4	117.1	111.3
December	129.1	122.5	116.7

Table 13: Monthly Probability of Exceedance Values (GWh). The monthly P75 and P90 values are not expected to sum to the annual values, since the variability of the monthly-means is greater than the variability of the annual-mean.

9 CONCLUSION

3TIER has conducted a wind resource assessment of the Rush Creek I project. The assessment is based on a wind turbine layout consisting of 200 Vestas V110-2.0 wind turbines at $80\,m$. The wind resource assessment yields a gross energy value of $1909.7\,GWh$. Loss factors were considered, leading to a net energy estimate of $1498.4\,GWh$. Turbine-wise values of gross energy, wake loss, and net energy are available in Appendix Turbine Means. Following the uncertainty assessment of wind speed measurement and energy modeling analysis, net probabilities of exceedance were calculated. 20-year P75 and P90 cases are $1425.0\,GWh$ and $1358.9\,GWh$, respectively.

10 APPENDIX TURBINE MEANS

This section contains turbine-specific elevation, wind speed, and air density, along with gross energy values, wake loss, and net energy values for each of the 200 turbines at the Rush Creek I project.

10.1 Vestas V110-2.0 wind turbines at 80 m

ID	Latitude (*degrees*)	Longitude (*degrees*)	Elevation (m)	Wind Speed ($\frac{m}{s}$)	Air Density ($\frac{kg}{m^3}$)	Gross Generation (MWh :: %)	Wake Loss (%)	Net Generation (MWh :: %)
T001	39.24318	-103.75590	1708	7.99	1.008	9118 :: 52.0	95.7	7339 :: 41.9
T002	39.23797	-103.76170	1718	8.07	1.007	9236 :: 52.7	94.7	7357 :: 42.0
T003	39.12624	-103.93746	1864	8.59	0.991	9978 :: 56.9	93.8	7833 :: 44.7
T004	39.23382	-103.76730	1731	8.15	1.005	9343 :: 53.3	95.3	7484 :: 42.7
T005	39.19856	-103.78707	1743	8.12	1.004	9356 :: 53.4	92.2	7264 :: 41.4
T006	39.21352	-103.72591	1701	8.03	1.008	9205 :: 52.5	94.1	7283 :: 41.5
T007	39.16334	-103.84012	1789	8.27	0.999	9584 :: 54.7	90.7	7289 :: 41.6
T008	39.20950	-103.73215	1706	8.06	1.008	9250 :: 52.8	94.5	7347 :: 41.9
T009	39.10220	-103.98783	1884	8.36	0.989	9696 :: 55.3	93.4	7605 :: 43.4
T010	39.10257	-104.00593	1897	8.34	0.988	9663 :: 55.1	93.0	7549 :: 43.1
T011	39.22004	-103.78256	1742	8.11	1.004	9290 :: 53.0	94.1	7362 :: 42.0
T012	39.14072	-103.92920	1850	8.46	0.993	9797 :: 55.9	93.0	7645 :: 43.6
T013	39.22110	-103.76776	1733	8.11	1.005	9300 :: 53.0	92.6	7249 :: 41.3
T014	39.21289	-103.79915	1757	8.18	1.003	9381 :: 53.5	93.1	7353 :: 41.9
T015	39.14140	-103.90634	1841	8.43	0.994	9774 :: 55.8	94.7	7759 :: 44.3
T016	39.20867	-103.81888	1768	8.18	1.002	9359 :: 53.4	92.5	7280 :: 41.5
T017	39.21060	-103.80204	1759	8.19	1.002	9387 :: 53.5	93.1	7353 :: 41.9
T020	39.19699	-103.81421	1763	8.15	1.002	9361 :: 53.4	92.8	7316 :: 41.7
T021	39.19218	-103.82300	1773	8.17	1.001	9396 :: 53.6	92.3	7286 :: 41.6
T022	39.12802	-103.93421	1860	8.55	0.992	9936 :: 56.7	94.4	7853 :: 44.8
T023	39.18343	-103.84850	1791	8.20	0.999	9441 :: 53.8	92.4	7323 :: 41.8
T024	39.19257	-103.86502	1805	8.25	0.998	9455 :: 53.9	94.1	7464 :: 42.6
T026	39.19024	-103.87211	1796	8.07	0.999	9211 :: 52.5	94.0	7280 :: 41.5
T027	39.18543	-103.87416	1810	8.22	0.998	9432 :: 53.8	93.1	7369 :: 42.0
T028	39.17434	-103.88005	1819	8.18	0.997	9402 :: 53.6	93.4	7375 :: 42.1
T029	39.18238	-103.88143	1806	8.10	0.998	9271 :: 52.9	93.5	7288 :: 41.6
T030	39.18018	-103.88740	1793	7.89	0.999	8969 :: 51.2	95.2	7194 :: 41.0
T031	39.16658	-103.87952	1818	8.18	0.997	9419 :: 53.7	93.9	7432 :: 42.4
T032	39.16860	-103.84846	1797	8.32	0.998	9635 :: 55.0	91.1	7358 :: 42.0
T033	39.23232	-103.75326	1717	8.10	1.007	9276 :: 52.9	94.0	7334 :: 41.8
T034	39.16317	-103.84930	1796	8.29	0.999	9599 :: 54.8	92.1	7417 :: 42.3
T035	39.16373	-103.74979	1723	8.10	1.006	9329 :: 53.2	93.5	7338 :: 41.9
T036	39.15864	-103.85916	1802	8.26	0.998	9560 :: 54.5	92.6	7427 :: 42.4
T037	39.19412	-103.81885	1770	8.19	1.001	9423 :: 53.7	92.9	7357 :: 42.0
T038	39.16737	-103.81523	1769	8.17	1.001	9463 :: 54.0	91.5	7288 :: 41.6
T039	39.18853	-103.83341	1780	8.20	1.000	9434 :: 53.8	92.1	7291 :: 41.6

Table 14: Turbine-specific 36-year mean values for 200 Vestas V110-2.0 wind turbines at 80 m. Generation values are provided in terms of energy and capacity factor. (continued on next page)

ID	Latitude (degrees)	Longitude (degrees)	Elevation (m)	Wind Speed ($\frac{m}{s}$)	Air Density ($\frac{kg}{m^3}$)	Gross Generation (MWh :: %)	Wake Loss (%)	Net Generation (MWh :: %)
T040	39.13490	-103.85404	1791	8.19	0.999	9471 :: 54.0	94.3	7496 :: 42.8
T041	39.14237	-103.82057	1771	8.19	1.001	9482 :: 54.1	92.2	7358 :: 42.0
T042	39.17855	-103.85860	1802	8.25	0.998	9506 :: 54.2	92.3	7360 :: 42.0
T043	39.18553	-103.84279	1788	8.24	0.999	9482 :: 54.1	92.7	7375 :: 42.1
T044	39.13029	-103.93123	1854	8.47	0.992	9824 :: 56.0	94.2	7763 :: 44.3
T045	39.12488	-103.92445	1853	8.42	0.992	9771 :: 55.7	92.5	7581 :: 43.2
T046	39.16865	-103.86931	1814	8.29	0.997	9578 :: 54.6	94.0	7555 :: 43.1
T047	39.14179	-103.86636	1808	8.31	0.997	9625 :: 54.9	94.4	7619 :: 43.5
T048	39.15985	-103.88042	1822	8.27	0.996	9548 :: 54.5	93.8	7517 :: 42.9
T049	39.17561	-103.86112	1802	8.22	0.998	9468 :: 54.0	92.9	7389 :: 42.1
T050	39.15885	-103.88502	1828	8.34	0.996	9646 :: 55.0	94.5	7650 :: 43.6
T051	39.15541	-103.88730	1829	8.34	0.995	9650 :: 55.0	94.4	7645 :: 43.6
T052	39.15257	-103.89000	1830	8.34	0.995	9646 :: 55.0	93.1	7538 :: 43.0
T053	39.15302	-103.89511	1829	8.30	0.995	9592 :: 54.7	94.3	7595 :: 43.3
T054	39.14904	-103.89696	1835	8.37	0.995	9684 :: 55.2	93.6	7607 :: 43.4
T055	39.15030	-103.90216	1840	8.45	0.994	9793 :: 55.9	94.5	7757 :: 44.2
T056	39.13786	-103.79708	1750	8.07	1.003	9300 :: 53.0	92.3	7235 :: 41.3
T057	39.18140	-103.85344	1796	8.23	0.999	9481 :: 54.1	92.8	7383 :: 42.1
T058	39.13500	-103.84790	1790	8.26	0.999	9555 :: 54.5	93.2	7468 :: 42.6
T059	39.11664	-103.92462	1850	8.35	0.993	9677 :: 55.2	94.5	7672 :: 43.8
T060	39.13955	-103.83586	1786	8.28	0.999	9589 :: 54.7	91.9	7390 :: 42.2
T061	39.13771	-103.82448	1777	8.25	1.000	9549 :: 54.5	92.4	7415 :: 42.3
T062	39.19919	-103.72241	1701	8.01	1.008	9188 :: 52.4	94.8	7327 :: 41.8
T063	39.20102	-103.71796	1699	8.02	1.009	9198 :: 52.5	94.8	7329 :: 41.8
T065	39.14192	-103.88042	1816	8.29	0.996	9604 :: 54.8	94.5	7620 :: 43.5
T067	39.16678	-103.83278	1785	8.27	1.000	9593 :: 54.7	91.1	7335 :: 41.8
T068	39.13596	-103.93011	1853	8.46	0.993	9805 :: 55.9	92.9	7644 :: 43.6
T069	39.13764	-103.92255	1848	8.35	0.993	9671 :: 55.2	93.0	7550 :: 43.1
T071	39.20949	-103.75010	1717	8.06	1.007	9259 :: 52.8	94.3	7348 :: 41.9
T072	39.22136	-103.77307	1737	8.12	1.005	9320 :: 53.2	93.7	7351 :: 41.9
T075	39.11916	-103.77948	1744	8.11	1.003	9302 :: 53.1	93.4	7308 :: 41.7
T076	39.12408	-103.77837	1738	8.04	1.004	9215 :: 52.6	91.9	7126 :: 40.6
T077	39.12484	-103.78749	1749	8.11	1.003	9323 :: 53.2	92.9	7293 :: 41.6
T079	39.13854	-103.76220	1727	8.03	1.005	9221 :: 52.6	93.5	7257 :: 41.4
T080	39.13895	-103.90939	1842	8.42	0.994	9763 :: 55.7	93.3	7636 :: 43.6
T081	39.16383	-103.82243	1778	8.25	1.000	9565 :: 54.6	90.7	7287 :: 41.6
T082	39.18017	-103.80563	1760	8.16	1.002	9438 :: 53.8	91.8	7300 :: 41.6
T083	39.14650	-103.90400	1835	8.34	0.995	9656 :: 55.1	94.1	7625 :: 43.5
T087	39.14950	-103.93182	1822	8.21	0.996	9462 :: 54.0	94.8	7541 :: 43.0
T088	39.14732	-103.92373	1827	8.25	0.995	9519 :: 54.3	93.9	7508 :: 42.8
T089	39.15142	-103.76013	1731	8.12	1.005	9362 :: 53.4	92.8	7308 :: 41.7
T090	39.11486	-103.75043	1719	7.97	1.006	9096 :: 51.9	94.1	7199 :: 41.1
T091	39.11481	-103.74611	1716	7.97	1.006	9080 :: 51.8	93.4	7135 :: 40.7
T092	39.20950	-103.81417	1768	8.22	1.002	9418 :: 53.7	92.0	7287 :: 41.6
T093	39.13831	-103.71817	1704	7.99	1.008	9134 :: 52.1	94.3	7244 :: 41.3
T094	39.14023	-103.72537	1707	8.00	1.008	9148 :: 52.2	94.4	7263 :: 41.4

Table 14: Turbine-specific 36-year mean values for 200 Vestas V110-2.0 wind turbines at $80\,m$. Generation values are provided in terms of energy and capacity factor. (continued on next page)

ID	Latitude $(degrees)$	Longitude $(degrees)$	Elevation (m)	Wind Speed $(\frac{m}{s})$	Air Density $(\frac{kg}{m^3})$	Gross Generation $(MWh$ :: $\%)$	Wake Loss $(\%)$	Net Generation $(MWh$ :: $\%)$
T096	39.13720	-103.82987	1780	8.24	1.000	9544 :: 54.4	91.5	7331 :: 41.8
T097	39.13929	-103.91397	1846	8.45	0.993	9794 :: 55.9	94.8	7790 :: 44.4
T098	39.18548	-103.79292	1749	8.16	1.003	9429 :: 53.8	91.7	7280 :: 41.5
T100	39.15993	-103.85427	1802	8.32	0.998	9639 :: 55.0	92.5	7475 :: 42.6
T102	39.16497	-103.74489	1720	8.09	1.006	9319 :: 53.2	93.4	7318 :: 41.7
T103	39.11574	-103.73730	1709	7.95	1.007	9047 :: 51.6	94.5	7194 :: 41.0
T107	39.15664	-103.72716	1709	8.05	1.007	9246 :: 52.7	93.3	7257 :: 41.4
T108	39.15540	-103.73098	1711	8.04	1.007	9230 :: 52.6	93.3	7241 :: 41.3
T109	39.13883	-103.78194	1741	8.07	1.004	9278 :: 52.9	92.1	7192 :: 41.0
T110	39.11451	-103.83359	1773	8.17	1.000	9409 :: 53.7	94.0	7425 :: 42.4
T111	39.11563	-103.84450	1781	8.19	1.000	9441 :: 53.8	95.5	7564 :: 43.1
T112	39.11027	-103.83678	1777	8.19	1.000	9431 :: 53.8	95.1	7525 :: 42.9
T113	39.22019	-103.77755	1740	8.12	1.004	9308 :: 53.1	92.6	7253 :: 41.4
T114	39.16568	-103.83718	1787	8.27	0.999	9587 :: 54.7	90.4	7269 :: 41.5
T115	39.12035	-103.79355	1752	8.09	1.003	9285 :: 53.0	94.4	7381 :: 42.1
T116	39.13229	-103.80735	1760	8.12	1.002	9356 :: 53.4	93.5	7370 :: 42.0
T117	39.21180	-103.79394	1755	8.19	1.003	9408 :: 53.7	92.3	7306 :: 41.7
T118	39.13756	-103.80494	1758	8.13	1.002	9376 :: 53.5	92.1	7276 :: 41.5
T121	39.12170	-103.93852	1864	8.48	0.991	9848 :: 56.2	93.2	7695 :: 43.9
T122	39.16634	-103.81939	1774	8.21	1.001	9519 :: 54.3	90.8	7271 :: 41.5
T123	39.12183	-103.72308	1703	7.95	1.008	9054 :: 51.6	95.6	7278 :: 41.5
T124	39.11375	-103.75420	1721	7.98	1.006	9109 :: 52.0	94.8	7267 :: 41.5
T125	39.13789	-103.84460	1789	8.28	0.999	9584 :: 54.7	92.6	7442 :: 42.4
T126	39.05626	-104.03077	1920	8.47	0.985	9801 :: 55.9	93.9	7709 :: 44.0
T127	39.12253	-103.98437	1890	8.55	0.989	9919 :: 56.6	92.7	7709 :: 44.0
T128	39.08237	-104.04155	1928	8.51	0.985	9901 :: 56.5	97.0	8054 :: 45.9
T129	39.12082	-103.95180	1868	8.51	0.991	9887 :: 56.4	94.1	7800 :: 44.5
T130	39.10164	-104.03194	1922	8.56	0.985	9946 :: 56.7	96.7	8063 :: 46.0
T131	39.06042	-104.04208	1932	8.48	0.984	9833 :: 56.1	95.8	7884 :: 45.0
T132	39.12244	-103.96243	1876	8.60	0.990	9994 :: 57.0	94.0	7872 :: 44.9
T133	39.09181	-104.04446	1929	8.52	0.985	9910 :: 56.5	97.6	8112 :: 46.3
T134	39.10304	-104.02830	1917	8.48	0.986	9855 :: 56.2	94.8	7843 :: 44.7
T135	39.06117	-104.00642	1903	8.43	0.987	9763 :: 55.7	94.9	7762 :: 44.3
T136	39.07721	-104.02759	1920	8.51	0.985	9897 :: 56.5	93.5	7752 :: 44.2
T137	39.07953	-104.02299	1912	8.43	0.986	9799 :: 55.9	93.8	7714 :: 44.0
T138	39.12091	-103.96589	1876	8.50	0.990	9865 :: 56.3	93.1	7705 :: 43.9
T139	39.12598	-103.99824	1900	8.59	0.988	9968 :: 56.9	93.6	7815 :: 44.6
T140	39.12138	-103.95660	1875	8.59	0.990	9978 :: 56.9	94.1	7867 :: 44.9
T141	39.11975	-104.01604	1914	8.49	0.987	9845 :: 56.2	95.0	7850 :: 44.8
T142	39.12042	-103.97017	1878	8.44	0.990	9789 :: 55.8	93.4	7675 :: 43.8
T143	39.12272	-103.94850	1871	8.61	0.991	10000 :: 57.0	94.3	7899 :: 45.1
T144	39.10605	-104.01974	1913	8.45	0.986	9806 :: 55.9	93.5	7700 :: 43.9
T145	39.12469	-103.99357	1895	8.54	0.988	9908 :: 56.5	91.9	7633 :: 43.5
T146	39.12302	-103.98883	1894	8.58	0.988	9958 :: 56.8	92.7	7735 :: 44.1
T147	39.05785	-104.02139	1911	8.40	0.986	9720 :: 55.4	94.8	7722 :: 44.0
T148	39.10402	-104.02272	1915	8.53	0.986	9910 :: 56.5	94.3	7838 :: 44.7

Table 14: Turbine-specific 36-year mean values for 200 Vestas V110-2.0 wind turbines at $80\,m$. Generation values are provided in terms of energy and capacity factor. (continued on next page)

ID	Latitude (*degrees*)	Longitude (*degrees*)	Elevation (m)	Wind Speed ($\frac{m}{s}$)	Air Density ($\frac{kg}{m^3}$)	Gross Generation (MWh :: %)	Wake Loss (%)	Net Generation (MWh :: %)
T149	39.10439	-103.97180	1876	8.38	0.990	9718 :: 55.4	94.4	7701 :: 43.9
T150	39.05926	-104.03715	1927	8.47	0.985	9819 :: 56.0	94.2	7745 :: 44.2
T151	39.12061	-103.97473	1883	8.47	0.989	9825 :: 56.0	93.1	7675 :: 43.8
T152	39.06301	-104.00252	1898	8.43	0.987	9761 :: 55.7	94.4	7724 :: 44.1
T153	39.12213	-104.01060	1908	8.46	0.987	9812 :: 56.0	94.8	7803 :: 44.5
T154	39.12593	-104.00462	1905	8.57	0.987	9945 :: 56.7	94.3	7858 :: 44.8
T155	39.08515	-104.00814	1902	8.48	0.987	9863 :: 56.3	93.7	7745 :: 44.2
T156	39.08364	-104.01232	1905	8.47	0.987	9847 :: 56.2	94.1	7775 :: 44.3
T157	39.12281	-103.97992	1887	8.57	0.989	9946 :: 56.7	92.9	7744 :: 44.2
T158	39.11538	-104.01712	1914	8.41	0.987	9750 :: 55.6	93.4	7652 :: 43.6
T159	39.07909	-103.98449	1881	8.45	0.989	9810 :: 56.0	93.3	7673 :: 43.8
T160	39.05709	-104.02648	1915	8.43	0.986	9753 :: 55.6	93.8	7666 :: 43.7
T161	39.12188	-104.00606	1907	8.49	0.987	9847 :: 56.2	91.9	7592 :: 43.3
T162	39.05531	-104.04382	1932	8.42	0.984	9736 :: 55.5	96.9	7900 :: 45.1
T163	39.11255	-104.01930	1917	8.50	0.986	9861 :: 56.2	94.4	7812 :: 44.6
T164	39.05883	-104.01050	1905	8.41	0.987	9733 :: 55.5	95.7	7806 :: 44.5
T165	39.06485	-103.99893	1894	8.43	0.988	9774 :: 55.7	94.3	7725 :: 44.1
T166	39.04738	-104.02994	1916	8.39	0.986	9671 :: 55.2	94.8	7682 :: 43.8
T167	39.06042	-103.98108	1880	8.39	0.989	9703 :: 55.3	94.8	7707 :: 44.0
T168	39.05946	-103.98643	1884	8.38	0.989	9683 :: 55.2	94.4	7658 :: 43.7
T169	39.07891	-104.01784	1909	8.44	0.987	9810 :: 56.0	93.2	7664 :: 43.7
T170	39.04409	-104.03293	1917	8.35	0.986	9613 :: 54.8	96.7	7788 :: 44.4
T171	39.07740	-103.98867	1882	8.40	0.989	9745 :: 55.6	92.8	7582 :: 43.2
T172	39.07649	-104.03152	1923	8.51	0.985	9892 :: 56.4	94.3	7812 :: 44.6
T174	39.10241	-104.00076	1895	8.37	0.988	9704 :: 55.4	91.7	7475 :: 42.6
T175	39.04815	-104.04352	1923	8.32	0.985	9589 :: 54.7	98.0	7872 :: 44.9
T176	39.10974	-103.99796	1894	8.37	0.988	9699 :: 55.3	93.0	7574 :: 43.2
T177	39.10847	-103.95112	1861	8.34	0.992	9668 :: 55.1	94.9	7701 :: 43.9
T178	39.09004	-104.02623	1910	8.43	0.986	9795 :: 55.9	94.6	7773 :: 44.3
T179	39.12286	-103.94383	1864	8.49	0.991	9859 :: 56.2	94.6	7818 :: 44.6
T180	39.05796	-103.99147	1887	8.34	0.989	9634 :: 55.0	94.6	7643 :: 43.6
T181	39.15596	-103.86250	1805	8.29	0.998	9605 :: 54.8	93.1	7506 :: 42.8
T182	39.18741	-103.83874	1784	8.21	1.000	9439 :: 53.8	92.8	7350 :: 41.9
T183	39.19134	-103.82925	1778	8.19	1.001	9416 :: 53.7	93.2	7369 :: 42.0
T184	39.18897	-103.74823	1719	8.07	1.006	9290 :: 53.0	93.9	7341 :: 41.9
T185	39.18184	-103.80187	1759	8.20	1.002	9479 :: 54.1	91.1	7273 :: 41.5
T186	39.18387	-103.79818	1758	8.24	1.002	9529 :: 54.4	91.4	7334 :: 41.8
T187	39.20745	-103.82402	1770	8.16	1.001	9332 :: 53.2	94.3	7396 :: 42.2
T188	39.21838	-103.78696	1746	8.13	1.004	9319 :: 53.2	94.4	7405 :: 42.2
T190	39.13165	-103.92399	1847	8.31	0.993	9626 :: 54.9	92.9	7510 :: 42.8
T191	39.21427	-103.81100	1762	8.14	1.002	9306 :: 53.1	93.7	7338 :: 41.9
T192	39.23105	-103.76105	1724	8.07	1.006	9237 :: 52.7	94.1	7316 :: 41.7
T194	39.08677	-104.00290	1893	8.40	0.988	9753 :: 55.6	93.5	7652 :: 43.6
T195	39.08700	-103.99817	1889	8.40	0.989	9755 :: 55.6	91.8	7511 :: 42.8
T196	39.11388	-103.99081	1888	8.34	0.989	9657 :: 55.1	93.0	7544 :: 43.0
T197	39.06890	-104.03250	1923	8.46	0.985	9823 :: 56.0	94.0	7742 :: 44.2

Table 14: Turbine-specific 36-year mean values for 200 Vestas V110-2.0 wind turbines at 80 m. Generation values are provided in terms of energy and capacity factor. (continued on next page)

ID	Latitude (degrees)	Longitude (degrees)	Elevation (m)	Wind Speed ($\frac{m}{s}$)	Air Density ($\frac{kg}{m^3}$)	Gross Generation (MWh :: %)	Wake Loss (%)	Net Generation (MWh :: %)
T198	39.07410	-103.99215	1882	8.35	0.989	9685 :: 55.2	92.5	7520 :: 42.9
T199	39.06640	-104.03619	1924	8.43	0.985	9780 :: 55.8	94.6	7753 :: 44.2
T200	39.07311	-103.99692	1886	8.35	0.989	9680 :: 55.2	92.5	7515 :: 42.9
T201	39.18517	-103.78211	1744	8.19	1.004	9470 :: 54.0	91.5	7296 :: 41.6
T203	39.18908	-103.77501	1735	8.12	1.005	9368 :: 53.4	92.5	7296 :: 41.6
T206	39.13952	-103.84051	1788	8.25	0.999	9545 :: 54.4	92.5	7411 :: 42.3
T211	39.12285	-103.79057	1749	8.08	1.003	9276 :: 52.9	92.6	7234 :: 41.3
T212	39.14001	-103.79335	1747	8.05	1.003	9271 :: 52.9	92.0	7188 :: 41.0
T214	39.14066	-103.77853	1739	8.07	1.004	9287 :: 53.0	92.1	7200 :: 41.1
T216	39.15078	-103.83977	1786	8.24	0.999	9544 :: 54.4	91.1	7299 :: 41.6
T217	39.15113	-103.83370	1784	8.27	1.000	9592 :: 54.7	90.4	7276 :: 41.5
T218	39.15182	-103.82425	1775	8.21	1.001	9509 :: 54.2	91.0	7273 :: 41.5
T220	39.16764	-103.80326	1760	8.17	1.002	9453 :: 53.9	92.3	7347 :: 41.9
T221	39.16691	-103.79729	1756	8.17	1.002	9452 :: 53.9	90.9	7234 :: 41.3
T222	39.16626	-103.78713	1750	8.16	1.003	9435 :: 53.8	90.3	7174 :: 40.9
T223	39.16729	-103.78350	1747	8.15	1.003	9423 :: 53.7	91.1	7224 :: 41.2
T224	39.16675	-103.77869	1744	8.14	1.004	9404 :: 53.6	91.2	7217 :: 41.2
T225	39.16612	-103.77366	1740	8.13	1.004	9392 :: 53.6	91.3	7220 :: 41.2
T226	39.13840	-103.75536	1723	8.01	1.006	9184 :: 52.4	93.3	7214 :: 41.2
T227	39.19941	-103.81055	1763	8.18	1.002	9410 :: 53.7	92.8	7350 :: 41.9
T228	39.17566	-103.76766	1735	8.15	1.005	9412 :: 53.7	92.7	7342 :: 41.9
T240	39.16269	-103.73865	1715	8.08	1.007	9294 :: 53.0	93.0	7272 :: 41.5
T245	39.21081	-103.72842	1702	8.04	1.008	9218 :: 52.6	93.6	7255 :: 41.4
T246	39.11542	-103.74186	1712	7.94	1.007	9040 :: 51.6	94.0	7148 :: 40.8
T250	39.16748	-103.79279	1755	8.20	1.003	9487 :: 54.1	91.4	7304 :: 41.7
T251	39.18408	-103.87766	1801	8.06	0.998	9216 :: 52.6	93.0	7210 :: 41.1

Table 14: Turbine-specific 36-year mean values for 200 Vestas V110-2.0 wind turbines at 80 m. Generation values are provided in terms of energy and capacity factor.

ID	Net P50 (MWh :: %)	Net P75 (MWh :: %)	Net P90 (MWh :: %)	Net P95 (MWh :: %)	Net P99 (MWh :: %)
T001	7339 :: 41.9	6989 :: 39.9	6674 :: 38.1	6486 :: 37.0	6132 :: 35.0
T002	7357 :: 42.0	7011 :: 40.0	6700 :: 38.2	6513 :: 37.2	6163 :: 35.2
T003	7833 :: 44.7	7428 :: 42.4	7063 :: 40.3	6845 :: 39.0	6435 :: 36.7
T004	7484 :: 42.7	7136 :: 40.7	6823 :: 38.9	6635 :: 37.8	6283 :: 35.8
T005	7264 :: 41.4	6941 :: 39.6	6650 :: 37.9	6476 :: 36.9	6150 :: 35.1
T006	7283 :: 41.5	6931 :: 39.5	6614 :: 37.7	6424 :: 36.6	6069 :: 34.6
T007	7289 :: 41.6	6962 :: 39.7	6668 :: 38.0	6492 :: 37.0	6161 :: 35.1
T008	7347 :: 41.9	6996 :: 39.9	6681 :: 38.1	6492 :: 37.0	6138 :: 35.0
T009	7605 :: 43.4	7164 :: 40.9	6768 :: 38.6	6530 :: 37.2	6085 :: 34.7
T010	7549 :: 43.1	7097 :: 40.5	6691 :: 38.2	6447 :: 36.8	5991 :: 34.2
T011	7362 :: 42.0	7026 :: 40.1	6724 :: 38.3	6543 :: 37.3	6203 :: 35.4
T012	7645 :: 43.6	7262 :: 41.4	6917 :: 39.5	6711 :: 38.3	6323 :: 36.1
T013	7249 :: 41.3	6916 :: 39.4	6616 :: 37.7	6436 :: 36.7	6100 :: 34.8
T014	7353 :: 41.9	7020 :: 40.0	6719 :: 38.3	6539 :: 37.3	6202 :: 35.4

Table 15: Turbine-specific 20-year generation probability of exceedance values (P-values) for 200 Vestas V110-2.0 wind turbines at 80 m. (continued on next page)

ID	Net P50 (MWh :: %)	Net P75 (MWh :: %)	Net P90 (MWh :: %)	Net P95 (MWh :: %)	Net P99 (MWh :: %)
T015	7759 :: 44.3	7384 :: 42.1	7047 :: 40.2	6845 :: 39.0	6466 :: 36.9
T016	7280 :: 41.5	6952 :: 39.7	6656 :: 38.0	6479 :: 37.0	6148 :: 35.1
T017	7353 :: 41.9	7020 :: 40.0	6720 :: 38.3	6541 :: 37.3	6204 :: 35.4
T020	7316 :: 41.7	6992 :: 39.9	6700 :: 38.2	6525 :: 37.2	6197 :: 35.3
T021	7286 :: 41.6	6965 :: 39.7	6675 :: 38.1	6502 :: 37.1	6178 :: 35.2
T022	7853 :: 44.8	7451 :: 42.5	7088 :: 40.4	6871 :: 39.2	6464 :: 36.9
T023	7323 :: 41.8	6999 :: 39.9	6708 :: 38.3	6533 :: 37.3	6206 :: 35.4
T024	7464 :: 42.6	7126 :: 40.6	6822 :: 38.9	6640 :: 37.9	6298 :: 35.9
T026	7280 :: 41.5	6951 :: 39.6	6655 :: 38.0	6478 :: 36.9	6145 :: 35.1
T027	7369 :: 42.0	7035 :: 40.1	6735 :: 38.4	6555 :: 37.4	6218 :: 35.5
T028	7375 :: 42.1	7039 :: 40.2	6737 :: 38.4	6556 :: 37.4	6216 :: 35.5
T029	7288 :: 41.6	6957 :: 39.7	6659 :: 38.0	6480 :: 37.0	6145 :: 35.1
T030	7194 :: 41.0	6865 :: 39.2	6570 :: 37.5	6393 :: 36.5	6062 :: 34.6
T031	7432 :: 42.4	7092 :: 40.5	6787 :: 38.7	6604 :: 37.7	6261 :: 35.7
T032	7358 :: 42.0	7031 :: 40.1	6736 :: 38.4	6560 :: 37.4	6229 :: 35.5
T033	7334 :: 41.8	6988 :: 39.9	6676 :: 38.1	6490 :: 37.0	6140 :: 35.0
T034	7417 :: 42.3	7085 :: 40.4	6786 :: 38.7	6607 :: 37.7	6271 :: 35.8
T035	7338 :: 41.9	6998 :: 39.9	6692 :: 38.2	6509 :: 37.1	6165 :: 35.2
T036	7427 :: 42.4	7092 :: 40.5	6790 :: 38.7	6609 :: 37.7	6271 :: 35.8
T037	7357 :: 42.0	7032 :: 40.1	6740 :: 38.4	6564 :: 37.4	6236 :: 35.6
T038	7288 :: 41.6	6961 :: 39.7	6666 :: 38.0	6490 :: 37.0	6160 :: 35.1
T039	7291 :: 41.6	6969 :: 39.8	6680 :: 38.1	6507 :: 37.1	6183 :: 35.3
T040	7496 :: 42.8	7149 :: 40.8	6838 :: 39.0	6651 :: 37.9	6301 :: 35.9
T041	7358 :: 42.0	7046 :: 40.2	6764 :: 38.6	6596 :: 37.6	6280 :: 35.8
T042	7360 :: 42.0	7032 :: 40.1	6738 :: 38.4	6561 :: 37.4	6230 :: 35.5
T043	7375 :: 42.1	7049 :: 40.2	6756 :: 38.5	6581 :: 37.5	6252 :: 35.7
T044	7763 :: 44.3	7369 :: 42.0	7013 :: 40.0	6801 :: 38.8	6402 :: 36.5
T045	7581 :: 43.2	7198 :: 41.1	6853 :: 39.1	6646 :: 37.9	6259 :: 35.7
T046	7555 :: 43.1	7214 :: 41.1	6907 :: 39.4	6723 :: 38.3	6379 :: 36.4
T047	7619 :: 43.5	7268 :: 41.5	6952 :: 39.7	6763 :: 38.6	6408 :: 36.6
T048	7517 :: 42.9	7172 :: 40.9	6861 :: 39.1	6675 :: 38.1	6326 :: 36.1
T049	7389 :: 42.1	7059 :: 40.3	6763 :: 38.6	6585 :: 37.6	6252 :: 35.7
T050	7650 :: 43.6	7296 :: 41.6	6977 :: 39.8	6786 :: 38.7	6429 :: 36.7
T051	7645 :: 43.6	7289 :: 41.6	6969 :: 39.8	6778 :: 38.7	6418 :: 36.6
T052	7538 :: 43.0	7186 :: 41.0	6868 :: 39.2	6679 :: 38.1	6322 :: 36.1
T053	7595 :: 43.3	7238 :: 41.3	6917 :: 39.5	6725 :: 38.4	6364 :: 36.3
T054	7607 :: 43.4	7247 :: 41.3	6923 :: 39.5	6729 :: 38.4	6365 :: 36.3
T055	7757 :: 44.2	7387 :: 42.1	7054 :: 40.2	6855 :: 39.1	6481 :: 37.0
T056	7235 :: 41.3	6966 :: 39.7	6723 :: 38.3	6578 :: 37.5	6307 :: 36.0
T057	7383 :: 42.1	7056 :: 40.2	6761 :: 38.6	6585 :: 37.6	6254 :: 35.7
T058	7468 :: 42.6	7122 :: 40.6	6811 :: 38.8	6624 :: 37.8	6275 :: 35.8
T059	7672 :: 43.8	7281 :: 41.5	6929 :: 39.5	6718 :: 38.3	6323 :: 36.1
T060	7390 :: 42.2	7049 :: 40.2	6741 :: 38.4	6557 :: 37.4	6212 :: 35.4
T061	7415 :: 42.3	7088 :: 40.4	6794 :: 38.8	6618 :: 37.7	6288 :: 35.9
T062	7327 :: 41.8	6974 :: 39.8	6657 :: 38.0	6466 :: 36.9	6110 :: 34.8
T063	7329 :: 41.8	6973 :: 39.8	6653 :: 37.9	6461 :: 36.9	6102 :: 34.8
T065	7620 :: 43.5	7265 :: 41.4	6946 :: 39.6	6755 :: 38.5	6397 :: 36.5
T067	7335 :: 41.8	7008 :: 40.0	6713 :: 38.3	6536 :: 37.3	6205 :: 35.4

Table 15: Turbine-specific 20-year generation probability of exceedance values (P-values) for 200 Vestas V110-2.0 wind turbines at $80\,m$. (continued on next page)

ID	Net P50 (MWh :: %)	Net P75 (MWh :: %)	Net P90 (MWh :: %)	Net P95 (MWh :: %)	Net P99 (MWh :: %)
T068	7644 :: 43.6	7258 :: 41.4	6911 :: 39.4	6703 :: 38.2	6314 :: 36.0
T069	7550 :: 43.1	7175 :: 40.9	6837 :: 39.0	6635 :: 37.8	6256 :: 35.7
T071	7348 :: 41.9	7006 :: 40.0	6699 :: 38.2	6515 :: 37.2	6170 :: 35.2
T072	7351 :: 41.9	7014 :: 40.0	6711 :: 38.3	6530 :: 37.2	6189 :: 35.3
T075	7308 :: 41.7	6968 :: 39.7	6662 :: 38.0	6479 :: 37.0	6136 :: 35.0
T076	7126 :: 40.6	6796 :: 38.8	6498 :: 37.1	6320 :: 36.1	5987 :: 34.1
T077	7293 :: 41.6	6970 :: 39.8	6679 :: 38.1	6505 :: 37.1	6179 :: 35.2
T079	7257 :: 41.4	6916 :: 39.4	6609 :: 37.7	6426 :: 36.7	6082 :: 34.7
T080	7636 :: 43.6	7265 :: 41.4	6931 :: 39.5	6731 :: 38.4	6355 :: 36.3
T081	7287 :: 41.6	6959 :: 39.7	6663 :: 38.0	6486 :: 37.0	6153 :: 35.1
T082	7300 :: 41.6	6979 :: 39.8	6690 :: 38.2	6517 :: 37.2	6192 :: 35.3
T083	7625 :: 43.5	7260 :: 41.4	6932 :: 39.5	6735 :: 38.4	6367 :: 36.3
T087	7541 :: 43.0	7168 :: 40.9	6832 :: 39.0	6631 :: 37.8	6253 :: 35.7
T088	7508 :: 42.8	7140 :: 40.7	6808 :: 38.8	6610 :: 37.7	6238 :: 35.6
T089	7308 :: 41.7	6968 :: 39.7	6662 :: 38.0	6479 :: 37.0	6135 :: 35.0
T090	7199 :: 41.1	6856 :: 39.1	6548 :: 37.3	6363 :: 36.3	6016 :: 34.3
T091	7135 :: 40.7	6794 :: 38.8	6487 :: 37.0	6303 :: 36.0	5959 :: 34.0
T092	7287 :: 41.6	6958 :: 39.7	6661 :: 38.0	6484 :: 37.0	6151 :: 35.1
T093	7244 :: 41.3	6893 :: 39.3	6576 :: 37.5	6387 :: 36.4	6032 :: 34.4
T094	7263 :: 41.4	6914 :: 39.4	6600 :: 37.6	6412 :: 36.6	6060 :: 34.6
T096	7331 :: 41.8	6997 :: 39.9	6697 :: 38.2	6518 :: 37.2	6181 :: 35.3
T097	7790 :: 44.4	7408 :: 42.3	7064 :: 40.3	6859 :: 39.1	6473 :: 36.9
T098	7280 :: 41.5	6959 :: 39.7	6670 :: 38.0	6497 :: 37.1	6172 :: 35.2
T100	7475 :: 42.6	7138 :: 40.7	6835 :: 39.0	6654 :: 38.0	6313 :: 36.0
T102	7318 :: 41.7	6977 :: 39.8	6671 :: 38.1	6488 :: 37.0	6144 :: 35.0
T103	7194 :: 41.0	6848 :: 39.1	6536 :: 37.3	6349 :: 36.2	5999 :: 34.2
T107	7257 :: 41.4	6912 :: 39.4	6601 :: 37.7	6415 :: 36.6	6066 :: 34.6
T108	7241 :: 41.3	6898 :: 39.3	6589 :: 37.6	6404 :: 36.5	6057 :: 34.5
T109	7192 :: 41.0	6874 :: 39.2	6587 :: 37.6	6416 :: 36.6	6095 :: 34.8
T110	7425 :: 42.4	7079 :: 40.4	6767 :: 38.6	6580 :: 37.5	6230 :: 35.5
T111	7564 :: 43.1	7210 :: 41.1	6893 :: 39.3	6703 :: 38.2	6346 :: 36.2
T112	7525 :: 42.9	7173 :: 40.9	6856 :: 39.1	6667 :: 38.0	6311 :: 36.0
T113	7253 :: 41.4	6922 :: 39.5	6623 :: 37.8	6445 :: 36.8	6110 :: 34.9
T114	7269 :: 41.5	6944 :: 39.6	6652 :: 37.9	6477 :: 36.9	6149 :: 35.1
T115	7381 :: 42.1	7052 :: 40.2	6756 :: 38.5	6578 :: 37.5	6246 :: 35.6
T116	7370 :: 42.0	7095 :: 40.5	6847 :: 39.1	6699 :: 38.2	6421 :: 36.6
T117	7306 :: 41.7	6976 :: 39.8	6678 :: 38.1	6500 :: 37.1	6166 :: 35.2
T118	7276 :: 41.5	7019 :: 40.0	6787 :: 38.7	6648 :: 37.9	6388 :: 36.4
T121	7695 :: 43.9	7295 :: 41.6	6934 :: 39.6	6718 :: 38.3	6314 :: 36.0
T122	7271 :: 41.5	6944 :: 39.6	6650 :: 37.9	6474 :: 36.9	6144 :: 35.0
T123	7278 :: 41.5	6923 :: 39.5	6604 :: 37.7	6413 :: 36.6	6054 :: 34.5
T124	7267 :: 41.5	6922 :: 39.5	6611 :: 37.7	6425 :: 36.6	6075 :: 34.7
T125	7442 :: 42.4	7097 :: 40.5	6787 :: 38.7	6602 :: 37.7	6254 :: 35.7
T126	7709 :: 44.0	7202 :: 41.1	6746 :: 38.5	6474 :: 36.9	5962 :: 34.0
T127	7709 :: 44.0	7273 :: 41.5	6881 :: 39.2	6646 :: 37.9	6206 :: 35.4
T128	8054 :: 45.9	7532 :: 43.0	7062 :: 40.3	6780 :: 38.7	6253 :: 35.7
T129	7800 :: 44.5	7384 :: 42.1	7010 :: 40.0	6786 :: 38.7	6366 :: 36.3
T130	8063 :: 46.0	7557 :: 43.1	7102 :: 40.5	6830 :: 39.0	6319 :: 36.0

Table 15: Turbine-specific 20-year generation probability of exceedance values (P-values) for 200 Vestas V110-2.0 wind turbines at $80\,m$. (continued on next page)

ID	Net P50 (MWh :: %)	Net P75 (MWh :: %)	Net P90 (MWh :: %)	Net P95 (MWh :: %)	Net P99 (MWh :: %)
T131	7884 :: 45.0	7360 :: 42.0	6889 :: 39.3	6606 :: 37.7	6077 :: 34.7
T132	7872 :: 44.9	7445 :: 42.5	7060 :: 40.3	6830 :: 39.0	6399 :: 36.5
T133	8112 :: 46.3	7588 :: 43.3	7117 :: 40.6	6835 :: 39.0	6306 :: 36.0
T134	7843 :: 44.7	7355 :: 42.0	6916 :: 39.4	6653 :: 37.9	6160 :: 35.1
T135	7762 :: 44.3	7273 :: 41.5	6832 :: 39.0	6569 :: 37.5	6074 :: 34.6
T136	7752 :: 44.2	7257 :: 41.4	6812 :: 38.9	6545 :: 37.3	6045 :: 34.5
T137	7714 :: 44.0	7227 :: 41.2	6788 :: 38.7	6526 :: 37.2	6033 :: 34.4
T138	7705 :: 43.9	7284 :: 41.5	6905 :: 39.4	6678 :: 38.1	6253 :: 35.7
T139	7815 :: 44.6	7363 :: 42.0	6956 :: 39.7	6713 :: 38.3	6257 :: 35.7
T140	7867 :: 44.9	7444 :: 42.5	7063 :: 40.3	6835 :: 39.0	6408 :: 36.5
T141	7850 :: 44.8	7379 :: 42.1	6954 :: 39.7	6700 :: 38.2	6224 :: 35.5
T142	7675 :: 43.8	7252 :: 41.4	6872 :: 39.2	6644 :: 37.9	6217 :: 35.5
T143	7899 :: 45.1	7481 :: 42.7	7104 :: 40.5	6879 :: 39.2	6456 :: 36.8
T144	7700 :: 43.9	7229 :: 41.2	6805 :: 38.8	6552 :: 37.4	6076 :: 34.7
T145	7633 :: 43.5	7195 :: 41.0	6801 :: 38.8	6565 :: 37.4	6123 :: 34.9
T146	7735 :: 44.1	7294 :: 41.6	6898 :: 39.3	6660 :: 38.0	6215 :: 35.4
T147	7722 :: 44.0	7223 :: 41.2	6773 :: 38.6	6504 :: 37.1	5999 :: 34.2
T148	7838 :: 44.7	7355 :: 42.0	6921 :: 39.5	6661 :: 38.0	6173 :: 35.2
T149	7701 :: 43.9	7268 :: 41.5	6879 :: 39.2	6646 :: 37.9	6208 :: 35.4
T150	7745 :: 44.2	7233 :: 41.3	6773 :: 38.6	6497 :: 37.1	5980 :: 34.1
T151	7675 :: 43.8	7248 :: 41.3	6864 :: 39.2	6634 :: 37.8	6203 :: 35.4
T152	7724 :: 44.1	7241 :: 41.3	6807 :: 38.8	6546 :: 37.3	6059 :: 34.6
T153	7803 :: 44.5	7340 :: 41.9	6924 :: 39.5	6674 :: 38.1	6207 :: 35.4
T154	7858 :: 44.8	7399 :: 42.2	6985 :: 39.8	6737 :: 38.4	6272 :: 35.8
T155	7745 :: 44.2	7271 :: 41.5	6843 :: 39.0	6588 :: 37.6	6108 :: 34.8
T156	7775 :: 44.3	7294 :: 41.6	6862 :: 39.1	6603 :: 37.7	6117 :: 34.9
T157	7744 :: 44.2	7310 :: 41.7	6919 :: 39.5	6686 :: 38.1	6247 :: 35.6
T158	7652 :: 43.6	7190 :: 41.0	6774 :: 38.6	6525 :: 37.2	6058 :: 34.6
T159	7673 :: 43.8	7217 :: 41.2	6807 :: 38.8	6562 :: 37.4	6102 :: 34.8
T160	7666 :: 43.7	7166 :: 40.9	6716 :: 38.3	6446 :: 36.8	5941 :: 33.9
T161	7592 :: 43.3	7145 :: 40.8	6742 :: 38.5	6502 :: 37.1	6050 :: 34.5
T162	7900 :: 45.1	7371 :: 42.0	6895 :: 39.3	6610 :: 37.7	6075 :: 34.7
T163	7812 :: 44.6	7337 :: 41.8	6909 :: 39.4	6654 :: 38.0	6173 :: 35.2
T164	7806 :: 44.5	7309 :: 41.7	6862 :: 39.1	6595 :: 37.6	6093 :: 34.8
T165	7725 :: 44.1	7246 :: 41.3	6815 :: 38.9	6557 :: 37.4	6073 :: 34.6
T166	7682 :: 43.8	7172 :: 40.9	6713 :: 38.3	6439 :: 36.7	5924 :: 33.8
T167	7707 :: 44.0	7239 :: 41.3	6818 :: 38.9	6565 :: 37.4	6092 :: 34.8
T168	7658 :: 43.7	7189 :: 41.0	6766 :: 38.6	6513 :: 37.1	6038 :: 34.4
T169	7664 :: 43.7	7184 :: 41.0	6751 :: 38.5	6492 :: 37.0	6006 :: 34.3
T170	7788 :: 44.4	7267 :: 41.4	6798 :: 38.8	6517 :: 37.2	5991 :: 34.2
T171	7582 :: 43.2	7128 :: 40.7	6719 :: 38.3	6474 :: 36.9	6016 :: 34.3
T172	7812 :: 44.6	7310 :: 41.7	6858 :: 39.1	6588 :: 37.6	6081 :: 34.7
T174	7475 :: 42.6	7032 :: 40.1	6633 :: 37.8	6394 :: 36.5	5946 :: 33.9
T175	7872 :: 44.9	7340 :: 41.9	6862 :: 39.1	6576 :: 37.5	6039 :: 34.4
T176	7574 :: 43.2	7130 :: 40.7	6731 :: 38.4	6492 :: 37.0	6044 :: 34.5
T177	7701 :: 43.9	7287 :: 41.6	6913 :: 39.4	6690 :: 38.2	6271 :: 35.8
T178	7773 :: 44.3	7285 :: 41.6	6846 :: 39.1	6584 :: 37.6	6091 :: 34.7
T179	7818 :: 44.6	7408 :: 42.3	7039 :: 40.1	6818 :: 38.9	6404 :: 36.5

Table 15: Turbine-specific 20-year generation probability of exceedance values (P-values) for 200 Vestas V110-2.0 wind turbines at $80\,m$. (continued on next page)

ID	Net P50 (MWh :: %)	Net P75 (MWh :: %)	Net P90 (MWh :: %)	Net P95 (MWh :: %)	Net P99 (MWh :: %)
T180	7643 :: 43.6	7170 :: 40.9	6744 :: 38.5	6489 :: 37.0	6011 :: 34.3
T181	7506 :: 42.8	7165 :: 40.9	6859 :: 39.1	6675 :: 38.1	6331 :: 36.1
T182	7350 :: 41.9	7026 :: 40.1	6734 :: 38.4	6560 :: 37.4	6232 :: 35.5
T183	7369 :: 42.0	7043 :: 40.2	6750 :: 38.5	6575 :: 37.5	6246 :: 35.6
T184	7341 :: 41.9	7002 :: 39.9	6697 :: 38.2	6515 :: 37.2	6173 :: 35.2
T185	7273 :: 41.5	6953 :: 39.7	6665 :: 38.0	6492 :: 37.0	6169 :: 35.2
T186	7334 :: 41.8	7011 :: 40.0	6721 :: 38.3	6547 :: 37.3	6221 :: 35.5
T187	7396 :: 42.2	7063 :: 40.3	6764 :: 38.6	6585 :: 37.6	6249 :: 35.6
T188	7405 :: 42.2	7067 :: 40.3	6764 :: 38.6	6582 :: 37.5	6241 :: 35.6
T190	7510 :: 42.8	7134 :: 40.7	6796 :: 38.8	6593 :: 37.6	6213 :: 35.4
T191	7338 :: 41.9	7005 :: 40.0	6705 :: 38.2	6526 :: 37.2	6189 :: 35.3
T192	7316 :: 41.7	6975 :: 39.8	6667 :: 38.0	6483 :: 37.0	6138 :: 35.0
T194	7652 :: 43.6	7188 :: 41.0	6771 :: 38.6	6521 :: 37.2	6053 :: 34.5
T195	7511 :: 42.8	7060 :: 40.3	6654 :: 38.0	6411 :: 36.6	5955 :: 34.0
T196	7544 :: 43.0	7110 :: 40.6	6719 :: 38.3	6485 :: 37.0	6047 :: 34.5
T197	7742 :: 44.2	7240 :: 41.3	6787 :: 38.7	6517 :: 37.2	6009 :: 34.3
T198	7520 :: 42.9	7065 :: 40.3	6656 :: 38.0	6411 :: 36.6	5951 :: 33.9
T199	7753 :: 44.2	7245 :: 41.3	6789 :: 38.7	6516 :: 37.2	6003 :: 34.2
T200	7515 :: 42.9	7056 :: 40.2	6643 :: 37.9	6396 :: 36.5	5933 :: 33.8
T201	7296 :: 41.6	6971 :: 39.8	6679 :: 38.1	6505 :: 37.1	6177 :: 35.2
T203	7296 :: 41.6	6970 :: 39.8	6676 :: 38.1	6500 :: 37.1	6170 :: 35.2
T206	7411 :: 42.3	7068 :: 40.3	6760 :: 38.6	6575 :: 37.5	6228 :: 35.5
T211	7234 :: 41.3	6914 :: 39.4	6626 :: 37.8	6453 :: 36.8	6129 :: 35.0
T212	7188 :: 41.0	6907 :: 39.4	6654 :: 38.0	6503 :: 37.1	6219 :: 35.5
T214	7200 :: 41.1	6874 :: 39.2	6581 :: 37.5	6406 :: 36.5	6077 :: 34.7
T216	7299 :: 41.6	6965 :: 39.7	6664 :: 38.0	6484 :: 37.0	6146 :: 35.1
T217	7276 :: 41.5	6942 :: 39.6	6643 :: 37.9	6463 :: 36.9	6126 :: 34.9
T218	7273 :: 41.5	6946 :: 39.6	6651 :: 37.9	6475 :: 36.9	6144 :: 35.0
T220	7347 :: 41.9	7016 :: 40.0	6719 :: 38.3	6541 :: 37.3	6207 :: 35.4
T221	7234 :: 41.3	6907 :: 39.4	6614 :: 37.7	6438 :: 36.7	6108 :: 34.8
T222	7174 :: 40.9	6848 :: 39.1	6555 :: 37.4	6379 :: 36.4	6050 :: 34.5
T223	7224 :: 41.2	6896 :: 39.3	6601 :: 37.6	6424 :: 36.6	6092 :: 34.7
T224	7217 :: 41.2	6888 :: 39.3	6592 :: 37.6	6415 :: 36.6	6082 :: 34.7
T225	7220 :: 41.2	6890 :: 39.3	6593 :: 37.6	6415 :: 36.6	6082 :: 34.7
T226	7214 :: 41.2	6875 :: 39.2	6570 :: 37.5	6387 :: 36.4	6044 :: 34.5
T227	7350 :: 41.9	7023 :: 40.1	6728 :: 38.4	6552 :: 37.4	6222 :: 35.5
T228	7342 :: 41.9	7009 :: 40.0	6709 :: 38.3	6530 :: 37.2	6194 :: 35.3
T240	7272 :: 41.5	6931 :: 39.5	6624 :: 37.8	6441 :: 36.7	6096 :: 34.8
T245	7255 :: 41.4	6906 :: 39.4	6593 :: 37.6	6405 :: 36.5	6053 :: 34.5
T246	7148 :: 40.8	6805 :: 38.8	6496 :: 37.1	6312 :: 36.0	5965 :: 34.0
T250	7304 :: 41.7	6974 :: 39.8	6677 :: 38.1	6499 :: 37.1	6165 :: 35.2
T251	7210 :: 41.1	6884 :: 39.3	6590 :: 37.6	6414 :: 36.6	6084 :: 34.7

Table 15: Turbine-specific 20-year generation probability of exceedance values (P-values) for 200 Vestas V110-2.0 wind turbines at 80 m.

11 APPENDIX GROSS LONG-TERM VARIABILITY

11.1 Summary

This section provides a retrospective analysis of the past 36 years of wind speed and power at the Rush Creek I location. These data were derived from a mesoscale Numerical Weather Prediction (NWP) model that has been statistically calibrated to match the observed data during the measurement period at each meteorological tower for which data were provided (Towers M2301 and M2327). Due to long-term climate variability and/or change the historic distributions of wind and power capacity described here may not be indicative of future conditions.

Based on the results of 3TIER's Energy Risk Framework, the last 36 years (January, 1980 – December, 2015) of data have been utilized for estimating the expected future generation at Rush Creek I. The average MOS-corrected simulated wind speed at hub height ($80\,m$) during the past 36 years of record (January, 1980 – December, 2015) across all 200 turbines is $\mathbf{8.27}\,\boldsymbol{m/s}$. The average MOS-corrected simulated gross power capacity at hub height during the past 36 years across all 200 turbines is $\mathbf{54.5\%}$. A map of average MOS-corrected gross power capacity values across the Rush Creek I project area using the power curve for the Vestas V110-2.0 wind turbines is displayed in Power Capacity Maps.

All power capacities presented in this section are gross power capacities.

11.2 Power Capacity Maps

This section contains a map of MOS-corrected long-term mean gross power capacity values across the Rush Creek I project area for each turbine model and hub height.

11.2.1 Vestas V110-2.0 at 80 m

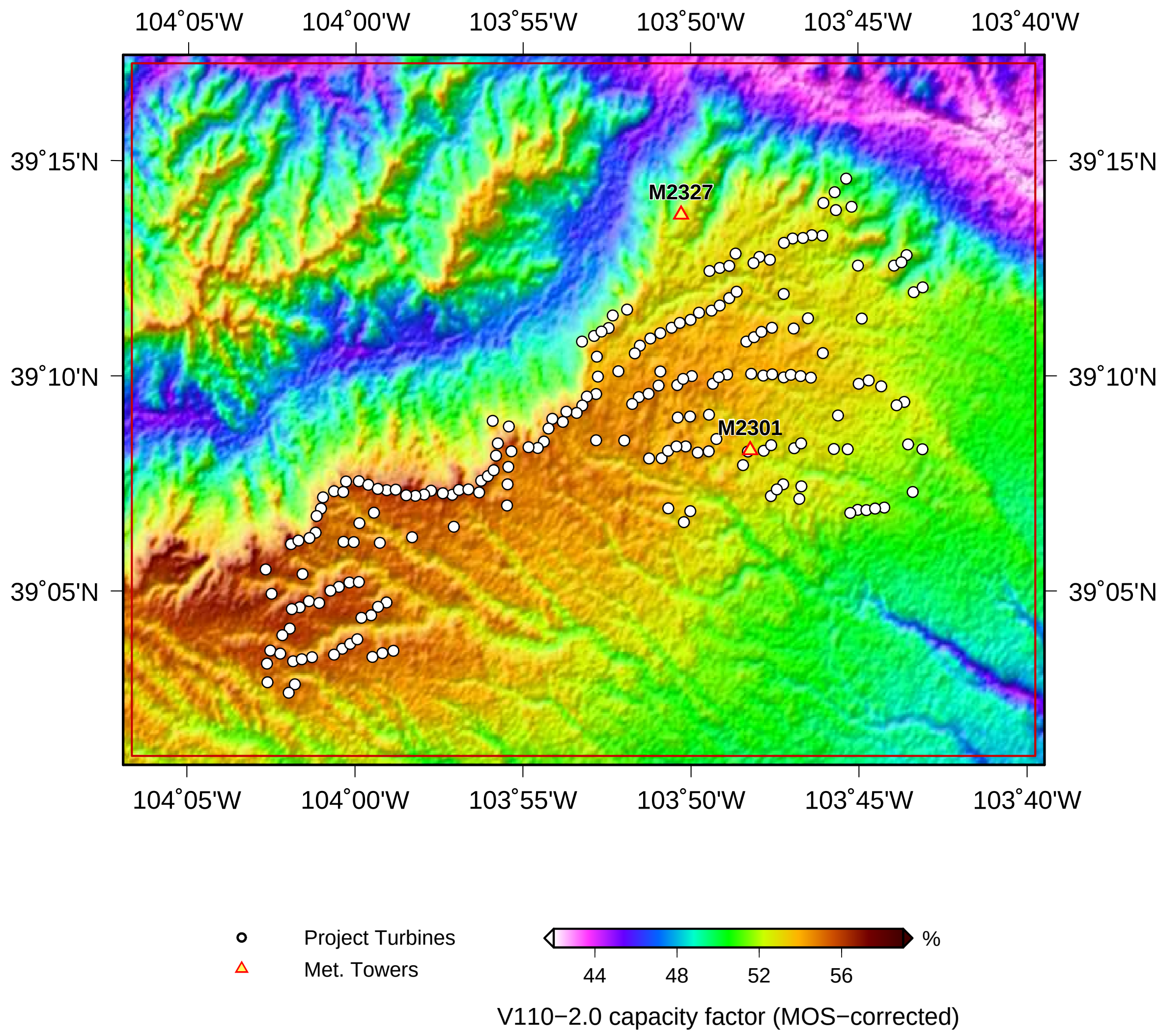

Figure 14: 36-year mean capacity factor at 80 m.

11.3 Model Simulations By 3TIER

The assessment of the wind resource across the Rush Creek I project presented in this section is based on 36 years of simulated data (January, 1980 – December, 2015) using a numerical weather prediction (NWP) model of the atmosphere.

The 36-year simulated data set is constructed from two separate model runs:

1. a 1-year, $500\,m$ resolution simulation (where the year of each calendar day is chosen sequentially from the last 10 years (2005 – 2014)), and
2. a 36-year continuous $4.5\,km$ resolution simulation.

The NWP model represents atmospheric processes in the boundary layer, including the roughness of the underlying terrain or water, stability within the boundary layer, heat and moisture fluxes into the atmosphere, wind shear, and turbulence within the boundary layer. The model outputs winds at fixed vertical levels, and there are 6 such levels in the lowest $600\,m$ of the atmosphere. To determine winds at specific hub heights, model data are interpolated between fixed vertical levels using "power-law interpolation". This process essentially uses the standard power-law shear formula, where the shear exponent is determined exactly from the winds at the two bracketing levels, rather than assuming a fixed shear exponent.

3TIER configured the NWP model using nested grids to simulate the wind resource over the Rush Creek I region. Some details of the NWP configuration are shown below in Table 16. The extent of the coarsest grid was selected to capture the effect of synoptic weather events on the wind resource at the site, as well as to allow the model to develop regional, thermally-driven circulations. The increasingly fine $40.5\,km$, $13.5\,km$, $4.5\,km$, $1.5\,km$ and $500\,m$ grids were selected to model the effect of local terrain and local scale atmospheric circulations.

After the NWP model simulations finished, a Time-Varying Microscale (TVM) model was employed to downscale the $500\,m$ horizontal resolution NWP model output to the final $90\,m$ horizontal resolution. All deliverables and model data shown in this section are derived from the $90\,m$ resolution model grids. A map of the $90\,m$ TVM grid is shown in Figure 15.

Based on a comparison of the NWP output with observations from each meteorological tower for which data were provided (Towers M2301 and M2327), a linear statistical model was constructed to remove the bias and adjust the variance of the raw NWP simulated winds.

Parameter	Value
Mesoscale numerical weather prediction model	WRF
Horizontal resolution of valid study area	$500\,m$
Final downscaled horizontal resolution	$90\,m$
Number of vertical levels	31
Elevation database	3 second SRTM
Vegetation database	10 second ESA Globcover
Surface parameterization	Monin-Obukhov similarity model
Boundary layer parameterization	YSU model (MRF with entrainment)
Land surface scheme	4-layer Noah-Land Surface Model

Table 16: Numerical weather prediction model configuration

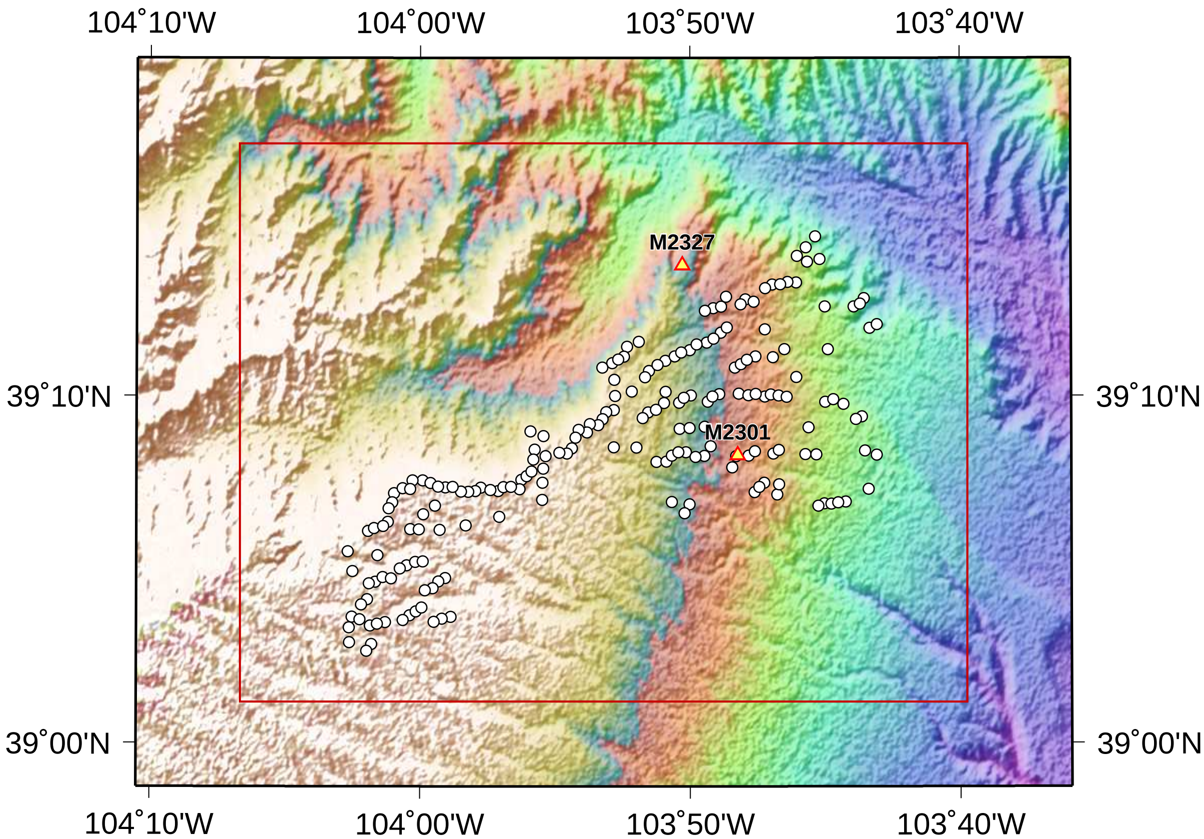

Figure 15: Map of the $90\,m$ resolution NWP model domain. The bold red box marks the boundary of the valid study area. The yellow triangles denote locations of meteorological towers and white dots indicate wind turbines.

11.4 Project-average Long-term Wind Resource Assessment

11.4.1 Monthly-mean Variability of Wind Speed

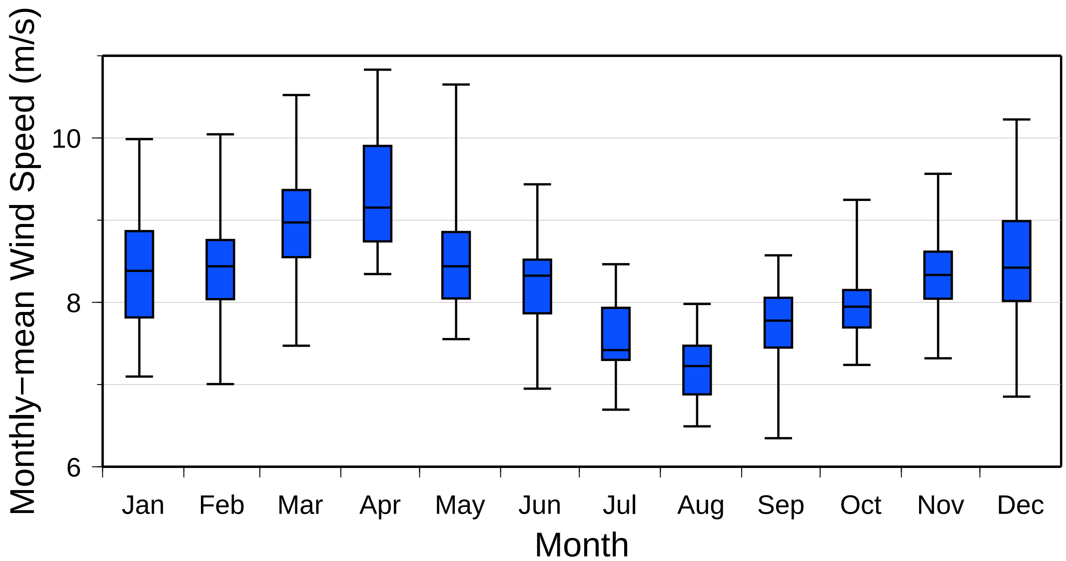

Figure 16: Box-and-whisker plot of monthly-mean project-average wind speed. This figure displays the expected variability of monthly-mean project-average wind speeds. Median wind speed denoted by solid line within the shaded box. Upper and lower boundaries of the shaded box correspond to the 75% and 25% quartiles, while the whiskers denote the maximum and minimum monthly-mean wind speeds.

11.4.2 Annual-mean Variability of Wind Speed

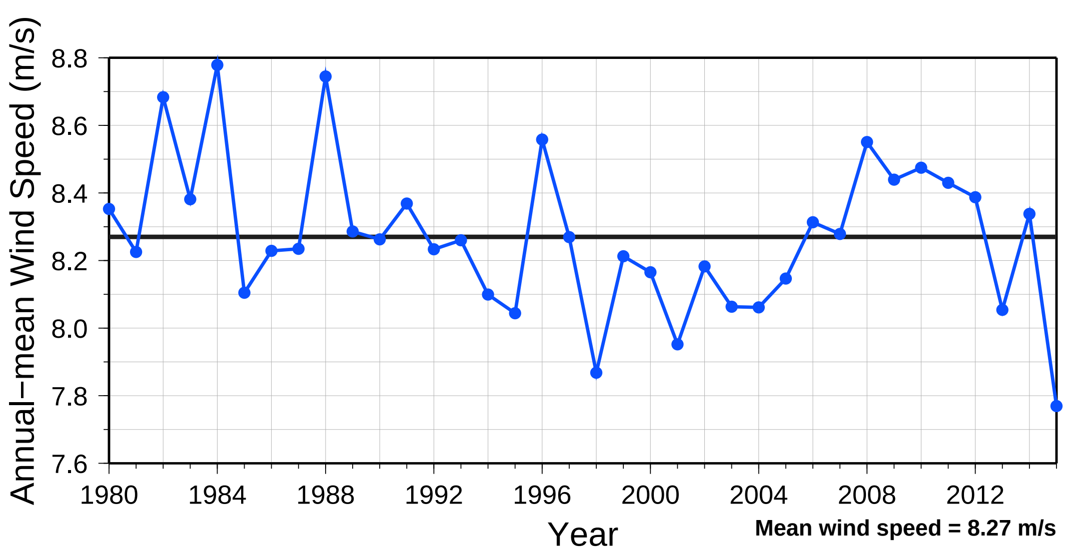

Figure 17: Time series of annual-mean project-average wind speed. Black line denotes the long-term mean.

11.4.3 Wind Speed Distribution

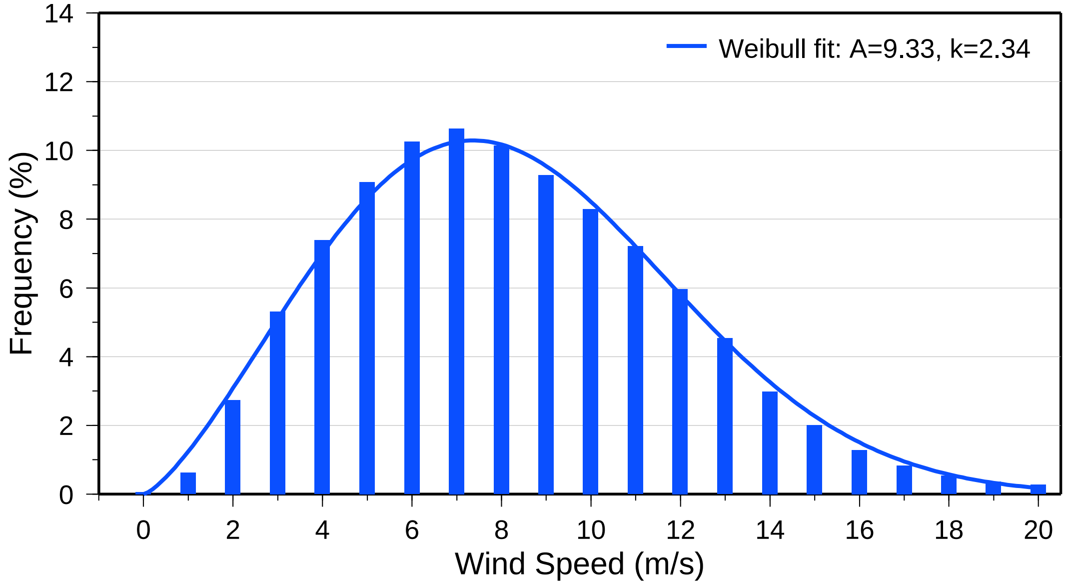

Figure 18: Hourly distribution of simulated project-average wind speed using $1\,m/s$ bins. ($0\,m/s$ bin contains only values ≤ 0.5.) Weibull distribution is also shown with the scale (A) and shape (k) parameters listed in the legend.

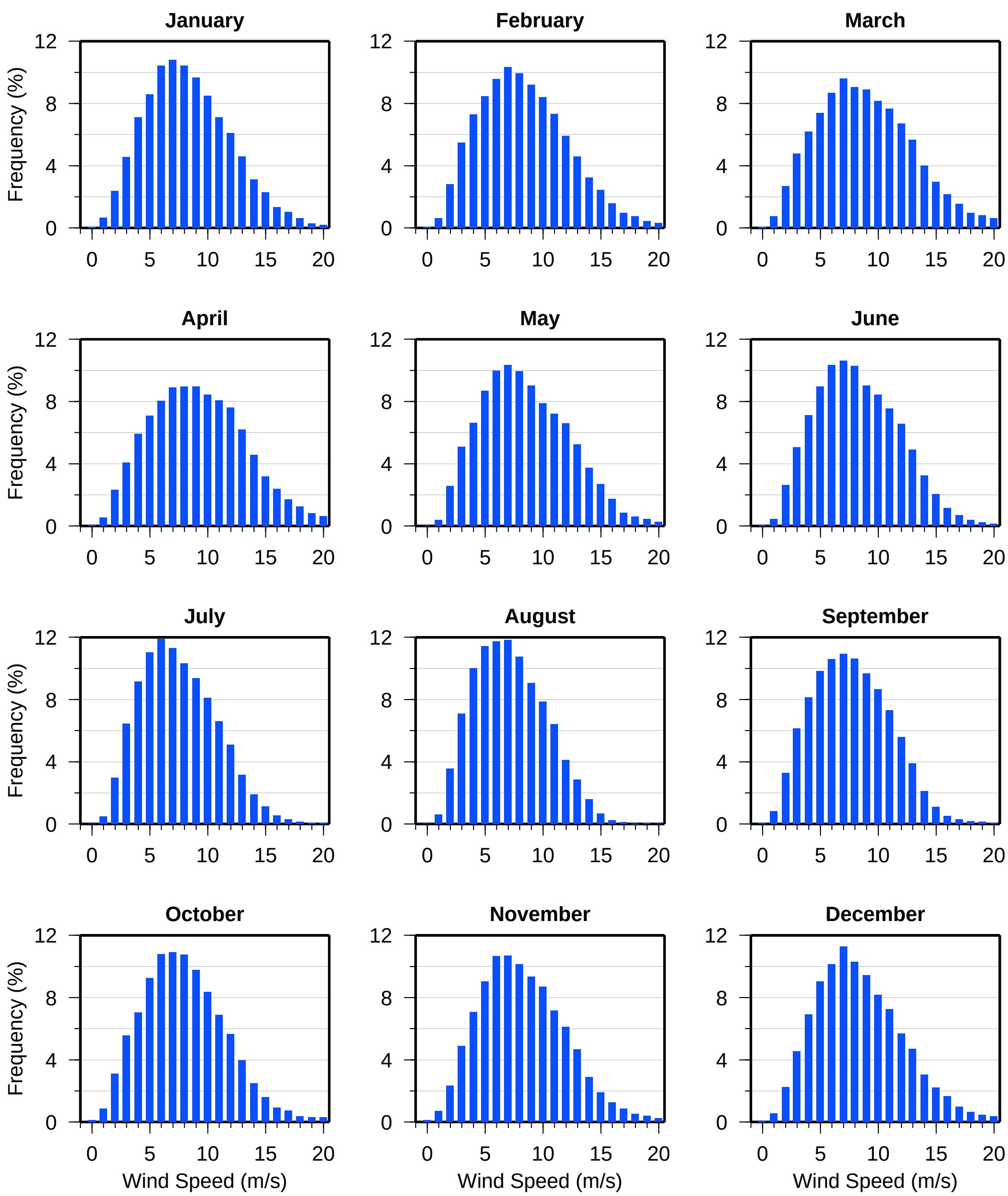

Figure 19: Hourly distribution of simulated project-average wind speed using $1\,m/s$ bins for each calendar month. ($0\,m/s$ bin contains only values ≤ 0.5.)

11.4.4 Wind Direction Distribution

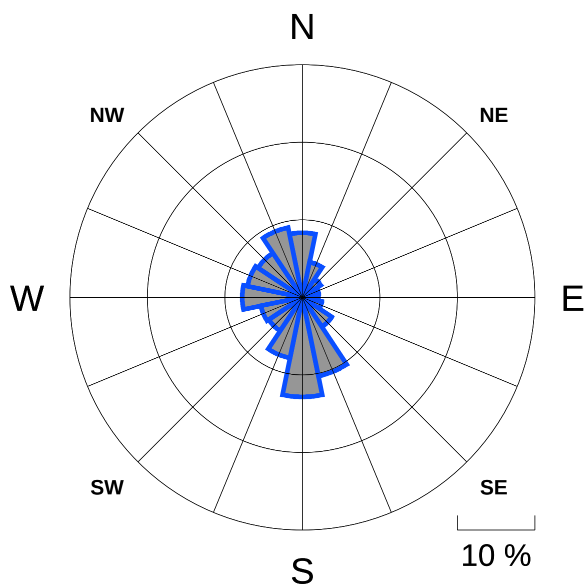

Figure 20: Annual wind rose of the hourly-mean project-average wind direction time series. Directional bins are 22.5° wide, and the radial contour interval is 10%.

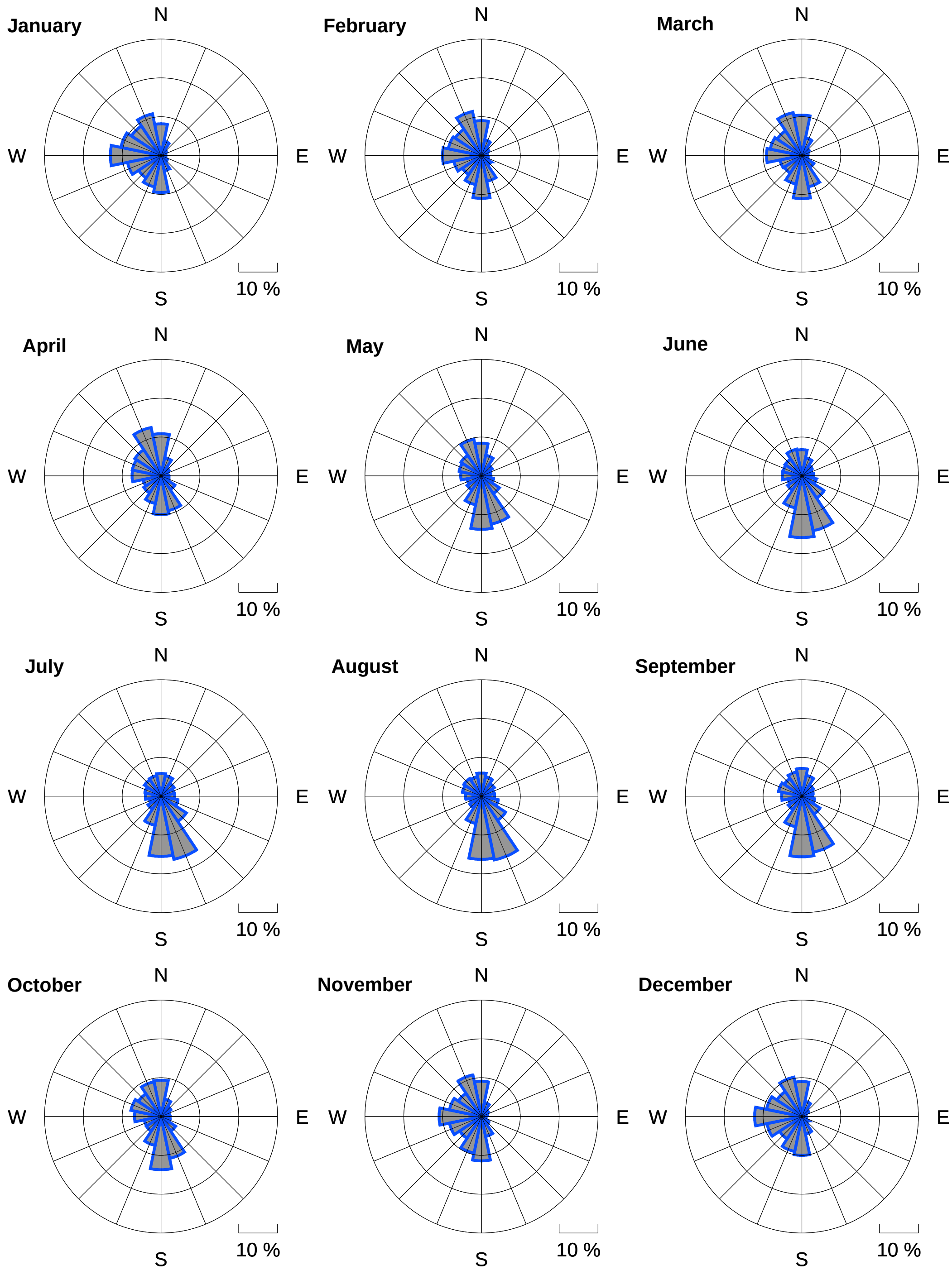

Figure 21: Wind roses of the hourly-mean project-average wind direction time series for each calendar month. Directional bins are 22.5° wide, and the radial contour interval is 10%.

11.4.5 Diurnal Variability of Wind Speed

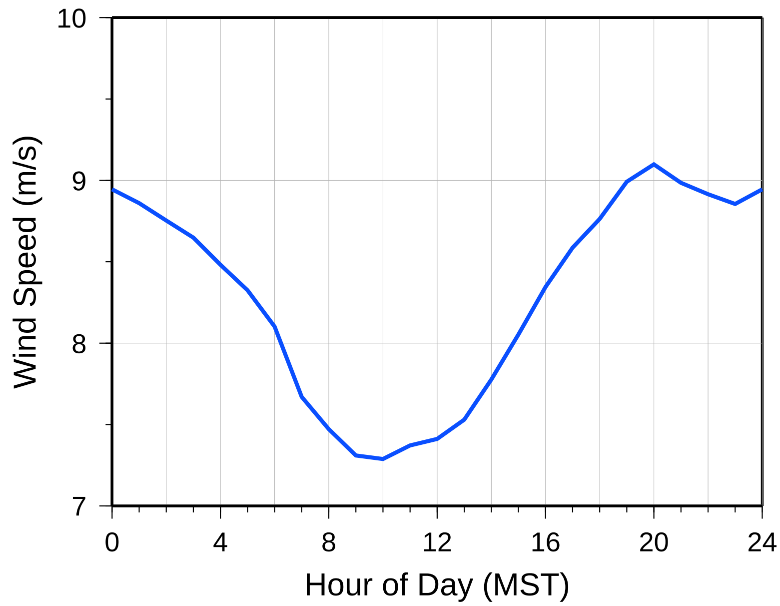

Figure 22: Diurnal cycle of simulated project-average wind speed. The horizontal axis is Mountain Standard Time (MST).

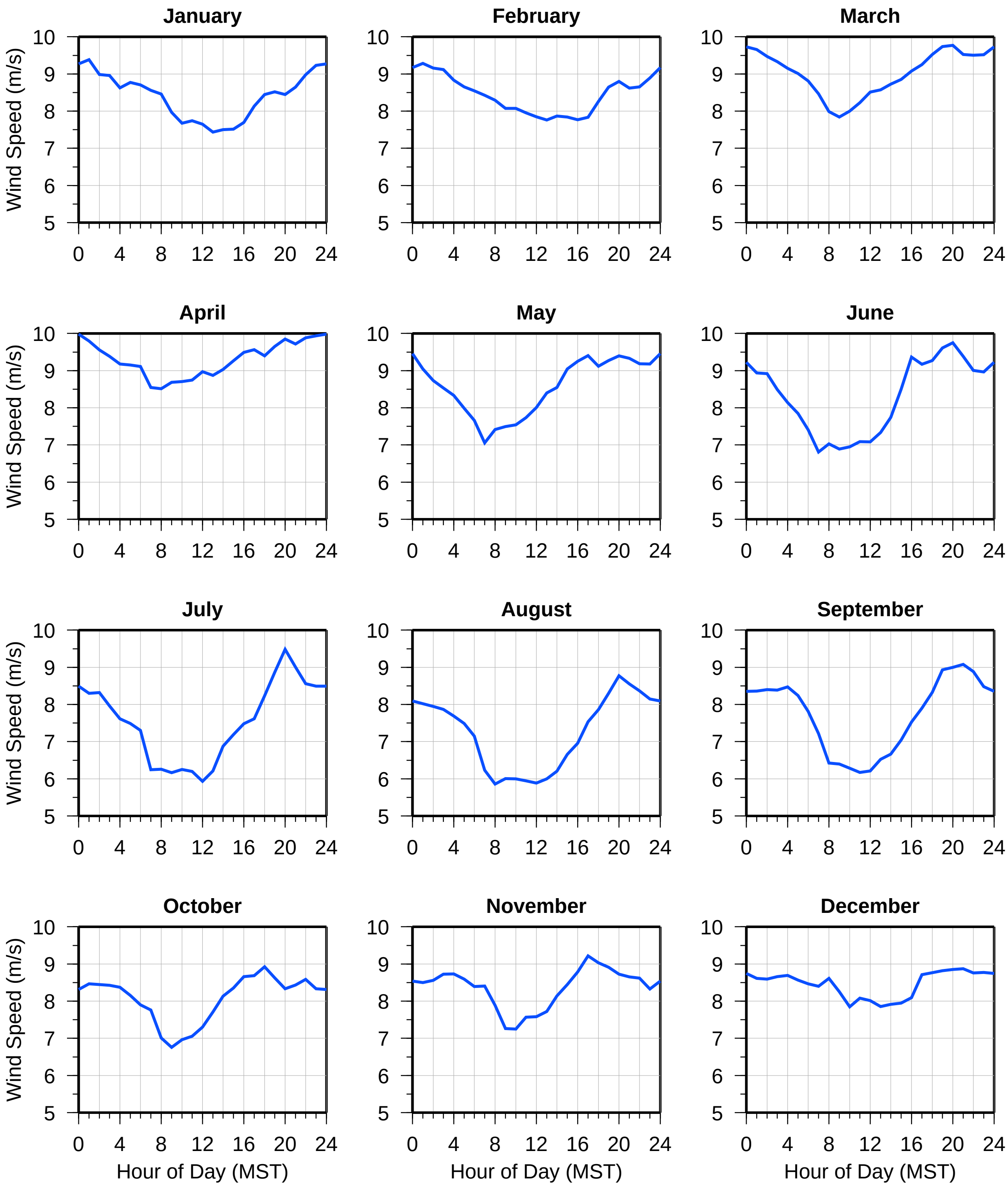

Figure 23: Diurnal cycle of simulated project-average wind speed for each calendar month. The horizontal axis is Mountain Standard Time (MST).

11.4.6 Wind Speed Variability and ENSO

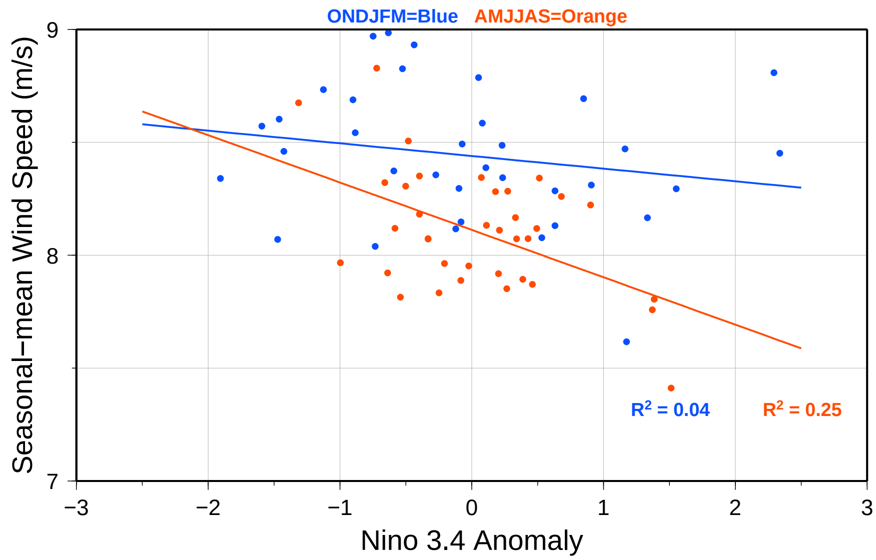

Figure 24: Scatter plot of Niño 3.4 anomalies vs. 6-month seasonal-mean project-average wind speed. Blue dots denote the mean during ONDJFM (October, November, December, January, February, and March); orange dots denote the mean during AMJJAS (April, May, June, July, August and September).

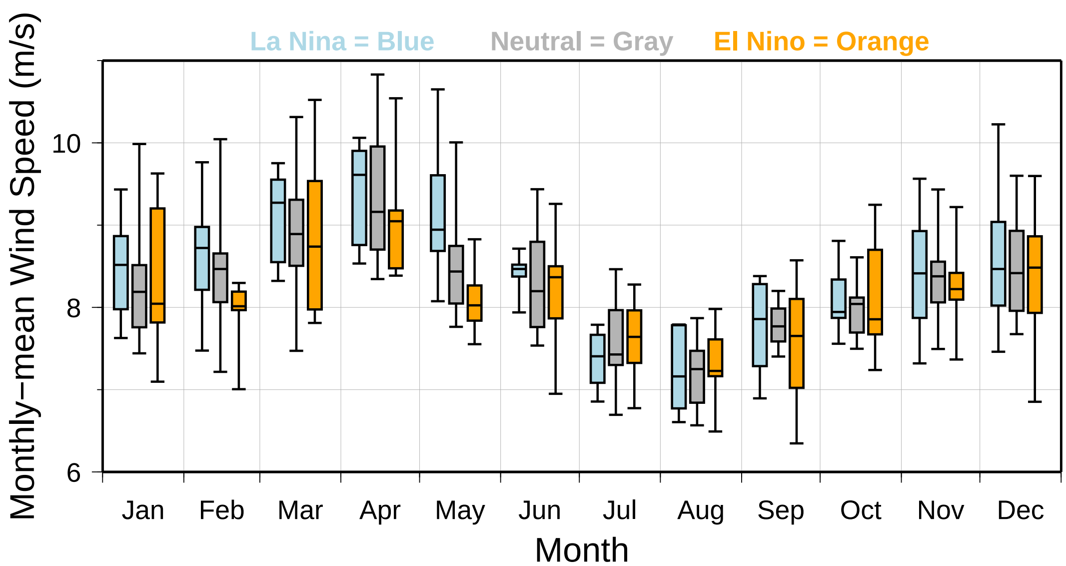

Figure 25: Box-and-whisker plot of monthly-mean project-average wind speed for La Niña (blue), neutral (gray), and El Niño (orange) phases of ENSO. Median wind speed denoted by solid line within the shaded box. Upper and lower boundaries of the shaded box correspond to the 75% and 25% quartiles, while the whiskers denote the maximum and minimum wind speeds.

11.4.7 Tabular Data

Hour of Day (MST)	Jan	Feb	Mar	Apr	May	Jun	Jly	Aug	Sep	Oct	Nov	Dec	Avg
0	9.27	9.17	9.73	9.98	9.46	9.22	8.49	8.09	8.35	8.31	8.54	8.75	8.95
1	9.39	9.28	9.66	9.80	9.04	8.94	8.30	8.02	8.36	8.47	8.50	8.61	8.86
2	8.99	9.16	9.47	9.56	8.74	8.92	8.32	7.95	8.40	8.44	8.56	8.59	8.75
3	8.96	9.12	9.33	9.38	8.53	8.49	7.96	7.87	8.38	8.43	8.72	8.66	8.65
4	8.63	8.83	9.15	9.18	8.33	8.14	7.62	7.69	8.47	8.37	8.74	8.69	8.48
5	8.77	8.65	9.01	9.15	7.99	7.85	7.49	7.49	8.24	8.15	8.59	8.57	8.33
6	8.70	8.55	8.81	9.11	7.66	7.41	7.30	7.15	7.81	7.90	8.39	8.47	8.10
7	8.56	8.43	8.46	8.55	7.06	6.81	6.24	6.23	7.22	7.76	8.40	8.40	7.67
8	8.46	8.29	7.99	8.52	7.41	7.03	6.25	5.86	6.43	7.01	7.88	8.61	7.47
9	7.97	8.07	7.84	8.68	7.49	6.89	6.17	6.00	6.39	6.75	7.26	8.26	7.31
10	7.67	8.08	8.00	8.70	7.54	6.95	6.25	6.00	6.29	6.96	7.25	7.85	7.29
11	7.74	7.96	8.23	8.75	7.74	7.09	6.19	5.95	6.17	7.06	7.57	8.08	7.37
12	7.65	7.85	8.51	8.97	8.00	7.08	5.93	5.89	6.21	7.30	7.58	8.01	7.41
13	7.44	7.76	8.58	8.87	8.40	7.33	6.21	6.00	6.52	7.71	7.72	7.85	7.53
14	7.50	7.87	8.73	9.03	8.54	7.74	6.87	6.20	6.66	8.13	8.14	7.91	7.78
15	7.51	7.84	8.85	9.26	9.04	8.50	7.19	6.66	7.04	8.35	8.45	7.95	8.05
16	7.69	7.77	9.08	9.49	9.25	9.37	7.48	6.96	7.53	8.66	8.78	8.09	8.34
17	8.19	7.80	9.17	9.61	9.41	9.18	7.67	7.50	7.91	8.65	9.19	8.75	8.59
18	8.49	8.21	9.45	9.46	9.12	9.26	8.27	7.85	8.34	8.88	9.01	8.81	8.76
19	8.55	8.60	9.69	9.71	9.23	9.63	8.92	8.28	8.96	8.58	8.88	8.87	8.99
20	8.47	8.73	9.74	9.90	9.38	9.74	9.53	8.77	9.04	8.29	8.68	8.91	9.10
21	8.66	8.57	9.49	9.76	9.33	9.38	9.03	8.54	9.11	8.40	8.60	8.93	8.99
22	9.00	8.61	9.48	9.91	9.19	9.01	8.58	8.35	8.91	8.57	8.58	8.80	8.92
23	9.26	8.86	9.49	9.96	9.20	8.95	8.52	8.14	8.48	8.33	8.30	8.79	8.85
Avg	8.40	8.42	9.00	9.30	8.55	8.29	7.53	7.23	7.72	8.06	8.35	8.47	8.27

Wind Speed (m/s): 5.5 6.0 6.5 7.0 7.5 8.0 8.5 9.0 9.5 10.0

Figure 26: Hourly-mean values of simulated project-average wind speed. Vertical axis is local time.

Year	Jan	Feb	Mar	Apr	May	Jun	Jly	Aug	Sep	Oct	Nov	Dec	Avg
1980	9.20	7.93	9.92	8.86	8.75	8.89	7.46	7.87	7.87	7.54	7.49	8.42	8.35
1981	7.46	8.98	8.81	8.70	9.10	8.33	7.99	6.77	7.53	8.10	8.43	8.56	8.23
1982	9.99	8.04	9.60	10.16	7.80	8.46	7.93	6.88	8.10	9.17	8.42	9.60	8.68
1983	8.56	8.19	8.90	9.15	8.83	7.50	7.97	6.87	8.12	7.89	9.56	9.04	8.38
1984	7.98	10.05	9.31	10.83	8.58	8.47	8.00	7.38	7.77	8.34	9.37	9.39	8.78
1985	7.63	7.91	9.75	8.76	8.08	7.94	7.08	7.47	8.20	7.94	8.56	7.96	8.10
1986	8.75	8.49	8.55	9.92	8.38	8.32	7.41	7.69	8.34	7.85	8.27	6.85	8.23
1987	9.34	7.99	10.52	9.05	8.09	7.87	8.28	7.20	6.35	7.24	8.10	8.73	8.23
1988	9.63	8.50	9.97	9.16	10.65	8.37	7.79	7.79	8.28	7.56	8.78	8.42	8.74
1989	8.53	7.47	9.27	8.53	9.02	8.25	8.38	7.80	7.95	8.12	8.35	7.68	8.29
1990	9.34	8.41	7.88	8.59	8.90	9.30	7.39	7.17	7.45	8.05	8.50	8.21	8.26
1991	7.76	8.08	10.31	8.77	9.82	9.26	7.04	7.16	7.99	7.67	8.48	8.08	8.37
1992	9.26	8.30	7.97	8.47	8.45	7.76	7.30	7.19	8.06	8.03	8.41	9.60	8.23
1993	8.32	8.07	9.08	9.18	7.84	8.50	8.46	7.11	7.62	7.50	8.32	9.12	8.26
1994	8.19	8.76	8.44	8.41	8.46	7.87	7.43	7.25	7.69	7.96	9.22	7.60	8.10
1995	8.12	8.04	8.93	8.34	8.86	8.23	7.46	6.83	7.29	8.71	8.03	7.69	8.04
1996	9.43	8.20	9.19	9.72	8.66	7.68	7.23	7.29	7.84	8.55	8.63	10.22	8.56
1997	8.52	8.65	9.01	8.68	7.96	8.37	8.03	6.49	7.02	9.25	8.22	9.03	8.27
1998	7.61	7.97	8.63	8.39	8.27	8.71	6.85	6.88	7.78	7.87	8.05	7.46	7.87
1999	8.51	9.56	9.31	9.57	8.87	8.46	7.41	6.60	6.89	7.69	7.32	8.47	8.21
2000	7.66	8.88	8.40	9.65	8.69	8.52	7.35	6.57	7.93	7.90	7.87	8.64	8.17
2001	8.13	8.21	7.47	9.69	8.17	7.77	7.01	7.28	7.40	8.15	7.92	8.26	7.95
2002	8.51	9.26	8.85	9.04	8.42	8.30	7.96	7.82	8.02	7.69	7.37	7.06	8.18
2003	7.59	7.26	8.74	9.97	7.85	7.61	7.33	7.46	7.49	7.87	8.62	8.93	8.06
2004	7.44	8.54	8.66	8.67	8.44	7.82	6.70	7.17	8.57	8.65	8.22	7.93	8.06
2005	7.96	7.22	8.49	9.98	8.05	8.20	8.09	6.58	7.77	7.93	9.43	8.07	8.15
2006	9.20	8.77	9.55	9.65	7.76	8.17	7.39	7.25	7.28	7.86	8.05	8.86	8.31
2007	7.98	8.47	8.51	8.95	7.91	9.02	7.56	7.27	8.38	8.81	7.56	8.99	8.28
2008	9.08	8.68	8.32	9.90	9.61	7.69	7.73	7.59	7.59	8.61	8.35	9.45	8.55
2009	8.87	8.88	9.75	9.95	7.96	7.53	7.32	7.61	8.06	8.70	7.85	8.81	8.44
2010	7.10	7.01	9.53	10.54	10.01	8.64	7.67	7.78	8.34	8.08	8.93	8.02	8.47
2011	7.75	9.76	9.07	10.06	9.28	8.86	7.30	7.16	7.17	7.99	8.90	8.02	8.43
2012	8.67	9.18	9.37	9.53	8.31	9.44	7.35	7.98	7.10	7.70	7.67	8.42	8.39
2013	7.90	8.49	8.71	8.98	7.76	8.51	7.69	6.84	7.99	8.06	8.06	7.74	8.05
2014	8.44	8.55	9.28	10.37	8.56	8.80	7.05	6.60	7.62	7.66	8.98	8.24	8.34
2015	7.82	8.28	7.81	8.74	7.55	6.95	6.77	7.45	7.00	7.53	8.21	9.30	7.77
Avg	8.40	8.42	9.00	9.30	8.55	8.29	7.53	7.23	7.72	8.06	8.35	8.47	8.27

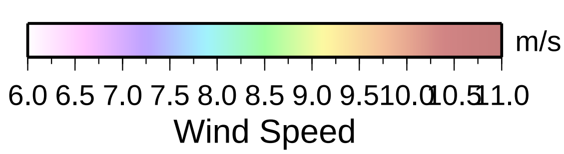

Figure 27: Monthly-mean values of simulated project-average wind speed.

Sector	Mean Speed(m/s)	Weibull Scale(A)	Weibull Shape(k)	Frequency(%)
N	9.22	10.40	2.40	8.33
NNE	6.87	7.75	2.36	4.63
NE	5.62	6.34	2.22	2.81
ENE	5.38	6.07	2.04	2.16
E	5.64	6.36	1.97	2.09
ESE	6.29	7.10	2.01	2.56
SE	7.44	8.40	2.12	4.56
SSE	8.70	9.80	2.56	10.35
S	8.78	9.87	2.78	12.82
SSW	8.36	9.42	2.54	7.98
SW	8.05	9.09	2.22	5.19
WSW	8.24	9.29	2.40	5.46
W	8.81	9.89	2.76	7.76
WNW	8.15	9.14	2.87	7.24
NW	8.23	9.28	2.52	6.87
NNW	9.73	10.99	2.30	9.18
ALL	**8.27**	**9.33**	**2.34**	**100.00**

Table 17: Simulated project-average mean wind speed, Weibull parameters, and frequency. Blank values correspond to times with less than 10 data points.

Wind Speed (m/s)	N	NNE	NE	ENE	E	ESE	SE	SSE	S	SSW	SW	WSW	W	WNW	NW	NNW	All
0 - 0.5	0.00	0.00	0.00	0.01	0.01	0.01	0.01	0.01	0.00	0.00	0.00	0.00	0.00	0.00	0.00	0.00	0.06
0.5 - 1.5	0.02	0.03	0.05	0.06	0.06	0.06	0.07	0.08	0.05	0.02	0.01	0.02	0.02	0.02	0.02	0.01	0.62
1.5 - 2.5	0.12	0.17	0.21	0.21	0.19	0.18	0.23	0.27	0.28	0.17	0.13	0.13	0.11	0.10	0.11	0.11	2.73
2.5 - 3.5	0.31	0.39	0.35	0.35	0.31	0.27	0.34	0.44	0.46	0.41	0.33	0.27	0.24	0.27	0.27	0.27	5.30
3.5 - 4.5	0.49	0.54	0.45	0.34	0.30	0.34	0.46	0.61	0.62	0.56	0.48	0.43	0.42	0.41	0.46	0.46	7.37
4.5 - 5.5	0.65	0.64	0.45	0.31	0.29	0.33	0.49	0.77	0.87	0.68	0.54	0.55	0.60	0.63	0.61	0.65	9.05
5.5 - 6.5	0.79	0.62	0.40	0.26	0.25	0.32	0.49	0.90	1.13	0.75	0.60	0.60	0.76	0.77	0.77	0.84	10.22
6.5 - 7.5	0.83	0.55	0.29	0.20	0.19	0.26	0.44	1.03	1.27	0.81	0.58	0.61	0.87	0.90	0.87	0.92	10.61
7.5 - 8.5	0.80	0.43	0.21	0.14	0.14	0.20	0.39	1.01	1.39	0.85	0.50	0.51	0.81	0.95	0.86	0.91	10.11
8.5 - 9.5	0.74	0.36	0.14	0.10	0.10	0.15	0.34	0.96	1.40	0.83	0.44	0.46	0.76	0.90	0.75	0.83	9.26
9.5 - 10.5	0.69	0.27	0.09	0.07	0.09	0.12	0.29	0.94	1.35	0.76	0.36	0.40	0.69	0.76	0.65	0.75	8.28
10.5 - 11.5	0.59	0.22	0.06	0.04	0.06	0.11	0.30	0.90	1.21	0.66	0.30	0.37	0.65	0.59	0.46	0.67	7.19
11.5 - 12.5	0.56	0.16	0.04	0.04	0.05	0.08	0.23	0.81	1.00	0.53	0.24	0.32	0.62	0.40	0.33	0.55	5.96
12.5 - 13.5	0.48	0.11	0.03	0.02	0.03	0.05	0.17	0.62	0.75	0.37	0.18	0.29	0.50	0.23	0.23	0.47	4.52
13.5 - 14.5	0.36	0.07	0.01	0.01	0.01	0.03	0.13	0.42	0.48	0.21	0.13	0.19	0.30	0.12	0.14	0.36	2.98
14.5 - 15.5	0.26	0.04	0.01	0.01	0.01	0.02	0.07	0.27	0.27	0.13	0.11	0.13	0.18	0.08	0.10	0.33	2.01
15.5 - 16.5	0.20	0.02	0.00	0.00	0.01	0.01	0.04	0.14	0.13	0.09	0.10	0.08	0.11	0.03	0.07	0.25	1.28
16.5 - 17.5	0.16	0.01	0.00	0.00	0.00	0.01	0.03	0.08	0.06	0.05	0.06	0.04	0.05	0.02	0.05	0.20	0.83
17.5 - 18.5	0.11	0.00	0.00	0.00	0.00	0.00	0.02	0.04	0.04	0.04	0.04	0.02	0.03	0.02	0.04	0.15	0.53
18.5 - 19.5	0.06	0.00	0.00	0.00	0.00	0.00	0.01	0.03	0.03	0.02	0.03	0.01	0.02	0.01	0.03	0.12	0.37
19.5 - 20.5	0.06	0.00	0.00	0.00	0.00	0.00	0.00	0.02	0.02	0.01	0.01	0.01	0.01	0.01	0.02	0.10	0.27
20.5 - 21.5	0.03	0.00	0.00	0.00	0.00	0.00	0.00	0.01	0.01	0.01	0.01	0.01	0.01	0.00	0.01	0.07	0.17
21.5 - 22.5	0.02	0.00	0.00	0.00	0.00	0.00	0.00	0.00	0.01	0.00	0.01	0.00	0.00	0.00	0.01	0.05	0.11
22.5 - 23.5	0.01	0.00	0.00	0.00	0.00	0.00	0.00	0.00	0.00	0.00	0.00	0.00	0.00	0.00	0.00	0.03	0.06
23.5 - 24.5	0.01	0.00	0.00	0.00	0.00	0.00	0.00	0.00	0.00	0.00	0.00	0.00	0.00	0.00	0.01	0.02	0.04
> 24.5	0.01	0.00	0.00	0.00	0.00	0.00	0.00	0.00	0.00	0.00	0.00	0.00	0.00	0.00	0.00	0.05	0.07

Table 18: Distribution of simulated project-average wind speed by direction.

11.5 Project-average Long-term Gross Power Capacity Assessment

11.5.1 Monthly-mean Variability of Power Capacity

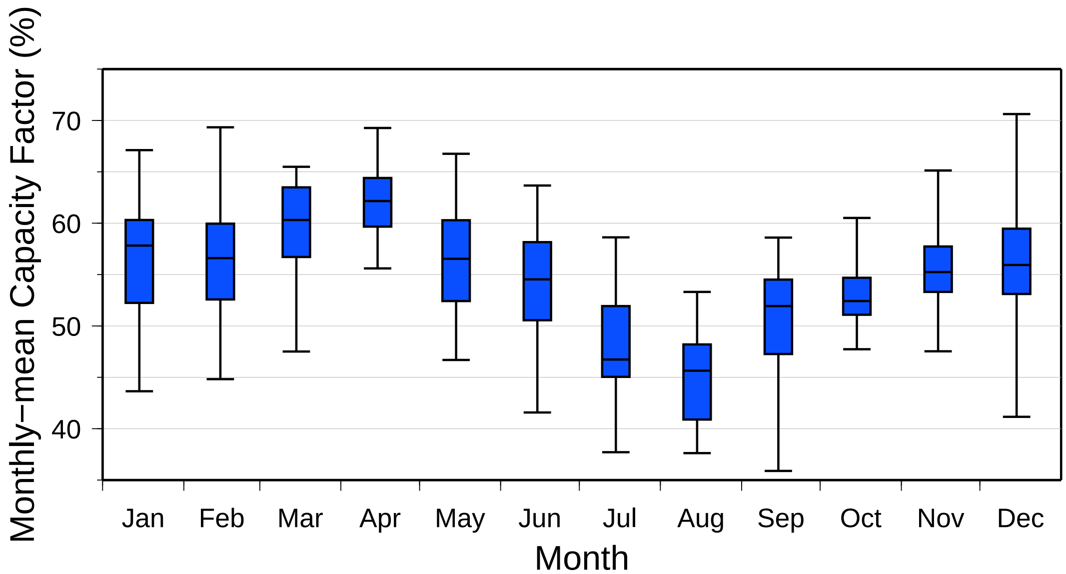

Figure 28: Box-and-whisker plot of monthly-mean project-average gross power capacity. This figure displays the expected variability of monthly-mean project-average gross power capacities. Median power capacity denoted by solid line within the shaded box. Upper and lower boundaries of the shaded box correspond to the 75% and 25% quartiles, while the whiskers denote the maximum and minimum monthly-mean power capacities.

11.5.2 Annual-mean Variability of Power Capacity

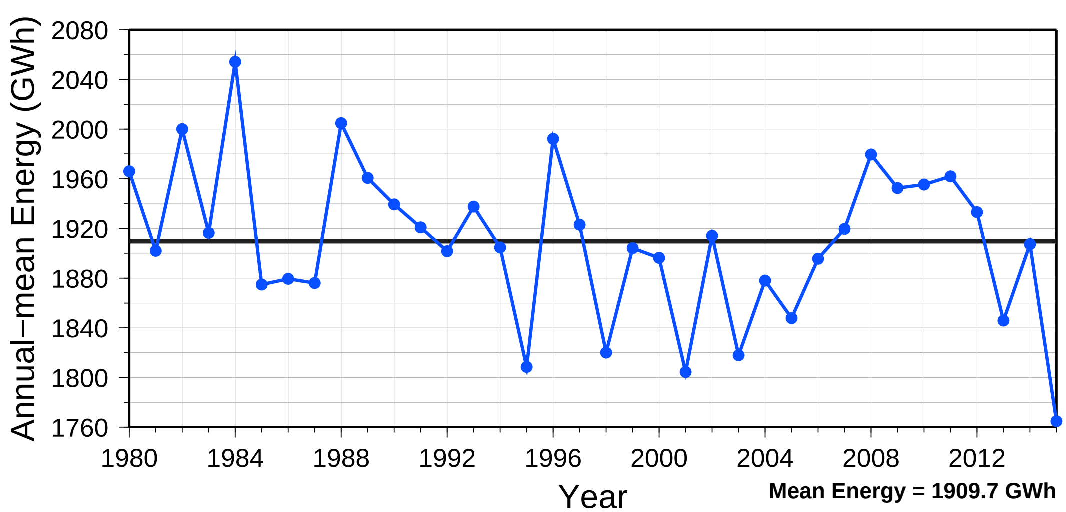

Figure 29: Time series of annual-mean project-average gross energy. Black line denotes the long-term mean.

11.5.3 Power Direction Distribution

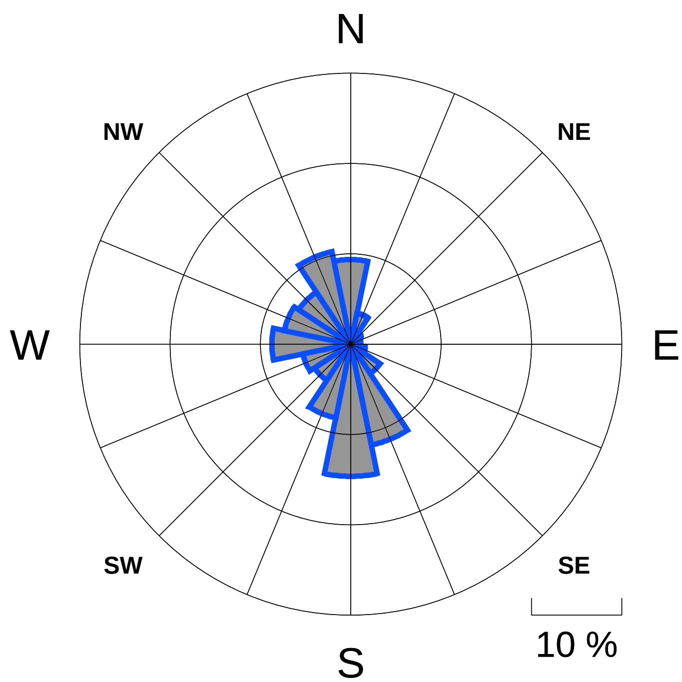

Figure 30: Annual power rose of the hourly-mean project-average gross capacity factor time series. Power rose shows the percent of total power within each sector. Directional bins are 22.5° wide, and the radial contour interval is 10%.

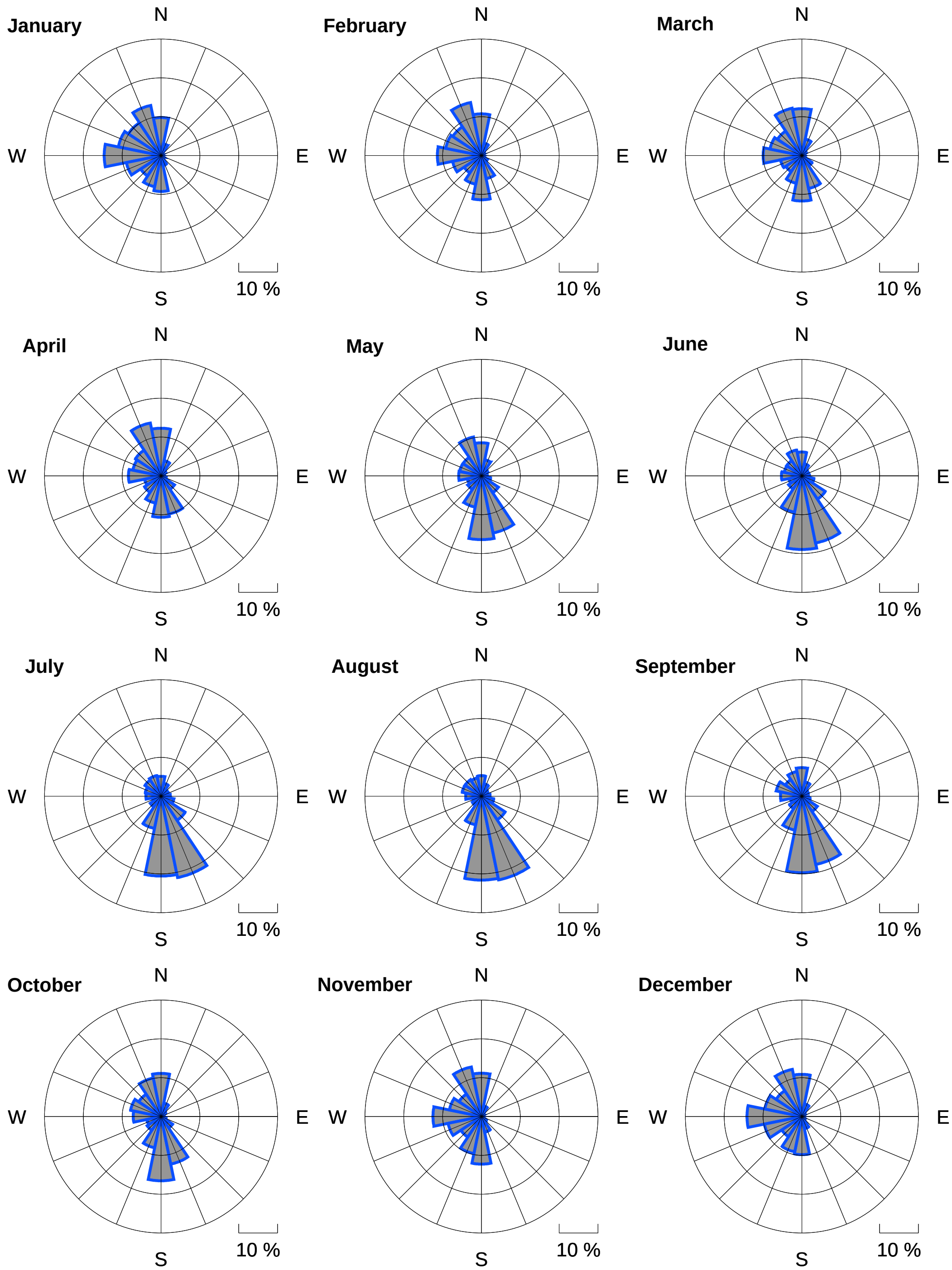

Figure 31: Power roses of the hourly-mean project-average gross capacity factor time series for each calendar month. Directional bins are 22.5° wide, and the radial contour interval is 10%.

11.5.4 Diurnal Variability of Power Capacity

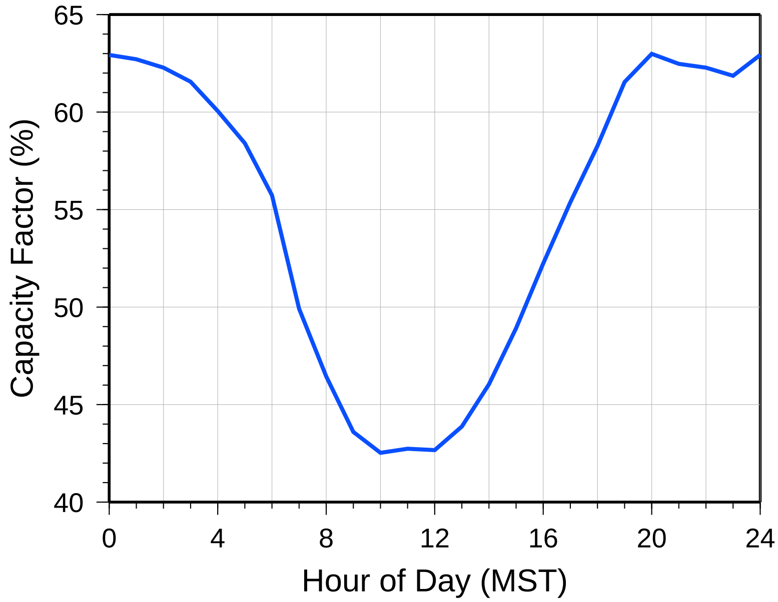

Figure 32: Diurnal cycle of simulated project-average gross power capacity. The horizontal axis is Mountain Standard Time (MST).

Appendix Gross Long-term Variability

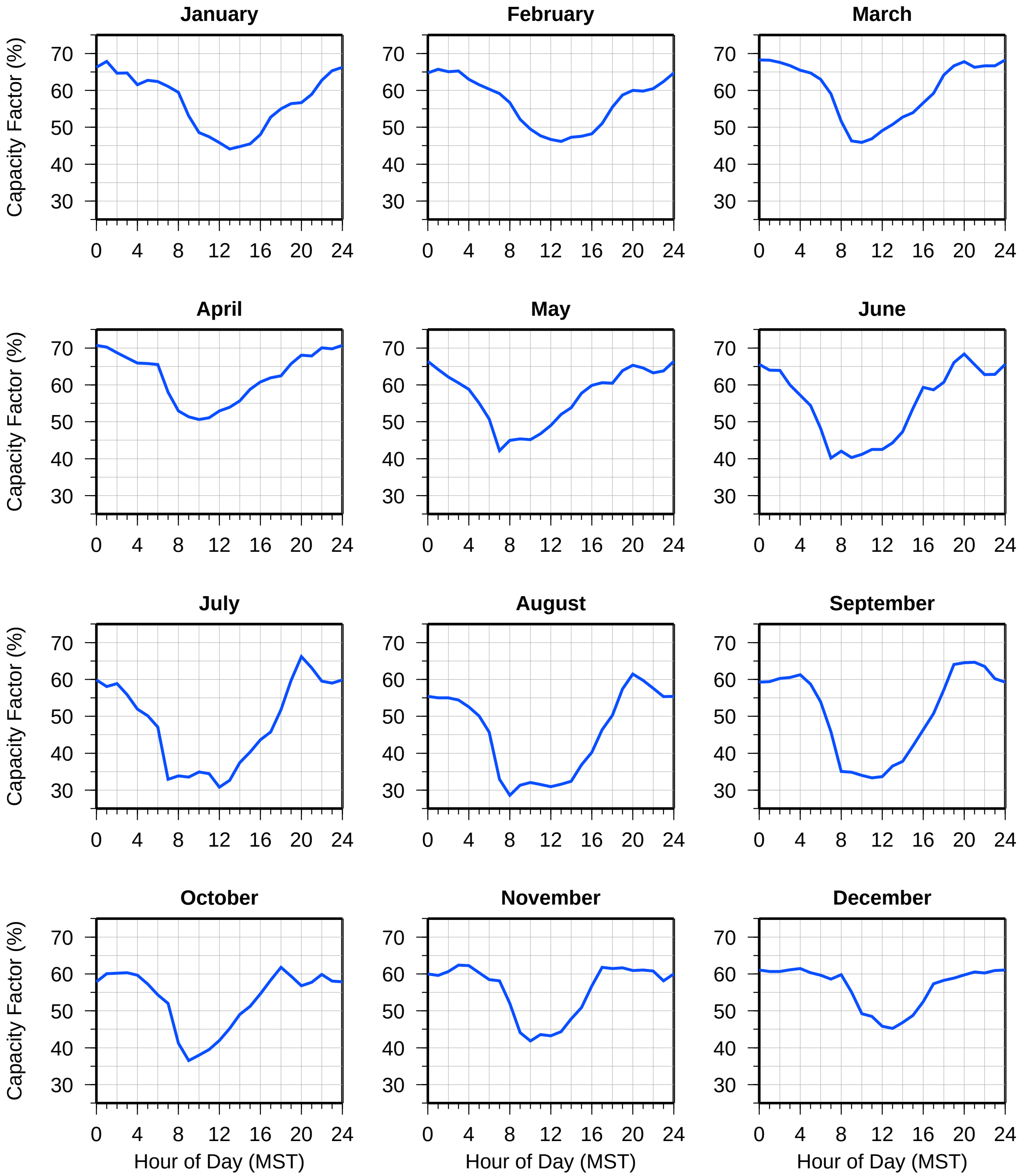

Figure 33: Diurnal cycle of simulated project-average gross power capacity for each calendar month. The horizontal axis is Mountain Standard Time (MST).

11.5.5 Power Capacity Variability and ENSO

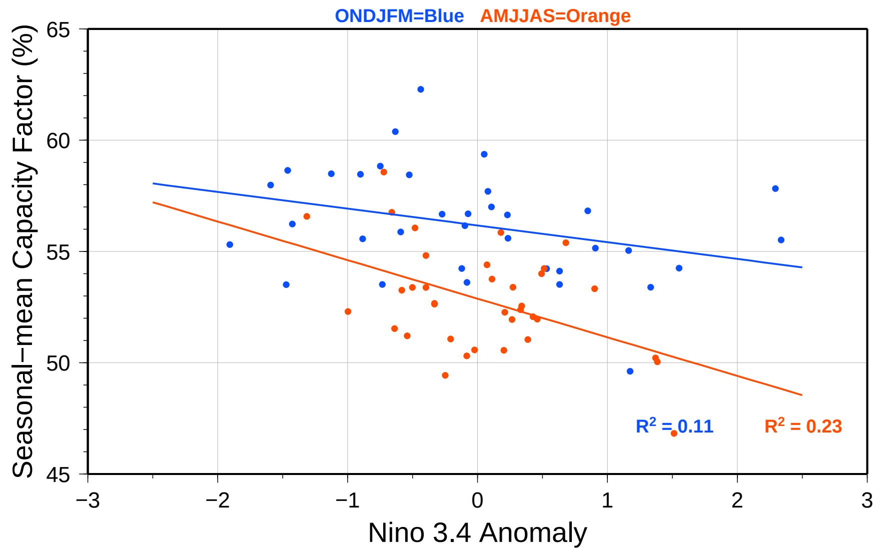

Figure 34: Scatter plot of Niño 3.4 anomalies vs. 6-month seasonal-mean gross power capacity. Blue dots denote the mean during ONDJFM (October, November, December, January, February, and March); orange dots denote the mean during AMJJAS (April, May, June, July, August and September).

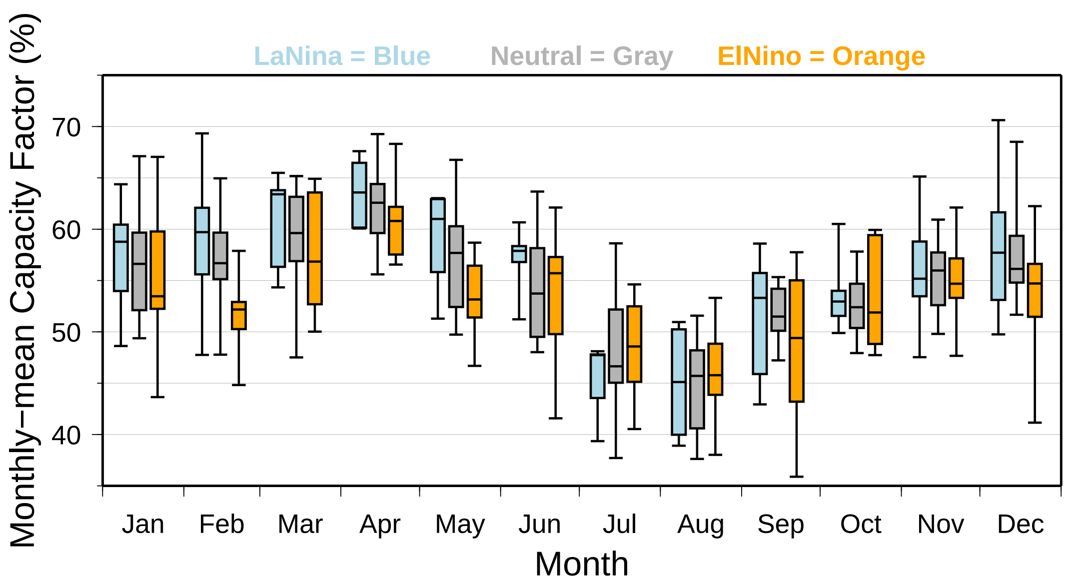

Figure 35: Box-and-whisker plot of monthly-mean project-average gross power capacity for La Niña (blue), neutral (gray), and El Niño (orange) phases of ENSO. Median power capacity denoted by solid line within the shaded box. Upper and lower boundaries of the shaded box correspond to the 75% and 25% quartiles, while the whiskers denote the maximum and minimum power capacities.

11.5.6 Tabular Data

Hour of Day (MST)	Jan	Feb	Mar	Apr	May	Jun	Jly	Aug	Sep	Oct	Nov	Dec	Avg
0	66.2	64.7	68.2	70.7	66.4	65.6	59.9	55.4	59.3	57.9	60.0	61.1	62.9
1	67.9	65.7	68.1	70.3	64.2	64.0	58.1	55.0	59.4	60.0	59.6	60.6	62.7
2	64.7	65.1	67.6	68.7	62.1	64.0	58.8	55.0	60.3	60.2	60.7	60.7	62.3
3	64.7	65.2	66.7	67.3	60.5	60.0	55.8	54.4	60.6	60.3	62.4	61.1	61.6
4	61.5	63.0	65.5	65.9	58.8	57.2	52.0	52.5	61.3	59.7	62.2	61.5	60.1
5	62.7	61.5	64.7	65.8	55.1	54.4	50.2	50.1	58.8	57.3	60.4	60.4	58.4
6	62.4	60.3	63.0	65.5	50.8	48.2	47.1	45.7	53.9	54.4	58.5	59.6	55.7
7	61.0	59.2	59.1	58.0	42.1	40.1	32.9	32.9	45.8	52.0	58.1	58.6	49.9
8	59.5	56.6	51.6	52.9	45.0	42.0	33.8	28.6	35.0	41.2	52.0	59.8	46.4
9	53.1	52.1	46.3	51.3	45.3	40.3	33.5	31.3	34.8	36.5	44.1	55.1	43.6
10	48.5	49.5	45.9	50.6	45.2	41.2	34.9	32.0	34.0	37.9	41.9	49.2	42.5
11	47.4	47.7	46.9	51.1	46.7	42.5	34.4	31.5	33.3	39.5	43.6	48.5	42.7
12	45.8	46.7	49.1	53.0	49.0	42.5	30.8	30.9	33.6	42.0	43.2	45.8	42.7
13	44.1	46.2	50.7	53.9	52.0	44.3	32.7	31.6	36.5	45.2	44.4	45.2	43.9
14	44.8	47.3	52.7	55.7	53.8	47.3	37.4	32.4	37.8	49.0	47.8	46.8	46.0
15	45.5	47.5	53.9	58.8	57.8	53.6	40.3	36.9	42.0	51.2	50.9	48.8	48.9
16	48.0	48.2	56.6	60.8	59.9	59.3	43.6	40.2	46.4	54.6	56.7	52.5	52.2
17	53.3	50.7	58.6	62.2	60.5	58.8	46.4	46.0	50.9	58.1	61.8	57.3	55.4
18	55.4	55.0	63.7	62.8	60.5	60.7	52.2	50.1	57.2	61.5	61.5	58.4	58.3
19	56.7	58.3	66.2	66.0	63.6	66.1	60.2	57.2	64.4	59.1	61.5	59.2	61.5
20	56.9	59.4	67.4	68.4	65.2	68.3	66.6	61.5	64.8	56.5	60.5	60.3	63.0
21	59.0	59.4	65.9	68.2	64.6	65.6	63.4	59.6	64.8	57.6	60.7	61.1	62.5
22	62.9	60.1	66.3	70.3	63.3	62.8	59.7	57.4	63.8	59.7	60.4	60.6	62.3
23	65.5	62.1	66.3	70.1	63.9	62.8	59.1	55.2	60.3	58.0	57.9	61.1	61.9
Avg	56.6	56.3	59.6	62.0	56.5	54.7	47.7	45.1	50.8	52.9	55.4	56.4	54.5

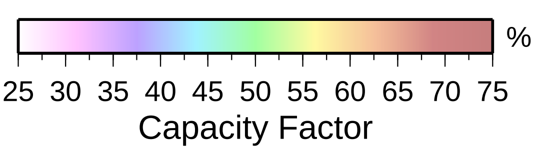

Figure 36: Hourly-mean values of simulated project-average gross capacity factor. Vertical axis is local time.

Year	Jan	Feb	Mar	Apr	May	Jun	Jly	Aug	Sep	Oct	Nov	Dec	Avg
1980	59.8	55.1	65.1	62.1	60.4	62.1	46.5	51.0	53.0	48.6	49.9	59.3	56.1
1981	50.6	62.8	54.2	60.5	60.3	54.4	52.2	40.0	48.7	55.1	54.6	58.4	54.2
1982	67.1	56.5	64.4	65.0	51.4	57.0	52.5	40.8	53.3	59.9	57.1	59.5	57.0
1983	61.1	52.6	56.7	62.0	56.6	48.3	53.3	40.9	54.2	52.9	56.1	61.0	54.7
1984	54.9	65.0	63.1	69.3	57.9	56.8	54.0	47.3	51.0	55.4	65.1	63.8	58.6
1985	48.9	52.2	65.5	60.1	51.3	51.2	43.6	48.2	54.9	51.5	59.6	55.0	53.5
1986	60.3	52.5	56.3	64.6	54.6	53.8	47.0	50.6	55.9	51.6	55.3	41.2	53.6
1987	67.0	50.3	64.9	60.8	53.6	49.8	54.6	45.6	35.9	48.5	53.7	56.6	53.5
1988	58.7	58.3	65.2	63.0	62.9	57.7	47.8	50.2	57.8	49.9	58.8	56.1	57.2
1989	58.2	47.8	61.0	60.1	61.3	54.6	58.4	51.6	54.5	54.7	56.4	51.7	55.9
1990	63.7	58.3	52.2	59.5	60.9	63.5	46.6	44.9	47.2	53.6	59.2	54.8	55.3
1991	53.8	56.1	62.4	59.6	63.6	62.1	41.7	43.9	54.5	48.8	57.4	54.0	54.8
1992	61.6	53.7	50.0	57.5	58.7	49.5	44.6	46.0	55.3	52.6	52.6	68.5	54.2
1993	58.1	51.4	62.9	62.2	51.2	57.3	58.6	44.3	50.4	47.9	57.7	60.8	55.3
1994	56.6	60.0	59.0	57.9	57.9	52.1	45.9	46.0	51.9	51.9	62.1	51.5	54.3
1995	53.1	52.9	59.4	55.7	58.2	50.3	46.7	40.6	45.1	53.0	53.7	50.2	51.6
1996	58.8	55.6	62.1	64.4	60.3	48.4	45.0	45.7	52.0	57.8	60.9	70.6	56.8
1997	60.4	60.6	63.3	59.7	52.8	55.7	51.9	38.0	43.2	55.4	55.2	62.2	54.8
1998	51.6	51.8	56.9	56.6	56.4	60.7	39.4	42.1	52.1	52.7	53.5	49.7	51.9
1999	57.5	60.6	63.4	62.8	63.0	58.1	48.1	38.9	42.9	51.6	47.5	57.7	54.3
2000	48.6	60.7	54.9	66.5	55.8	58.3	46.8	37.6	54.5	53.0	54.3	58.9	54.1
2001	51.8	55.6	47.5	63.1	55.7	49.0	41.3	45.5	47.3	55.7	49.8	55.7	51.5
2002	59.7	59.7	59.6	64.2	53.7	54.5	53.7	51.2	55.0	52.3	47.7	44.5	54.6
2003	50.4	44.8	58.1	64.1	52.1	48.0	43.7	47.4	48.2	51.8	55.7	57.5	51.8
2004	49.4	59.6	59.6	57.5	57.7	51.0	37.7	44.6	57.8	59.4	54.2	54.8	53.6
2005	52.2	47.8	56.9	62.6	53.6	54.0	53.4	37.9	52.2	51.1	56.8	54.1	52.7
2006	64.4	60.6	63.8	64.7	49.7	53.7	46.3	46.0	42.9	49.8	52.8	54.6	54.1
2007	53.1	53.7	57.0	61.3	52.0	58.3	47.1	45.8	55.7	60.5	50.8	61.6	54.7
2008	61.7	58.9	54.3	67.6	60.7	50.5	50.1	49.2	50.7	52.2	56.3	65.3	56.5
2009	61.0	62.1	65.5	64.0	52.2	48.1	45.1	48.8	54.1	59.7	53.3	54.8	55.7
2010	43.6	45.3	63.6	68.3	66.8	59.0	47.7	51.0	58.6	54.0	57.9	53.1	55.8
2011	54.0	69.3	63.6	64.4	61.6	58.1	45.1	45.1	45.9	51.3	61.4	53.0	56.0
2012	59.2	62.3	63.5	60.2	52.4	63.7	45.2	53.3	45.5	50.4	50.1	56.1	55.1
2013	52.1	56.7	56.2	55.6	51.9	59.1	49.4	39.3	51.1	53.1	55.2	52.7	52.6
2014	59.4	57.7	62.0	66.0	58.6	57.3	44.2	38.2	50.1	48.8	61.7	49.8	54.4
2015	53.8	57.9	52.7	59.3	46.7	41.6	40.5	48.0	44.9	47.7	51.7	60.8	50.3
Avg	56.6	56.3	59.6	62.0	56.5	54.7	47.7	45.1	50.8	52.9	55.4	56.4	54.5

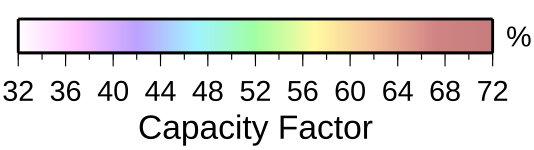

Figure 37: Monthly-mean values of simulated project-average gross capacity factor.

Sector	Mean Capacity Factor(%)	Percent Total Power(%)
N	61.2	9.4
NNE	41.0	3.5
NE	27.4	1.4
ENE	25.3	1.0
E	28.7	1.1
ESE	34.9	1.6
SE	46.6	3.9
SSE	59.9	11.4
S	62.1	14.6
SSW	56.8	8.3
SW	50.4	4.8
WSW	53.8	5.4
W	61.3	8.7
WNW	56.4	7.5
NW	54.8	6.9
NNW	61.9	10.4
ALL	**54.5**	**100.0**

Table 19: Simulated project-average gross mean power capacity factor and percent of total power. Blank values correspond to times with less than 10 data points.

Power Capacity (%)	N	NNE	NE	ENE	E	ESE	SE	SSE	S	SSW	SW	WSW	W	WNW	NW	NNW	All
0 - 5%	0.61	0.70	0.72	0.69	0.63	0.61	0.75	0.90	0.89	0.72	0.56	0.49	0.44	0.45	0.48	0.64	10.29
5% - 15%	0.76	0.79	0.63	0.46	0.40	0.45	0.65	0.95	1.01	0.81	0.67	0.64	0.66	0.67	0.71	0.76	11.00
15% - 25%	0.71	0.60	0.40	0.27	0.26	0.31	0.49	0.83	0.97	0.70	0.55	0.54	0.66	0.68	0.68	0.72	9.36
25% - 35%	0.59	0.44	0.26	0.17	0.15	0.22	0.32	0.72	0.90	0.58	0.45	0.47	0.58	0.60	0.58	0.68	7.73
35% - 45%	0.50	0.32	0.17	0.11	0.11	0.15	0.26	0.62	0.77	0.49	0.37	0.39	0.56	0.55	0.54	0.56	6.47
45% - 55%	0.45	0.26	0.12	0.10	0.09	0.12	0.23	0.55	0.74	0.48	0.32	0.32	0.49	0.53	0.50	0.52	5.81
55% - 65%	0.41	0.21	0.10	0.06	0.07	0.11	0.19	0.53	0.71	0.47	0.27	0.30	0.42	0.51	0.44	0.49	5.31
65% - 75%	0.40	0.19	0.09	0.07	0.07	0.09	0.20	0.50	0.73	0.45	0.27	0.27	0.43	0.51	0.43	0.48	5.19
75% - 85%	0.43	0.20	0.08	0.06	0.07	0.10	0.23	0.59	0.83	0.51	0.28	0.29	0.46	0.54	0.46	0.53	5.65
85% - 95%	0.61	0.23	0.09	0.06	0.08	0.13	0.30	0.88	1.30	0.74	0.36	0.41	0.66	0.69	0.57	0.71	7.83
95% - 100%	2.88	0.67	0.15	0.11	0.15	0.28	0.93	3.28	3.96	2.03	1.10	1.35	2.41	1.50	1.47	3.09	25.36

Table 20: Distribution of simulated project-average gross power capacity by direction.

11.6 Long-term Wind Resource Assessment for Tower M2301 at 80 m

11.6.1 Tabular Data

Sector	Mean Speed(m/s)	Weibull Scale(A)	Weibull Shape(k)	Frequency(%)
N	9.27	10.46	2.38	8.62
NNE	6.77	7.64	2.33	4.47
NE	5.68	6.42	2.12	2.79
ENE	5.38	6.07	1.95	2.21
E	5.54	6.24	1.83	2.23
ESE	5.80	6.52	1.78	2.74
SE	6.86	7.74	1.94	5.03
SSE	8.01	9.03	2.43	10.88
S	8.25	9.27	2.69	12.70
SSW	7.98	9.00	2.49	7.68
SW	7.87	8.88	2.11	4.71
WSW	7.90	8.92	2.18	4.08
W	9.11	10.25	2.65	6.80
WNW	8.66	9.71	2.92	7.86
NW	8.64	9.73	2.56	7.33
NNW	10.14	11.44	2.30	9.86
ALL	**8.16**	**9.22**	**2.25**	**100.00**

Table 21: Simulated mean wind speed, Weibull parameters, and frequency for Tower M2301 at 80 m. Blank values correspond to times with less than 10 data points.

Wind Speed (m/s)	N	NNE	NE	ENE	E	ESE	SE	SSE	S	SSW	SW	WSW	W	WNW	NW	NNW	All
0 - 0.5	0.00	0.00	0.00	0.00	0.01	0.04	0.04	0.01	0.00	0.00	0.00	0.00	0.00	0.00	0.00	0.00	0.12
0.5 - 1.5	0.02	0.03	0.05	0.08	0.11	0.15	0.18	0.17	0.08	0.04	0.03	0.02	0.02	0.02	0.02	0.02	1.04
1.5 - 2.5	0.17	0.21	0.24	0.25	0.26	0.26	0.33	0.42	0.34	0.23	0.18	0.14	0.13	0.12	0.12	0.14	3.54
2.5 - 3.5	0.33	0.38	0.36	0.35	0.31	0.31	0.45	0.56	0.55	0.46	0.38	0.29	0.24	0.25	0.25	0.30	5.77
3.5 - 4.5	0.52	0.53	0.43	0.31	0.28	0.33	0.51	0.72	0.71	0.55	0.46	0.39	0.35	0.37	0.42	0.42	7.31
4.5 - 5.5	0.65	0.59	0.41	0.29	0.26	0.34	0.54	0.88	0.96	0.65	0.48	0.44	0.48	0.55	0.55	0.62	8.68
5.5 - 6.5	0.77	0.59	0.37	0.25	0.25	0.30	0.51	1.03	1.22	0.77	0.48	0.44	0.63	0.72	0.72	0.75	9.82
6.5 - 7.5	0.83	0.53	0.29	0.20	0.21	0.25	0.49	1.18	1.48	0.88	0.50	0.42	0.69	0.87	0.84	0.94	10.61
7.5 - 8.5	0.79	0.43	0.21	0.15	0.16	0.21	0.39	1.15	1.48	0.87	0.41	0.35	0.66	0.92	0.87	0.88	9.92
8.5 - 9.5	0.71	0.34	0.14	0.11	0.11	0.14	0.37	1.08	1.45	0.84	0.38	0.31	0.59	0.94	0.83	0.89	9.22
9.5 - 10.5	0.69	0.26	0.10	0.07	0.09	0.13	0.32	0.99	1.32	0.68	0.31	0.25	0.57	0.87	0.73	0.82	8.18
10.5 - 11.5	0.63	0.20	0.06	0.05	0.07	0.09	0.27	0.87	1.06	0.58	0.26	0.23	0.51	0.77	0.61	0.72	6.99
11.5 - 12.5	0.62	0.16	0.04	0.04	0.05	0.07	0.24	0.71	0.85	0.45	0.23	0.23	0.58	0.61	0.48	0.68	6.04
12.5 - 13.5	0.54	0.10	0.04	0.02	0.03	0.05	0.16	0.49	0.54	0.27	0.18	0.19	0.51	0.42	0.28	0.60	4.41
13.5 - 14.5	0.38	0.06	0.02	0.01	0.01	0.02	0.09	0.25	0.27	0.14	0.13	0.14	0.32	0.20	0.18	0.42	2.63
14.5 - 15.5	0.30	0.03	0.01	0.01	0.01	0.02	0.06	0.16	0.17	0.10	0.10	0.09	0.24	0.11	0.14	0.39	1.93
15.5 - 16.5	0.23	0.02	0.01	0.00	0.00	0.01	0.04	0.09	0.08	0.07	0.08	0.06	0.13	0.06	0.08	0.33	1.28
16.5 - 17.5	0.14	0.01	0.00	0.00	0.00	0.00	0.02	0.04	0.04	0.03	0.05	0.03	0.07	0.03	0.06	0.23	0.77
17.5 - 18.5	0.10	0.00	0.00	0.00	0.00	0.00	0.01	0.03	0.03	0.02	0.04	0.02	0.04	0.02	0.04	0.17	0.53
18.5 - 19.5	0.07	0.00	0.00	0.00	0.00	0.00	0.01	0.02	0.02	0.01	0.02	0.02	0.02	0.01	0.03	0.14	0.37
19.5 - 20.5	0.06	0.00	0.00	0.00	0.00	0.00	0.00	0.01	0.02	0.01	0.02	0.01	0.01	0.01	0.02	0.13	0.31
20.5 - 21.5	0.03	0.00	0.00	0.00	0.00	0.00	0.00	0.01	0.01	0.01	0.01	0.00	0.01	0.00	0.01	0.09	0.18
21.5 - 22.5	0.02	0.00	0.00	0.00	0.00	0.00	0.00	0.00	0.01	0.00	0.00	0.00	0.00	0.00	0.01	0.06	0.11
22.5 - 23.5	0.01	0.00	0.00	0.00	0.00	0.00	0.00	0.00	0.00	0.00	0.01	0.00	0.00	0.00	0.01	0.04	0.08
23.5 - 24.5	0.01	0.00	0.00	0.00	0.00	0.00	0.00	0.00	0.00	0.00	0.00	0.00	0.00	0.00	0.01	0.03	0.05
> 24.5	0.01	0.00	0.00	0.00	0.00	0.00	0.00	0.00	0.00	0.00	0.00	0.00	0.00	0.00	0.01	0.07	0.11

Table 22: Distribution of simulated wind speed by direction for Tower M2301 at $80\,m$.

11.7 Long-term Wind Resource Assessment for Tower M2327 at 80 m

11.7.1 Tabular Data

Sector	Mean Speed(m/s)	Weibull Scale(A)	Weibull Shape(k)	Frequency(%)
N	8.87	10.02	2.30	8.01
NNE	6.87	7.76	2.23	4.90
NE	5.53	6.24	1.98	2.97
ENE	5.19	5.84	1.80	2.43
E	5.42	6.07	1.67	2.55
ESE	6.03	6.76	1.68	3.34
SE	7.50	8.43	1.81	5.01
SSE	9.19	10.37	2.33	11.09
S	9.43	10.62	2.58	12.13
SSW	8.59	9.70	2.28	7.28
SW	8.14	9.19	2.19	5.87
WSW	8.49	9.56	2.53	6.93
W	8.40	9.47	2.52	6.86
WNW	7.80	8.79	2.57	5.71
NW	8.04	9.08	2.35	6.19
NNW	9.36	10.57	2.29	8.75
ALL	**8.24**	**9.31**	**2.17**	**100.00**

Table 23: Simulated mean wind speed, Weibull parameters, and frequency for Tower M2327 at 80 m. Blank values correspond to times with less than 10 data points.

Wind Speed (m/s)	N	NNE	NE	ENE	E	ESE	SE	SSE	S	SSW	SW	WSW	W	WNW	NW	NNW	All
0 - 0.5	0.00	0.00	0.00	0.02	0.04	0.06	0.06	0.03	0.01	0.00	0.00	0.00	0.00	0.00	0.00	0.00	0.24
0.5 - 1.5	0.03	0.03	0.06	0.10	0.15	0.15	0.17	0.15	0.08	0.04	0.02	0.01	0.01	0.01	0.01	0.01	1.05
1.5 - 2.5	0.15	0.23	0.32	0.34	0.33	0.36	0.34	0.39	0.37	0.25	0.20	0.15	0.12	0.12	0.12	0.13	3.95
2.5 - 3.5	0.34	0.42	0.43	0.37	0.35	0.38	0.36	0.44	0.45	0.43	0.34	0.30	0.27	0.24	0.27	0.27	5.66
3.5 - 4.5	0.55	0.57	0.45	0.32	0.32	0.37	0.43	0.53	0.53	0.51	0.48	0.45	0.43	0.42	0.43	0.46	7.23
4.5 - 5.5	0.80	0.71	0.46	0.35	0.32	0.40	0.53	0.75	0.69	0.65	0.62	0.69	0.67	0.62	0.70	0.78	9.75
5.5 - 6.5	0.79	0.61	0.35	0.25	0.26	0.34	0.47	0.83	0.82	0.61	0.63	0.71	0.70	0.67	0.78	0.91	9.73
6.5 - 7.5	0.82	0.55	0.27	0.21	0.20	0.28	0.44	1.00	0.96	0.63	0.64	0.75	0.84	0.76	0.83	0.92	10.09
7.5 - 8.5	0.75	0.42	0.20	0.14	0.15	0.21	0.35	0.93	1.07	0.61	0.56	0.67	0.78	0.73	0.70	0.85	9.11
8.5 - 9.5	0.64	0.35	0.12	0.10	0.11	0.17	0.34	0.91	1.12	0.61	0.49	0.60	0.69	0.64	0.60	0.77	8.28
9.5 - 10.5	0.54	0.27	0.10	0.07	0.09	0.15	0.28	0.85	1.10	0.59	0.39	0.55	0.55	0.47	0.46	0.62	7.06
10.5 - 11.5	0.56	0.24	0.07	0.06	0.08	0.13	0.28	0.92	1.19	0.62	0.38	0.57	0.51	0.36	0.37	0.59	6.94
11.5 - 12.5	0.49	0.17	0.05	0.04	0.05	0.11	0.25	0.83	1.02	0.50	0.28	0.50	0.39	0.25	0.25	0.49	5.65
12.5 - 13.5	0.43	0.13	0.03	0.03	0.04	0.07	0.21	0.78	0.93	0.41	0.22	0.38	0.29	0.16	0.18	0.41	4.70
13.5 - 14.5	0.30	0.08	0.02	0.01	0.03	0.05	0.17	0.56	0.60	0.26	0.16	0.25	0.20	0.09	0.13	0.35	3.24
14.5 - 15.5	0.24	0.05	0.01	0.01	0.02	0.03	0.10	0.40	0.47	0.17	0.12	0.14	0.13	0.06	0.08	0.28	2.31
15.5 - 16.5	0.22	0.03	0.01	0.01	0.01	0.03	0.08	0.32	0.33	0.14	0.12	0.10	0.10	0.04	0.08	0.25	1.86
16.5 - 17.5	0.15	0.02	0.01	0.01	0.01	0.02	0.06	0.21	0.18	0.09	0.08	0.06	0.07	0.02	0.07	0.21	1.26
17.5 - 18.5	0.08	0.01	0.00	0.00	0.00	0.01	0.03	0.10	0.07	0.05	0.04	0.02	0.03	0.01	0.03	0.12	0.60
18.5 - 19.5	0.06	0.00	0.00	0.00	0.00	0.01	0.02	0.07	0.05	0.04	0.03	0.02	0.02	0.01	0.03	0.10	0.47
19.5 - 20.5	0.04	0.00	0.00	0.00	0.00	0.00	0.01	0.03	0.03	0.02	0.02	0.01	0.01	0.01	0.02	0.08	0.29
20.5 - 21.5	0.04	0.00	0.00	0.00	0.00	0.00	0.01	0.02	0.03	0.02	0.02	0.01	0.01	0.01	0.02	0.07	0.26
21.5 - 22.5	0.02	0.00	0.00	0.00	0.00	0.00	0.00	0.01	0.01	0.01	0.01	0.00	0.01	0.00	0.01	0.04	0.13
22.5 - 23.5	0.00	0.00	0.00	0.00	0.00	0.00	0.00	0.00	0.00	0.00	0.00	0.00	0.00	0.00	0.00	0.01	0.03
23.5 - 24.5	0.00	0.00	0.00	0.00	0.00	0.00	0.00	0.00	0.00	0.00	0.00	0.00	0.00	0.00	0.00	0.01	0.03
> 24.5	0.00	0.00	0.00	0.00	0.00	0.00	0.00	0.01	0.01	0.00	0.00	0.00	0.00	0.00	0.01	0.02	0.06

Table 24: Distribution of simulated wind speed by direction for Tower M2327 at $80\,m$.

12 APPENDIX VALIDATION OF MODEL RESULTS

12.1 Validation of Model Results at Tower M2301

This section examines the quality of the NWP simulations used at a single point within the study area. For this section, the observations were taken at Tower M2301 (latitude 39.13808, longitude -103.80388).

The average observed wind speed (for all valid observational times) at $60.0\,m$ during the 48 months of the period of record (June, 2010 to May, 2014) is $7.89\,m/s$ with an hourly standard deviation of $3.71\,m/s$ at Tower M2301. This compares to a modeled $60\,m$ wind speed of $6.86\,m/s$ with a $3.20\,m/s$ standard deviation for these same times.

Based on a comparison of the NWP model output with observations from each of the meteorological towers for which data were provided, Model Output Statistics (MOS) was constructed. MOS uses a multilinear regression model designed to remove the bias and adjust the variance of the raw NWP simulated wind speed and direction. Applying this statistical model to the simulated data at Tower M2301 results in a MOS-corrected mean value of $7.90\,m/s$ and an hourly standard deviation of $3.71\,m/s$.

This section presents a comparison of the simulated winds with the observations at the reference tower (Tower M2301). The focus of the verification is on the model's ability to reproduce the observed variability of the wind resource at daily and monthly time scales, while preserving the distribution of hourly wind speeds and the diurnal characteristics of the wind.

12.1.1 Observational Data

Approximately 48 months of wind speed data at $60.0\,meters$ and wind direction data at $58.0\,meters$ (June, 2010 to May, 2014) from a meteorological tower (Tower M2301) at Rush Creek I were used in this analysis. This tower will be referred to as the reference tower throughout this section. The data at $60\,m$ were used to assess the quality of the model simulations at $60\,m$.

It should be noted that meteorological observations provided to 3TIER are not allowed to influence the raw model simulations.

12.1.2 Model Validation Statistics

Table 25 presents some basic statistical measures of the model performance relative to the measured winds at the reference tower during the observational period. Also shown are values (labeled "MOS-corrected") for model data with the statistical model applied. For reference, the correlation of the reference tower data to itself is perfect and hence the explained variance (r^2) value is 1.0.

The observed and modeled winds in this section represent the mean of all times during the month for which a valid wind speed or direction observation was available. Therefore they should not be interpreted as estimates of the true winds at the site, but rather a verification of the model's ability to reproduce the available observations. Any month or hour missing greater than 50% of the available observations is omitted from the following figures, tables, and statistics.

Comparison	Value
Correlation of monthly-mean simulated wind speed to observed	0.91
RMS error of monthly-mean simulated wind speed	1.08 m/s
Correlation of monthly-mean MOS-corrected wind speed to observed	0.97
RMS error of monthly-mean MOS-corrected wind speed	0.18 m/s
Correlation of daily-mean simulated wind speed to observed	0.84
RMS error of daily-mean simulated wind speed	1.69 m/s
Correlation of daily-mean MOS-corrected wind speed to observed	0.87
RMS error of daily-mean MOS-corrected wind speed	1.20 m/s

Table 25: Correlation and root mean square (RMS) error statistics of modeled wind speeds.

12.1.3 Monthly Mean Wind Speed

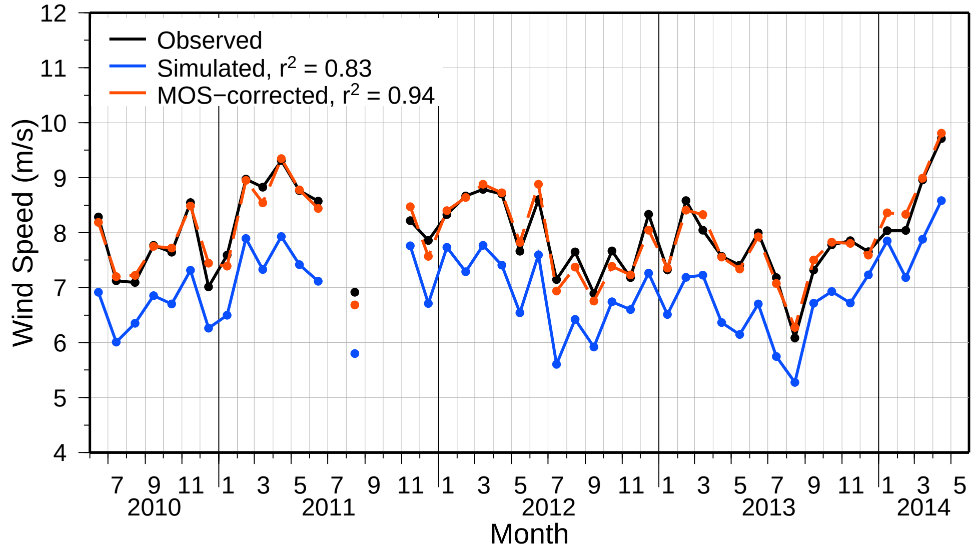

Figure 38: A comparison of the observed, simulated, and MOS-corrected monthly-mean $60\,m$ wind speed at Tower M2301. Explained variance(r^2) value of each data source relative to the monthly reference tower wind speeds are shown in the legend. Months missing greater than 50% of the available observations are not plotted. Tabular formatted data are available in Table 26 (p. 79).

12.1.4 Wind Speed Distribution

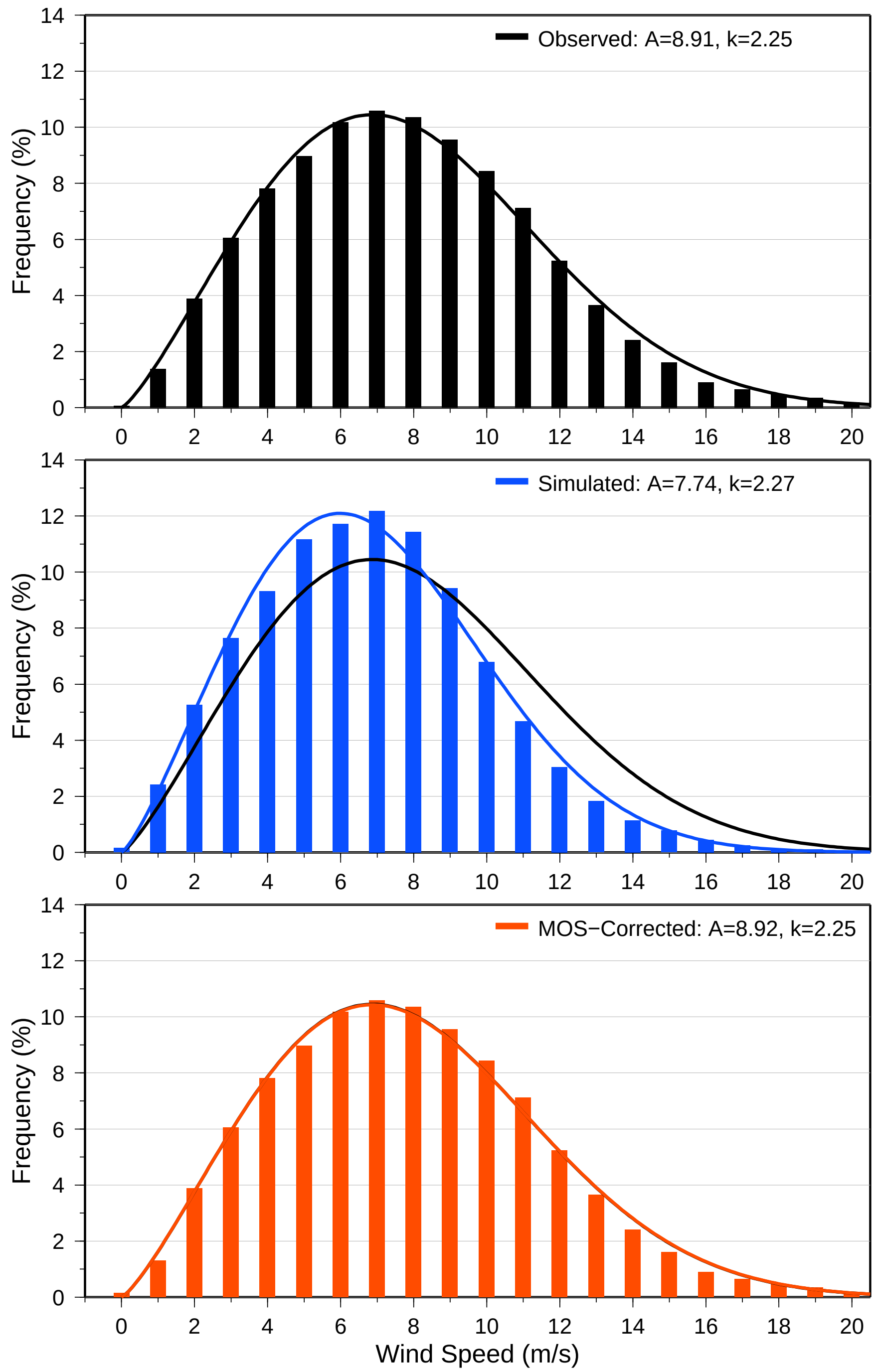

Figure 39: A comparison of the observed, simulated, and MOS-corrected hourly wind speed distributions at $60\,m$ at Tower M2301 during the period of record, using $1\,m/s$ bins. ($0\,m/s$ bin contains only values ≤ 0.5) Fitted Weibull distributions are also displayed with the scale(A) and shape(k) parameters listed in the legend.

12.1.5 Wind Direction Distribution

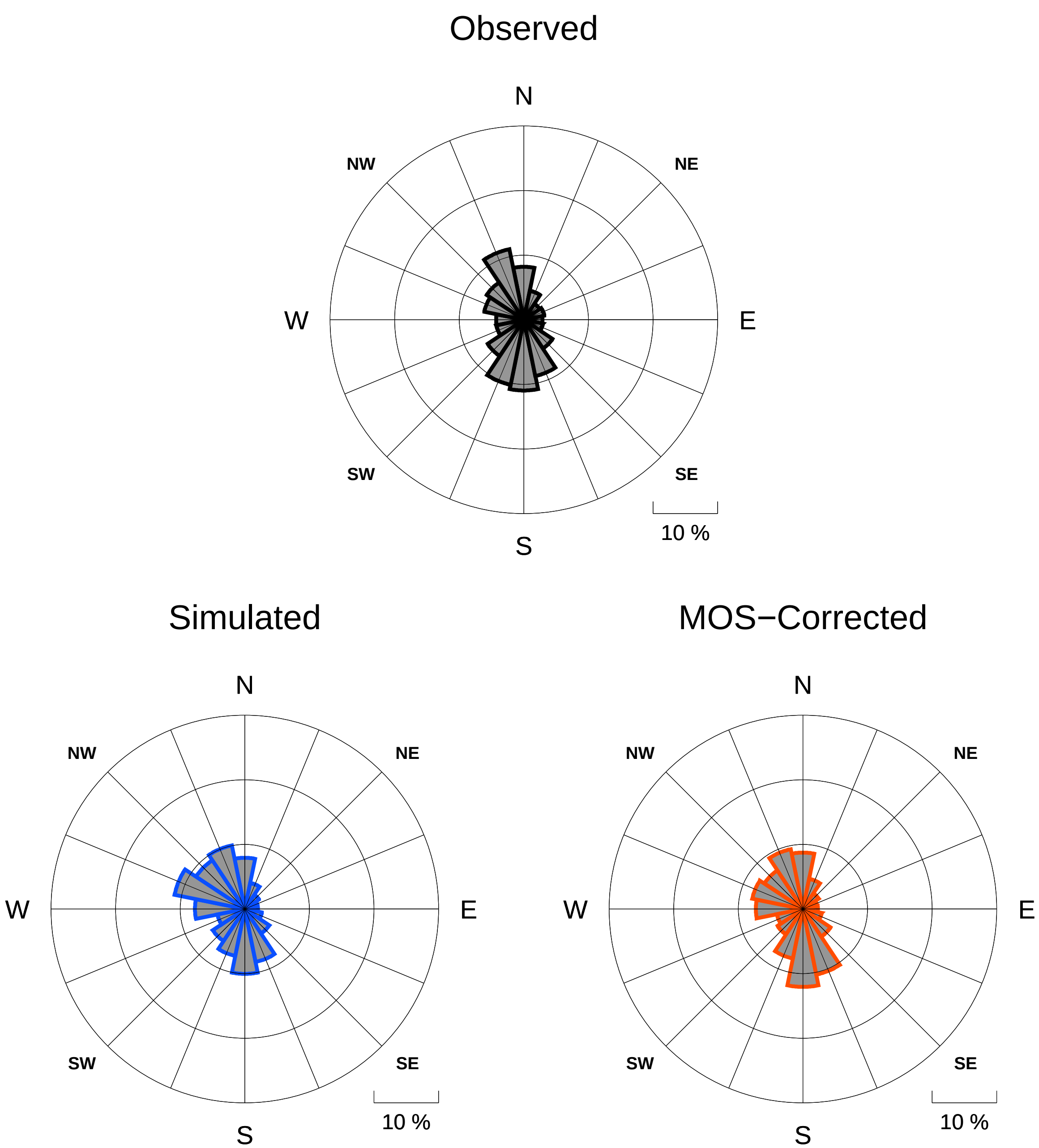

Figure 40: Wind roses at 58 m at Tower M2301 for observational data and simulated model data, averaged over the period of record (June, 2010–May, 2014). Directional bins are 22.5° wide, and the radial contour interval is 10%. Tabular formatted data, including mean wind speed values and Weibull parameters for each wind direction sector, are available in Tables 29 and 30 (p. 84).

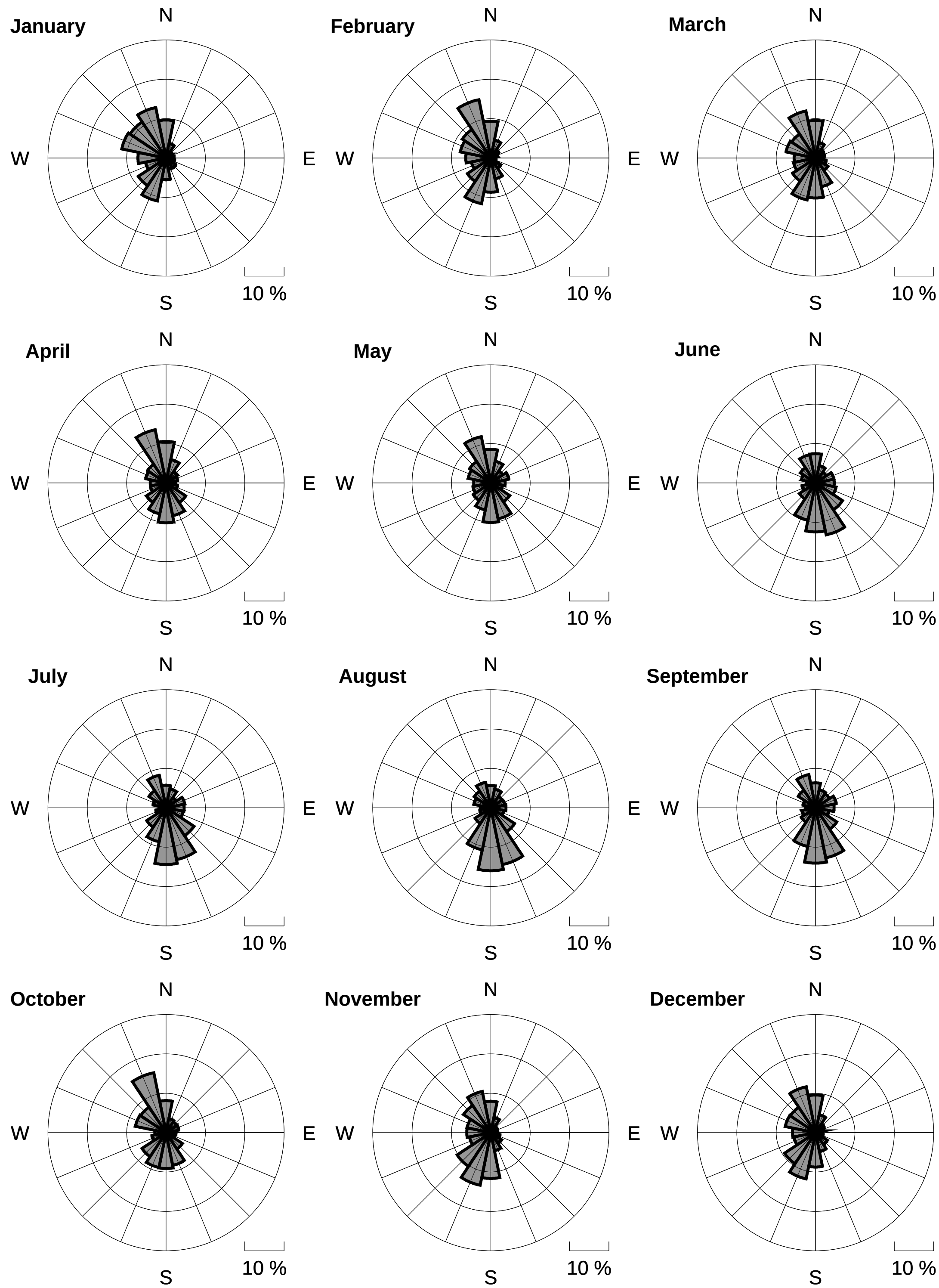

Figure 41: Wind rose of observed wind direction at 58 m at Tower M2301 for each calendar month. Directional bins are 22.5° wide, and the radial contour interval is 10%. Months missing greater than 50% of the available observations are not plotted.

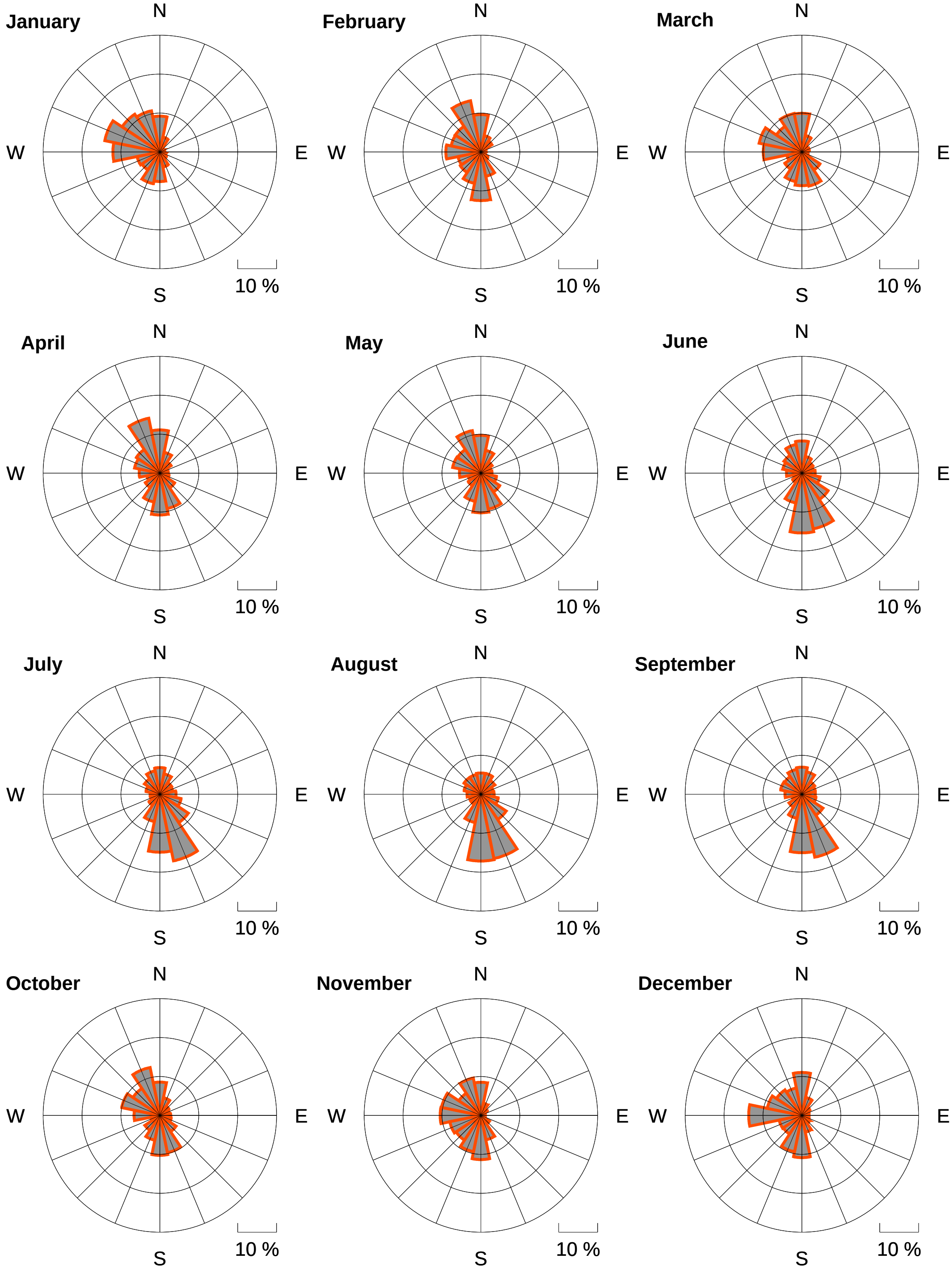

Figure 42: Wind rose of MOS-corrected wind direction at 58 m at Tower M2301 for each calendar month. Directional bins are 22.5° wide, and the radial contour interval is 10%. Months missing greater than 50% of the available observations are not plotted.

12.1.6 Diurnal Variability of Wind Speed

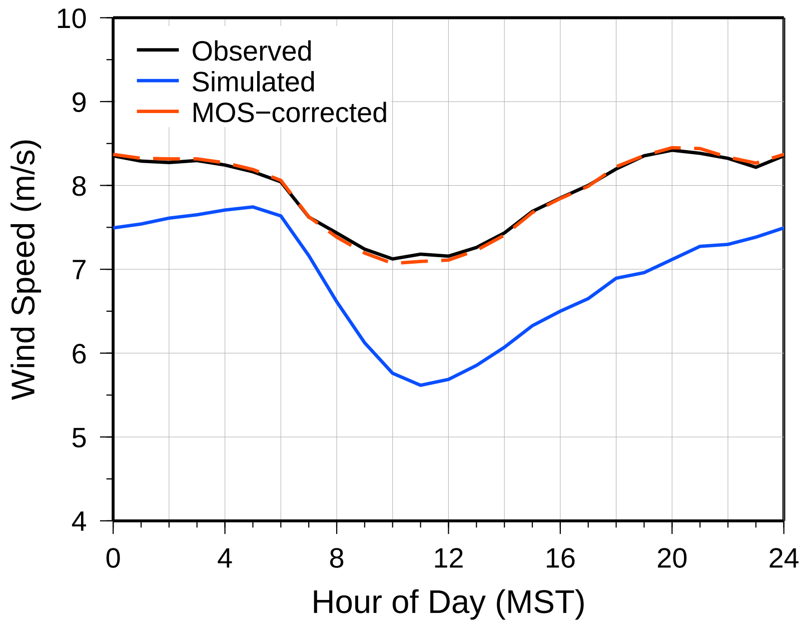

Figure 43: A comparison of the diurnal cycle of observed, simulated, and MOS-corrected 60 m wind speed at Tower M2301. Data are averaged over the period of record (June, 2010–May, 2014). Hours missing greater than 15% of the available observations are not plotted. The horizontal axis is Mountain Standard Time (MST). Tabular formatted data are available in Figures 45 and 46 (p. 80 and 81).

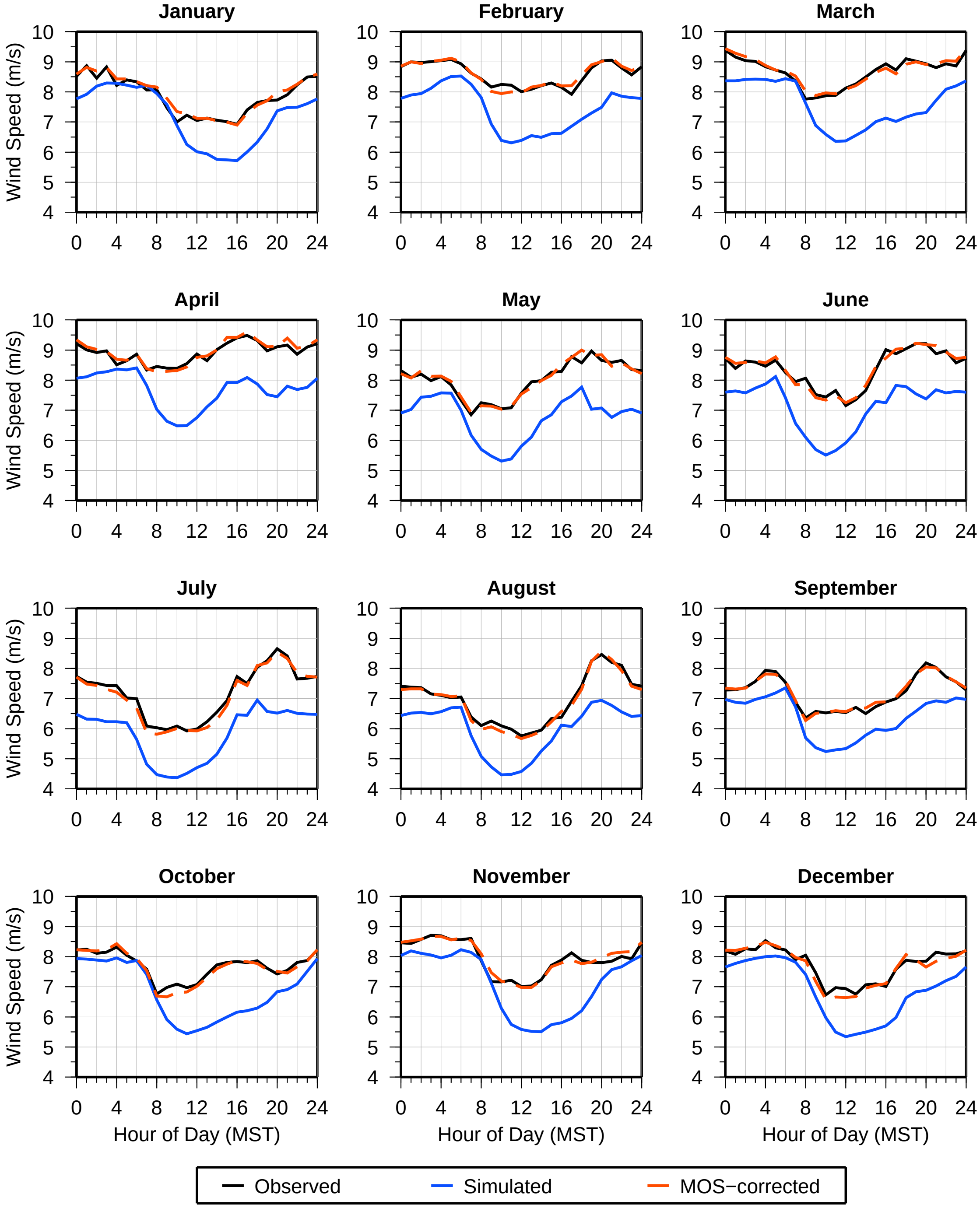

Figure 44: A comparison of the diurnal cycle of observed, simulated, and MOS-corrected $60\,m$ wind speed for each calendar month at Tower M2301. Hours missing greater than 50% of the available observations are not plotted. The horizontal axis is Mountain Standard Time (MST). Tabular formatted data available in Figures 45 and 46 (p. 80 and 81).

12.1.7 Tabular Data

Month	Observed	Simulated	Bias	MOS-corrected	Availability(%)
06/2010	8.28	6.91	-1.37	8.19	64.0
07/2010	7.13	6.01	-1.12	7.20	99.9
08/2010	7.09	6.35	-0.74	7.22	99.9
09/2010	7.77	6.86	-0.91	7.75	99.6
10/2010	7.65	6.70	-0.94	7.72	99.9
11/2010	8.55	7.31	-1.23	8.48	92.4
12/2010	7.01	6.26	-0.75	7.44	96.0
01/2011	7.59	6.50	-1.09	7.39	94.1
02/2011	8.97	7.89	-1.08	8.95	83.0
03/2011	8.83	7.33	-1.50	8.54	93.0
04/2011	9.31	7.93	-1.38	9.34	98.5
05/2011	8.76	7.42	-1.35	8.78	99.2
06/2011	8.57	7.11	-1.46	8.44	86.5
07/2011	7.04	5.85	-1.20	6.90	35.5
08/2011	6.92	5.80	-1.12	6.68	98.9
09/2011	6.35	5.55	-0.80	6.44	43.6
10/2011	–	–	–	–	0.0
11/2011	8.22	7.76	-0.46	8.47	60.3
12/2011	7.86	6.71	-1.15	7.57	93.5
01/2012	8.33	7.73	-0.60	8.40	99.7
02/2012	8.67	7.29	-1.38	8.64	70.8
03/2012	8.79	7.77	-1.02	8.88	95.2
04/2012	8.70	7.41	-1.30	8.73	94.7
05/2012	7.66	6.54	-1.12	7.82	100.0
06/2012	8.60	7.59	-1.01	8.88	100.0
07/2012	7.15	5.60	-1.54	6.94	100.0
08/2012	7.65	6.42	-1.23	7.37	100.0
09/2012	6.89	5.92	-0.98	6.76	100.0
10/2012	7.67	6.74	-0.92	7.39	94.6
11/2012	7.18	6.60	-0.58	7.23	93.9
12/2012	8.33	7.26	-1.07	8.04	93.8
01/2013	7.32	6.51	-0.81	7.36	97.8
02/2013	8.58	7.19	-1.39	8.41	86.8
03/2013	8.04	7.23	-0.82	8.33	98.3
04/2013	7.57	6.36	-1.21	7.56	78.1
05/2013	7.41	6.15	-1.27	7.34	95.0
06/2013	8.00	6.70	-1.29	7.92	99.7
07/2013	7.18	5.75	-1.44	7.08	99.9
08/2013	6.08	5.28	-0.81	6.28	99.6
09/2013	7.32	6.72	-0.61	7.50	96.7

Table 26: Monthly-mean 60 m wind speeds (m/s) at Tower M2301. Time series graph of data is available in Figure 38 (p. 71). (continued on next page)

Month	Observed	Simulated	Bias	MOS-corrected	Availability(%)
10/2013	7.78	6.93	-0.85	7.83	96.4
11/2013	7.85	6.72	-1.13	7.80	96.9
12/2013	7.65	7.23	-0.42	7.59	72.7
01/2014	8.04	7.85	-0.19	8.36	98.4
02/2014	8.04	7.18	-0.86	8.33	82.1
03/2014	8.96	7.88	-1.08	8.99	85.5
04/2014	9.71	8.58	-1.13	9.81	94.2
05/2014	11.15	9.32	-1.83	10.58	5.9
All	**7.89**	**6.86**	**-1.04**	**7.90**	**86.8**

Table 26: Monthly-mean $60\,m$ wind speeds (m/s) at Tower M2301. Time series graph of data is available in Figure 38 (p. 71). The average values shown at the bottom of the table, labeled 'All', are computed as the mean of monthly means.

Observed = mean of all available wind speed observations
Simulated = mean of simulated model output for times with observations
Bias = Simulated – Observed
MOS-corrected = mean of MOS-corrected output for times with observations

Observations

Hour of Day (MST)	Jan	Feb	Mar	Apr	May	Jun	Jly	Aug	Sep	Oct	Nov	Dec	Avg
0	8.52	8.84	9.38	9.21	8.32	8.73	7.74	7.41	7.28	8.22	8.46	8.19	8.35
1	8.87	9.00	9.16	9.00	8.10	8.39	7.54	7.38	7.29	8.25	8.44	8.08	8.29
2	8.46	8.97	9.04	8.91	8.20	8.64	7.51	7.36	7.36	8.11	8.57	8.27	8.27
3	8.83	9.00	9.01	8.98	7.99	8.60	7.44	7.15	7.57	8.15	8.71	8.23	8.30
4	8.22	9.04	8.84	8.51	8.12	8.46	7.42	7.11	7.94	8.32	8.70	8.54	8.24
5	8.40	9.08	8.72	8.65	7.84	8.66	7.02	7.03	7.90	8.05	8.56	8.30	8.16
6	8.34	8.94	8.63	8.87	7.34	8.26	6.99	7.05	7.54	7.86	8.56	8.23	8.04
7	8.06	8.62	8.36	8.33	6.85	7.96	6.08	6.39	6.87	7.59	8.60	7.90	7.62
8	8.08	8.43	7.76	8.46	7.25	8.07	6.03	6.10	6.35	6.76	7.87	8.05	7.43
9	7.47	8.16	7.80	8.40	7.18	7.52	5.96	6.25	6.57	6.98	7.17	7.46	7.24
10	7.01	8.25	7.87	8.39	7.05	7.44	6.09	6.09	6.52	7.09	7.16	6.73	7.12
11	7.22	8.22	7.89	8.55	7.08	7.66	5.92	5.98	6.57	6.97	7.22	6.97	7.18
12	7.05	8.01	8.13	8.87	7.57	7.16	5.99	5.76	6.53	7.07	7.01	6.93	7.16
13	7.13	8.08	8.26	8.65	7.94	7.35	6.23	5.85	6.71	7.41	7.03	6.76	7.26
14	7.06	8.21	8.50	9.02	7.98	7.66	6.55	5.94	6.50	7.73	7.23	7.06	7.43
15	7.01	8.29	8.75	9.23	8.27	8.35	6.93	6.33	6.73	7.81	7.71	7.10	7.69
16	6.92	8.15	8.93	9.41	8.29	9.01	7.73	6.38	6.88	7.84	7.88	7.01	7.85
17	7.45	7.93	8.61	9.45	8.87	8.91	7.52	6.88	7.05	7.86	8.05	7.57	8.00
18	7.70	8.34	9.04	9.26	8.67	9.14	7.97	7.39	7.34	7.95	7.84	7.83	8.20
19	7.68	8.81	9.01	8.93	9.01	9.20	8.27	8.22	7.89	7.68	7.83	7.78	8.35
20	7.68	8.99	8.99	9.07	8.72	9.16	8.70	8.47	8.17	7.53	7.81	7.81	8.42
21	7.85	9.03	8.85	9.13	8.66	8.83	8.34	8.30	8.02	7.63	7.85	8.13	8.38
22	8.22	8.76	8.94	8.83	8.65	8.99	7.66	8.15	7.69	7.85	7.96	8.12	8.32
23	8.49	8.52	8.84	9.05	8.37	8.56	7.74	7.50	7.47	8.00	7.89	8.15	8.22
Avg	7.82	8.56	8.64	8.89	8.02	8.36	7.14	6.94	7.20	7.70	7.92	7.71	7.89

Wind Speed (m/s): 5 6 7 8 9 10

Figure 45: Hourly-mean values of observed 60 m wind speed at Tower M2301. Hours missing greater than 50% of the available observations are not plotted. The vertical axis is Mountain Standard Time (MST). Time series graphs of data are available in Figures 43 and 44 (p. 76 and 77).

MOS−Corrected

Hour of Day (MST)

	Jan	Feb	Mar	Apr	May	Jun	Jly	Aug	Sep	Oct	Nov	Dec	Avg
0	8.59	8.86	9.44	9.34	8.21	8.76	7.72	7.30	7.34	8.23	8.48	8.21	8.37
1	8.82	9.00	9.28	9.11	8.07	8.56	7.48	7.32	7.31	8.21	8.52	8.21	8.32
2	8.70	8.94	9.17	9.02	8.31	8.59	7.43	7.32	7.35	8.19	8.59	8.28	8.32
3	8.82	9.02	9.08	8.95	8.12	8.64	7.30	7.15	7.58	8.23	8.67	8.35	8.32
4	8.43	9.06	8.88	8.70	8.13	8.57	7.21	7.13	7.82	8.43	8.67	8.48	8.27
5	8.43	9.12	8.72	8.66	7.96	8.78	6.95	7.07	7.80	8.11	8.56	8.36	8.19
6	8.34	9.00	8.70	8.86	7.44	8.32	6.68	7.09	7.59	7.95	8.61	8.23	8.06
7	8.21	8.63	8.53	8.39	6.92	7.85	5.86	6.26	6.93	7.54	8.54	7.98	7.63
8	8.16	8.42	8.02	8.28	7.15	7.86	5.81	5.98	6.26	6.69	8.10	7.86	7.38
9	7.78	8.02	7.88	8.29	7.14	7.42	5.89	6.06	6.51	6.66	7.47	7.18	7.19
10	7.34	7.94	7.97	8.32	7.03	7.34	6.01	5.90	6.54	6.80	7.18	6.59	7.07
11	7.27	8.00	7.94	8.44	7.13	7.49	5.94	5.81	6.60	6.83	7.12	6.66	7.09
12	7.12	7.97	8.09	8.76	7.53	7.25	5.93	5.67	6.56	7.01	6.98	6.64	7.11
13	7.12	8.16	8.21	8.80	7.75	7.41	6.04	5.78	6.71	7.32	6.98	6.68	7.23
14	7.04	8.22	8.42	9.00	7.99	7.83	6.29	5.91	6.69	7.60	7.21	6.95	7.41
15	7.00	8.33	8.64	9.42	8.16	8.45	6.77	6.23	6.87	7.76	7.67	7.05	7.68
16	6.90	8.20	8.79	9.42	8.52	8.73	7.60	6.57	6.89	7.87	7.79	7.11	7.84
17	7.37	8.22	8.47	9.59	8.84	8.94	7.57	6.79	7.03	7.86	7.96	7.49	7.99
18	7.57	8.59	8.83	9.35	9.04	9.00	8.14	7.39	7.42	7.77	7.81	7.97	8.22
19	7.67	8.90	8.96	9.10	8.90	9.17	8.18	8.32	7.86	7.63	7.80	7.84	8.36
20	7.92	8.94	8.97	9.03	8.91	9.17	8.57	8.55	8.15	7.58	7.88	7.73	8.45
21	7.98	9.10	8.98	9.28	8.53	9.10	8.36	8.33	8.04	7.60	7.99	7.96	8.44
22	8.18	8.78	9.13	8.89	8.63	8.96	7.84	7.97	7.76	7.75	8.04	8.08	8.34
23	8.42	8.62	9.12	8.99	8.43	8.75	7.70	7.46	7.56	7.94	8.10	8.13	8.27
Avg	7.88	8.58	8.68	8.92	8.04	8.37	7.05	6.89	7.22	7.65	7.95	7.66	7.90

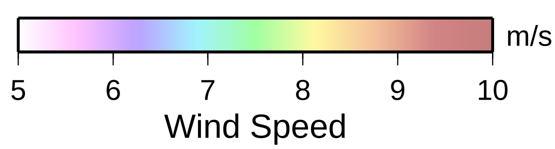

Figure 46: Hourly-mean values of MOS-corrected 60 m wind speed at Tower M2301. Hours missing greater than 50% of the available observations are not plotted. The vertical axis is Mountain Standard Time (MST). Time series graphs of data are available in Figures 43 and 44 (p. 76 and 77).

Wind Speed (m/s)	N	NNE	NE	ENE	E	ESE	SE	SSE	S	SSW	SW	WSW	W	WNW	NW	NNW	All
0 - 0.5	0.00	0.00	0.01	0.00	0.00	0.01	0.00	0.01	0.00	0.00	0.01	0.00	0.01	0.01	0.01	0.01	0.07
0.5 - 1.5	0.11	0.10	0.10	0.11	0.10	0.09	0.07	0.05	0.06	0.07	0.08	0.08	0.10	0.09	0.10	0.08	1.38
1.5 - 2.5	0.26	0.25	0.26	0.29	0.27	0.24	0.26	0.28	0.20	0.25	0.20	0.21	0.23	0.22	0.26	0.22	3.88
2.5 - 3.5	0.36	0.33	0.33	0.46	0.34	0.41	0.42	0.42	0.36	0.37	0.32	0.30	0.30	0.37	0.39	0.42	5.91
3.5 - 4.5	0.48	0.39	0.37	0.51	0.45	0.53	0.50	0.60	0.50	0.57	0.37	0.40	0.36	0.44	0.44	0.52	7.43
4.5 - 5.5	0.55	0.50	0.41	0.50	0.42	0.40	0.66	0.73	0.72	0.74	0.45	0.35	0.35	0.60	0.55	0.65	8.58
5.5 - 6.5	0.67	0.53	0.41	0.38	0.39	0.37	0.65	0.89	1.12	0.95	0.57	0.34	0.42	0.62	0.66	0.90	9.86
6.5 - 7.5	0.68	0.54	0.32	0.32	0.27	0.24	0.64	1.06	1.30	1.12	0.63	0.36	0.43	0.68	0.76	1.04	10.38
7.5 - 8.5	0.77	0.51	0.31	0.25	0.22	0.20	0.51	0.98	1.44	1.19	0.59	0.37	0.37	0.64	0.79	1.07	10.22
8.5 - 9.5	0.70	0.40	0.20	0.22	0.18	0.14	0.43	0.93	1.44	1.19	0.59	0.33	0.35	0.54	0.73	1.12	9.51
9.5 - 10.5	0.63	0.26	0.08	0.08	0.09	0.14	0.37	0.85	1.22	1.16	0.62	0.29	0.31	0.63	0.62	1.04	8.41
10.5 - 11.5	0.67	0.27	0.05	0.06	0.05	0.08	0.23	0.69	0.92	0.97	0.62	0.32	0.29	0.44	0.54	0.90	7.09
11.5 - 12.5	0.50	0.16	0.05	0.02	0.03	0.05	0.19	0.51	0.62	0.72	0.52	0.28	0.23	0.34	0.33	0.67	5.22
12.5 - 13.5	0.40	0.12	0.03	0.00	0.01	0.02	0.13	0.32	0.44	0.42	0.36	0.26	0.17	0.23	0.21	0.50	3.63
13.5 - 14.5	0.34	0.08	0.01	0.00	0.01	0.01	0.08	0.18	0.21	0.17	0.32	0.16	0.13	0.16	0.12	0.43	2.40
14.5 - 15.5	0.28	0.03	0.00	0.00	0.01	0.00	0.05	0.12	0.10	0.10	0.19	0.10	0.09	0.08	0.09	0.37	1.61
15.5 - 16.5	0.16	0.03	0.00	0.00	0.00	0.01	0.03	0.07	0.04	0.04	0.09	0.04	0.03	0.04	0.06	0.24	0.89
16.5 - 17.5	0.17	0.01	0.00	0.00	0.00	0.00	0.01	0.02	0.03	0.02	0.05	0.05	0.03	0.01	0.04	0.19	0.65
17.5 - 18.5	0.12	0.00	0.00	0.00	0.00	0.01	0.01	0.02	0.03	0.03	0.03	0.03	0.01	0.01	0.03	0.15	0.47
18.5 - 19.5	0.09	0.00	0.00	0.00	0.00	0.00	0.01	0.00	0.00	0.02	0.02	0.01	0.00	0.01	0.04	0.13	0.35
19.5 - 20.5	0.03	0.00	0.00	0.00	0.00	0.00	0.00	0.01	0.01	0.01	0.01	0.00	0.01	0.00	0.01	0.09	0.19
20.5 - 21.5	0.04	0.01	0.00	0.00	0.00	0.00	0.00	0.01	0.01	0.01	0.00	0.00	0.00	0.00	0.00	0.07	0.14
21.5 - 22.5	0.02	0.00	0.00	0.00	0.00	0.00	0.00	0.00	0.01	0.00	0.00	0.00	0.00	0.01	0.00	0.05	0.09
22.5 - 23.5	0.01	0.00	0.00	0.00	0.00	0.00	0.00	0.00	0.01	0.00	0.00	0.00	0.00	0.00	0.00	0.03	0.06
23.5 - 24.5	0.01	0.00	0.00	0.00	0.00	0.00	0.00	0.00	0.01	0.00	0.00	0.00	0.00	0.00	0.00	0.03	0.05
> 24.5	0.01	0.00	0.00	0.00	0.00	0.00	0.00	0.00	0.01	0.00	0.00	0.00	0.00	0.01	0.00	0.05	0.08

Table 27: Distribution of observed 60 m wind speed by direction at Tower M2301. Histogram of data is available in Figure 39 (p. 72).

Wind Speed (m/s)	N	NNE	NE	ENE	E	ESE	SE	SSE	S	SSW	SW	WSW	W	WNW	NW	NNW	All
0 - 0.5	0.00	0.00	0.00	0.00	0.01	0.04	0.06	0.04	0.00	0.00	0.00	0.00	0.00	0.00	0.00	0.00	0.15
0.5 - 1.5	0.02	0.03	0.06	0.13	0.14	0.19	0.19	0.26	0.09	0.02	0.02	0.01	0.03	0.03	0.03	0.03	1.28
1.5 - 2.5	0.15	0.21	0.30	0.27	0.29	0.26	0.34	0.44	0.40	0.27	0.13	0.17	0.15	0.13	0.13	0.16	3.82
2.5 - 3.5	0.42	0.51	0.41	0.32	0.34	0.30	0.40	0.52	0.50	0.41	0.42	0.24	0.23	0.25	0.31	0.35	5.92
3.5 - 4.5	0.62	0.55	0.46	0.32	0.29	0.43	0.59	0.68	0.66	0.58	0.42	0.39	0.35	0.46	0.42	0.45	7.67
4.5 - 5.5	0.62	0.66	0.42	0.31	0.25	0.40	0.65	0.89	0.96	0.57	0.52	0.39	0.44	0.60	0.50	0.60	8.79
5.5 - 6.5	0.80	0.56	0.31	0.23	0.23	0.30	0.61	1.08	1.12	0.75	0.48	0.49	0.62	0.81	0.77	0.77	9.94
6.5 - 7.5	0.85	0.47	0.30	0.16	0.19	0.25	0.46	1.09	1.29	0.91	0.46	0.40	0.72	0.94	0.87	0.95	10.33
7.5 - 8.5	0.79	0.38	0.21	0.16	0.19	0.21	0.44	1.08	1.41	1.04	0.44	0.36	0.75	0.99	0.90	0.81	10.14
8.5 - 9.5	0.69	0.35	0.12	0.10	0.14	0.15	0.36	1.01	1.36	0.79	0.42	0.40	0.87	0.96	0.82	0.83	9.38
9.5 - 10.5	0.67	0.31	0.09	0.10	0.12	0.11	0.27	0.86	1.24	0.69	0.37	0.28	0.77	0.97	0.72	0.74	8.30
10.5 - 11.5	0.65	0.23	0.06	0.05	0.04	0.10	0.26	0.81	1.04	0.65	0.28	0.29	0.63	0.65	0.59	0.70	7.03
11.5 - 12.5	0.57	0.18	0.07	0.02	0.01	0.07	0.18	0.63	0.72	0.30	0.22	0.20	0.59	0.51	0.35	0.60	5.21
12.5 - 13.5	0.49	0.12	0.03	0.01	0.03	0.04	0.08	0.32	0.50	0.27	0.13	0.18	0.46	0.26	0.22	0.50	3.62
13.5 - 14.5	0.42	0.05	0.01	0.01	0.02	0.03	0.09	0.23	0.27	0.13	0.10	0.10	0.23	0.17	0.13	0.40	2.39
14.5 - 15.5	0.27	0.05	0.02	0.01	0.00	0.01	0.04	0.13	0.15	0.12	0.08	0.05	0.14	0.07	0.08	0.39	1.60
15.5 - 16.5	0.16	0.01	0.01	0.00	0.01	0.01	0.02	0.06	0.07	0.04	0.06	0.03	0.10	0.03	0.05	0.26	0.89
16.5 - 17.5	0.13	0.00	0.00	0.00	0.01	0.00	0.01	0.03	0.02	0.04	0.05	0.02	0.08	0.02	0.07	0.17	0.65
17.5 - 18.5	0.08	0.01	0.00	0.00	0.00	0.00	0.01	0.02	0.03	0.04	0.02	0.01	0.02	0.00	0.04	0.21	0.47
18.5 - 19.5	0.07	0.01	0.00	0.00	0.00	0.00	0.00	0.02	0.00	0.03	0.02	0.02	0.01	0.01	0.03	0.13	0.34
19.5 - 20.5	0.07	0.00	0.00	0.00	0.00	0.00	0.00	0.00	0.01	0.02	0.00	0.00	0.00	0.00	0.01	0.07	0.19
20.5 - 21.5	0.04	0.00	0.00	0.00	0.00	0.00	0.00	0.00	0.01	0.00	0.01	0.00	0.00	0.01	0.01	0.07	0.14
21.5 - 22.5	0.03	0.00	0.00	0.00	0.00	0.00	0.00	0.00	0.01	0.01	0.00	0.00	0.00	0.00	0.00	0.02	0.09
22.5 - 23.5	0.01	0.00	0.00	0.00	0.00	0.00	0.00	0.00	0.00	0.01	0.00	0.00	0.00	0.00	0.01	0.03	0.06
23.5 - 24.5	0.02	0.00	0.00	0.00	0.00	0.00	0.00	0.00	0.00	0.01	0.00	0.00	0.00	0.00	0.01	0.01	0.05
> 24.5	0.00	0.00	0.00	0.00	0.00	0.00	0.00	0.00	0.01	0.00	0.00	0.00	0.00	0.00	0.01	0.05	0.08

Table 28: Distribution of MOS-corrected 60 m wind speed by direction at Tower M2301. All model values are computed only for times with valid observations. Histogram of data is available in Figure 39 (p. 72).

Sector	Mean Speed(m/s)	Weibull Scale(A)	Weibull Shape(k)	Frequency(%)
N	9.12	10.30	2.22	8.20
NNE	7.01	7.92	2.26	4.58
NE	5.65	6.38	2.23	2.97
ENE	5.27	5.95	2.25	3.23
E	5.42	6.12	2.21	2.88
ESE	5.57	6.29	2.02	3.00
SE	6.98	7.88	2.29	5.34
SSE	7.98	8.98	2.63	8.87
S	8.34	9.35	2.87	10.95
SSW	8.31	9.33	2.84	10.27
SW	8.70	9.80	2.51	6.74
WSW	8.05	9.09	2.13	4.34
W	7.61	8.60	2.12	4.29
WNW	7.78	8.78	2.38	6.26
NW	7.93	8.95	2.33	6.92
NNW	9.50	10.72	2.27	11.15
ALL	**7.89**	**8.91**	**2.25**	**100.00**

Table 29: Observed 60 m mean wind speed, Weibull parameters, and frequency at Tower M2301. Blank values correspond to times with less than 10 data points. Wind rose of data is available in Figure 40 (p. 73).

Sector	Mean Speed(m/s)	Weibull Scale(A)	Weibull Shape(k)	Frequency(%)
N	9.08	10.25	2.32	8.74
NNE	6.74	7.61	2.25	4.76
NE	5.53	6.24	2.04	2.91
ENE	5.15	5.80	1.93	2.25
E	5.32	5.99	1.81	2.32
ESE	5.58	6.27	1.78	2.96
SE	6.43	7.25	1.97	5.13
SSE	7.70	8.69	2.35	10.36
S	8.18	9.21	2.63	12.05
SSW	8.00	9.03	2.43	7.81
SW	7.66	8.64	2.23	4.72
WSW	7.68	8.67	2.37	4.10
W	8.85	9.93	2.87	7.29
WNW	8.25	9.24	2.98	7.99
NW	8.32	9.38	2.54	7.17
NNW	9.74	10.99	2.29	9.44
ALL	**7.90**	**8.92**	**2.25**	**100.00**

Table 30: MOS-corrected 60 m mean wind speed, Weibull parameters, and frequency at Tower M2301. All MOS-corrected model values are computed only for times with valid observations; blank values correspond to times with less than 10 data points. Wind rose of data is available in Figure 40 (p. 73).

12.2 Validation of Model Results at Tower M2327

This section examines the quality of the NWP simulations used at a single point within the study area. For this section, the observations were taken at Tower M2327 (latitude 39.22934, longitude -103.83809).

The average observed wind speed (for all valid observational times) at $60.0\,m$ during the 43 months of the period of record (November, 2010 to May, 2014) is $8.14\,m/s$ with an hourly standard deviation of $4.01\,m/s$ at Tower M2327. This compares to a modeled $60\,m$ wind speed of $7.00\,m/s$ with a $3.30\,m/s$ standard deviation for these same times.

Based on a comparison of the NWP model output with observations from each of the meteorological towers for which data were provided, Model Output Statistics (MOS) was constructed. MOS uses a multilinear regression model designed to remove the bias and adjust the variance of the raw NWP simulated wind speed and direction. Applying this statistical model to the simulated data at Tower M2327 results in a MOS-corrected mean value of $8.14\,m/s$ and an hourly standard deviation of $4.01\,m/s$.

This section presents a comparison of the simulated winds with the observations at the reference tower (Tower M2327). The focus of the verification is on the model's ability to reproduce the observed variability of the wind resource at daily and monthly time scales, while preserving the distribution of hourly wind speeds and the diurnal characteristics of the wind.

12.2.1 Observational Data

Approximately 43 months of wind speed data at $60.0\,meters$ and wind direction data at $59.0\,meters$ (November, 2010 to May, 2014) from a meteorological tower (Tower M2327) at Rush Creek I were used in this analysis. This tower will be referred to as the reference tower throughout this section. The data at $60\,m$ were used to assess the quality of the model simulations at $60\,m$.

It should be noted that meteorological observations provided to 3TIER are not allowed to influence the raw model simulations.

12.2.2 Model Validation Statistics

Table 31 presents some basic statistical measures of the model performance relative to the measured winds at the reference tower during the observational period. Also shown are values (labeled "MOS-corrected") for model data with the statistical model applied. For reference, the correlation of the reference tower data to itself is perfect and hence the explained variance (r^2) value is 1.0.

The observed and modeled winds in this section represent the mean of all times during the month for which a valid wind speed or direction observation was available. Therefore they should not be interpreted as estimates of the true winds at the site, but rather a verification of the model's ability to reproduce the available observations. Any month or hour missing greater than 50% of the available observations is omitted from the following figures, tables, and statistics.

Comparison	Value
Correlation of monthly-mean simulated wind speed to observed	0.90
RMS error of monthly-mean simulated wind speed	1.15 m/s
Correlation of monthly-mean MOS-corrected wind speed to observed	0.96
RMS error of monthly-mean MOS-corrected wind speed	0.24 m/s
Correlation of daily-mean simulated wind speed to observed	0.85
RMS error of daily-mean simulated wind speed	1.79 m/s
Correlation of daily-mean MOS-corrected wind speed to observed	0.89
RMS error of daily-mean MOS-corrected wind speed	1.20 m/s

Table 31: Correlation and root mean square (RMS) error statistics of modeled wind speeds.

12.2.3 Monthly Mean Wind Speed

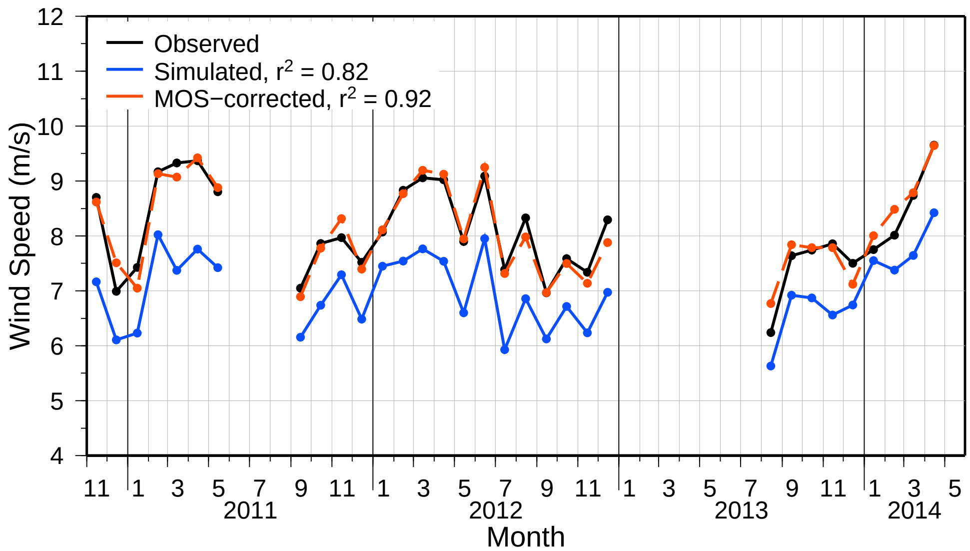

Figure 47: A comparison of the observed, simulated, and MOS-corrected monthly-mean $60\,m$ wind speed at Tower M2327. Explained variance(r^2) value of each data source relative to the monthly reference tower wind speeds are shown in the legend. Months missing greater than 50% of the available observations are not plotted. Tabular formatted data are available in Table 32 (p. 95).

12.2.4 Wind Speed Distribution

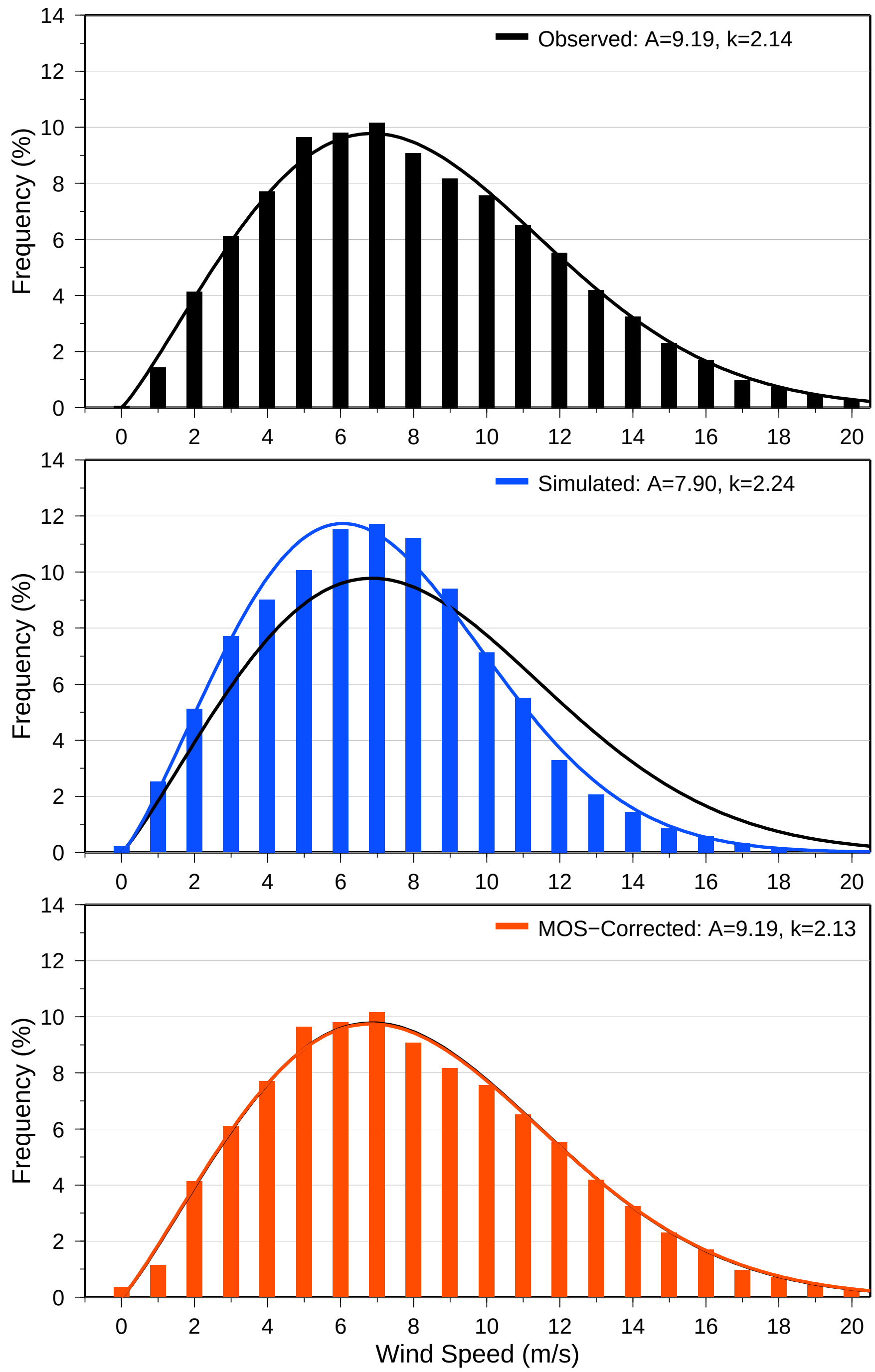

Figure 48: A comparison of the observed, simulated, and MOS-corrected hourly wind speed distributions at $60\,m$ at Tower M2327 during the period of record, using $1\,m/s$ bins. ($0\,m/s$ bin contains only values ≤ 0.5) Fitted Weibull distributions are also displayed with the scale(A) and shape(k) parameters listed in the legend.

12.2.5 Wind Direction Distribution

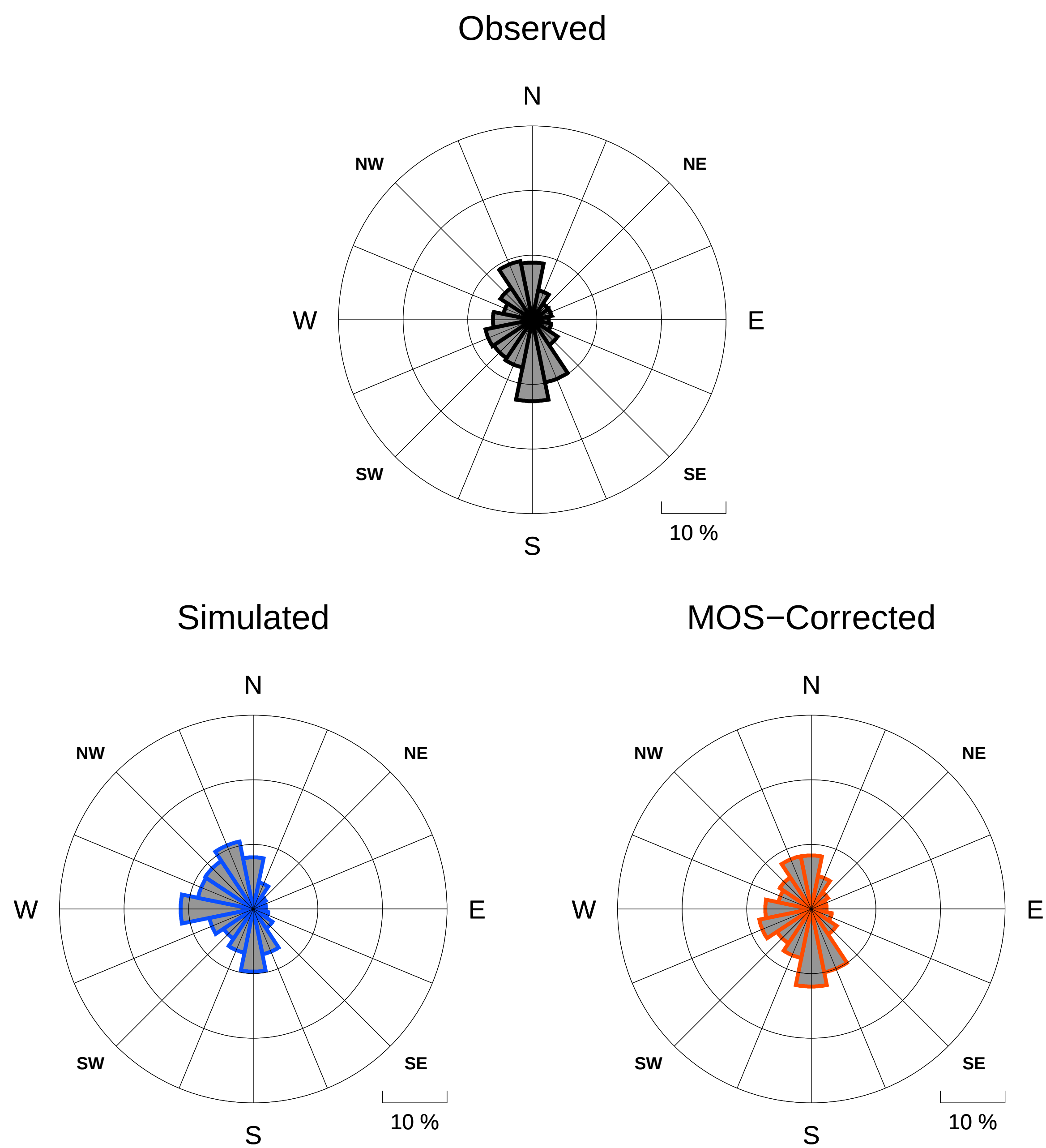

Figure 49: Wind roses at 59 m at Tower M2327 for observational data and simulated model data, averaged over the period of record (November, 2010–May, 2014). Directional bins are 22.5° wide, and the radial contour interval is 10%. Tabular formatted data, including mean wind speed values and Weibull parameters for each wind direction sector, are available in Tables 35 and 36 (p. 100).

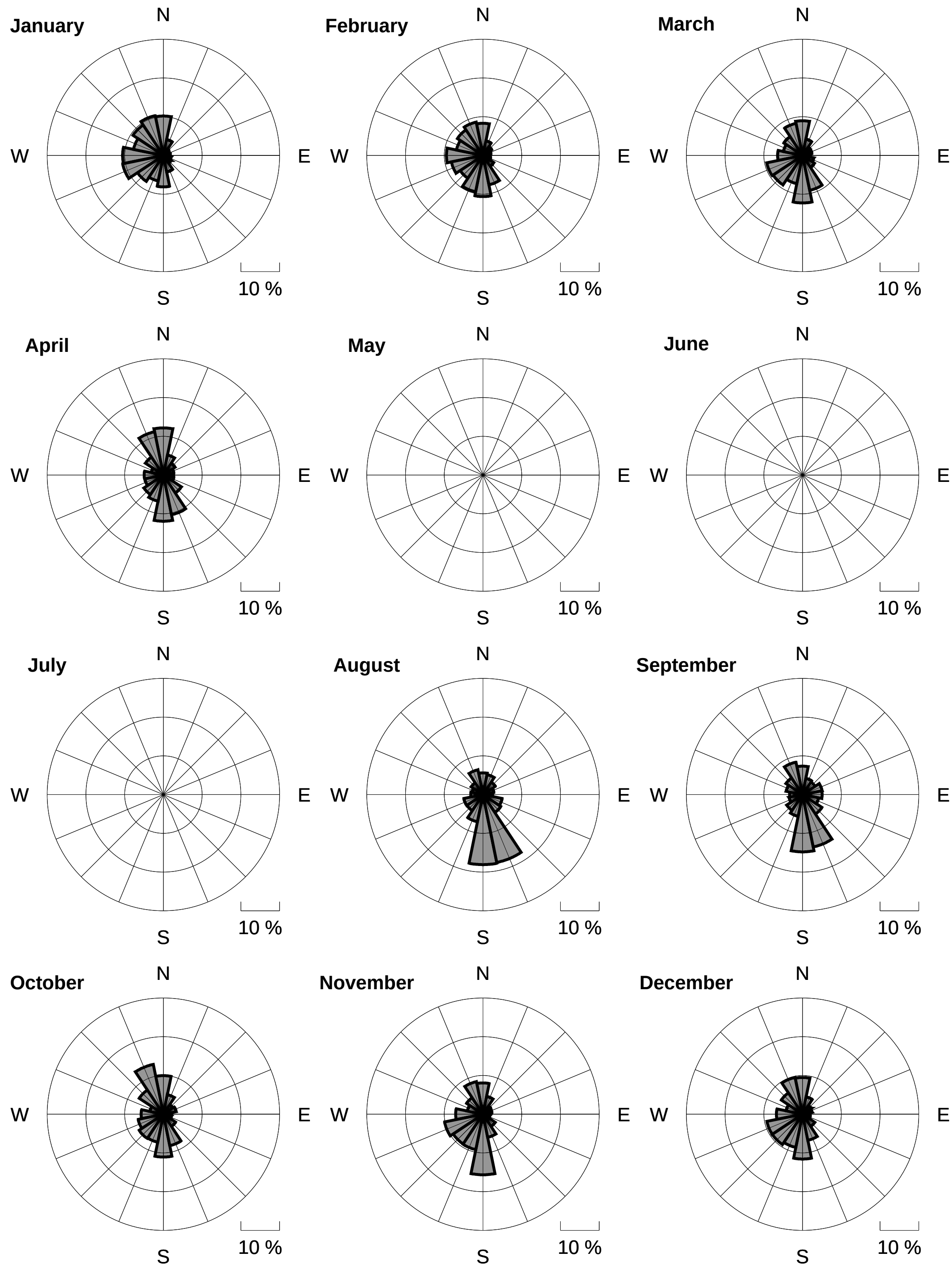

Figure 50: Wind rose of observed wind direction at $59\,m$ at Tower M2327 for each calendar month. Directional bins are 22.5° wide, and the radial contour interval is 10%. Months missing greater than 50% of the available observations are not plotted.

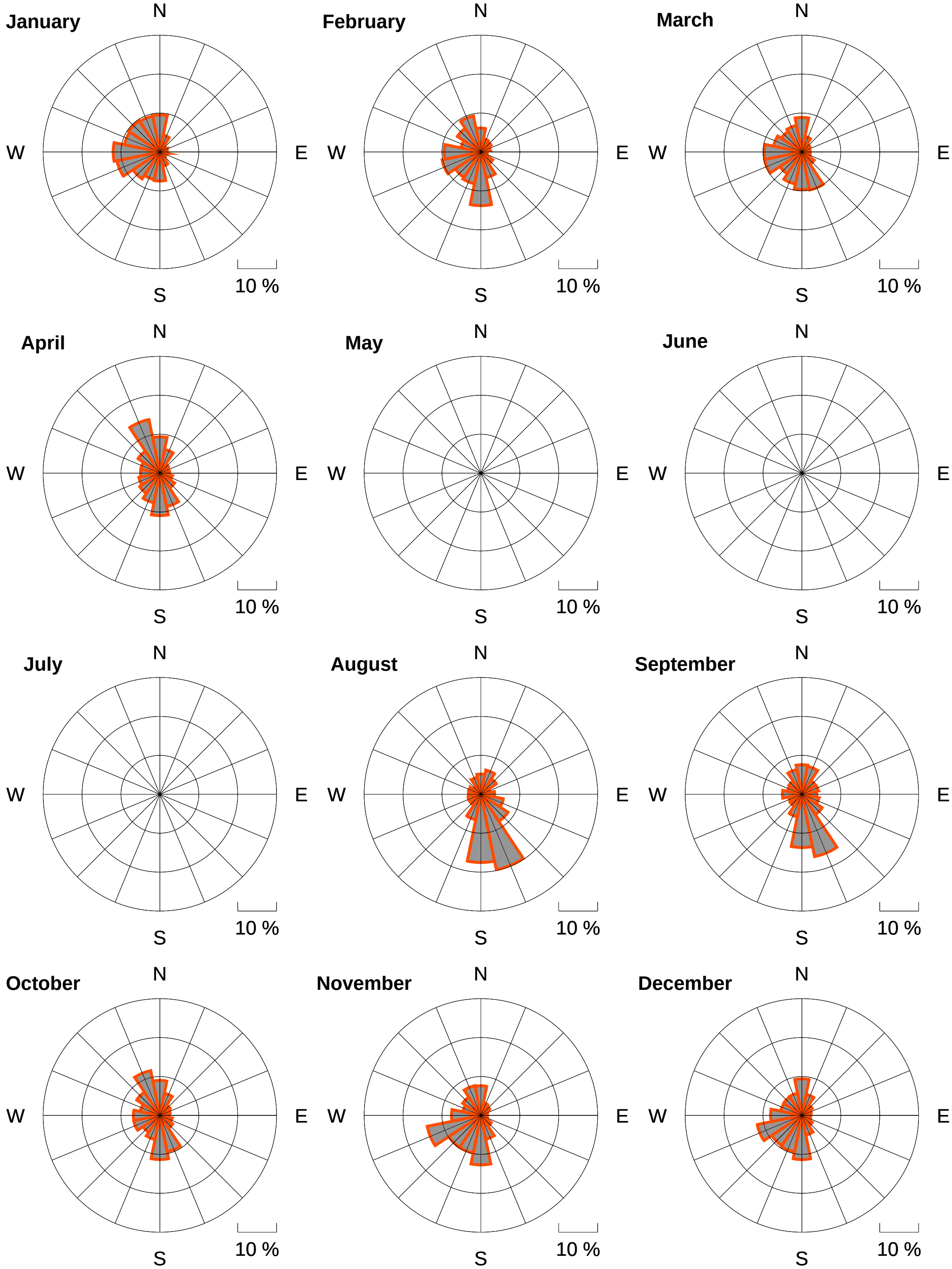

Figure 51: Wind rose of MOS-corrected wind direction at 59 m at Tower M2327 for each calendar month. Directional bins are 22.5° wide, and the radial contour interval is 10%. Months missing greater than 50% of the available observations are not plotted.

12.2.6 Diurnal Variability of Wind Speed

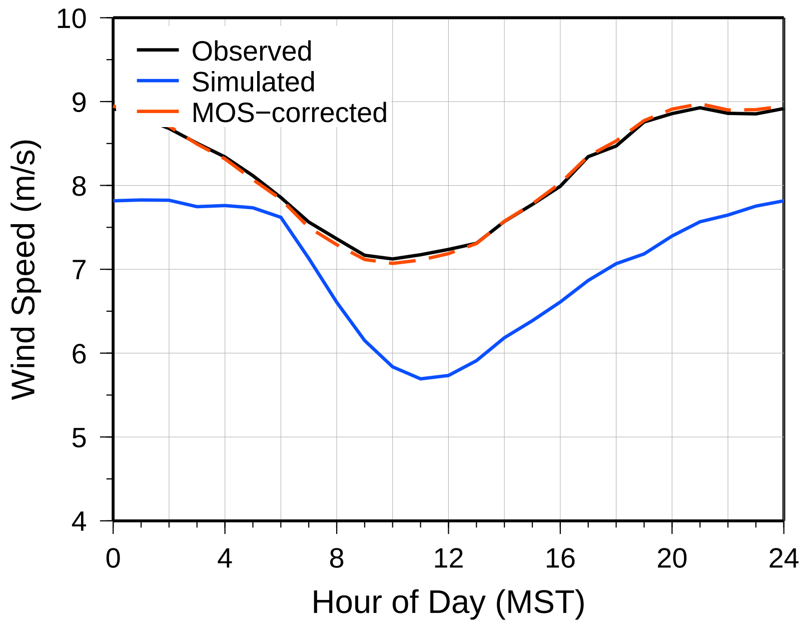

Figure 52: A comparison of the diurnal cycle of observed, simulated, and MOS-corrected 60 m wind speed at Tower M2327. Data are averaged over the period of record (November, 2010–May, 2014). Hours missing greater than 15% of the available observations are not plotted. The horizontal axis is Mountain Standard Time (MST). Tabular formatted data are available in Figures 54 and 55 (p. 96 and 97).

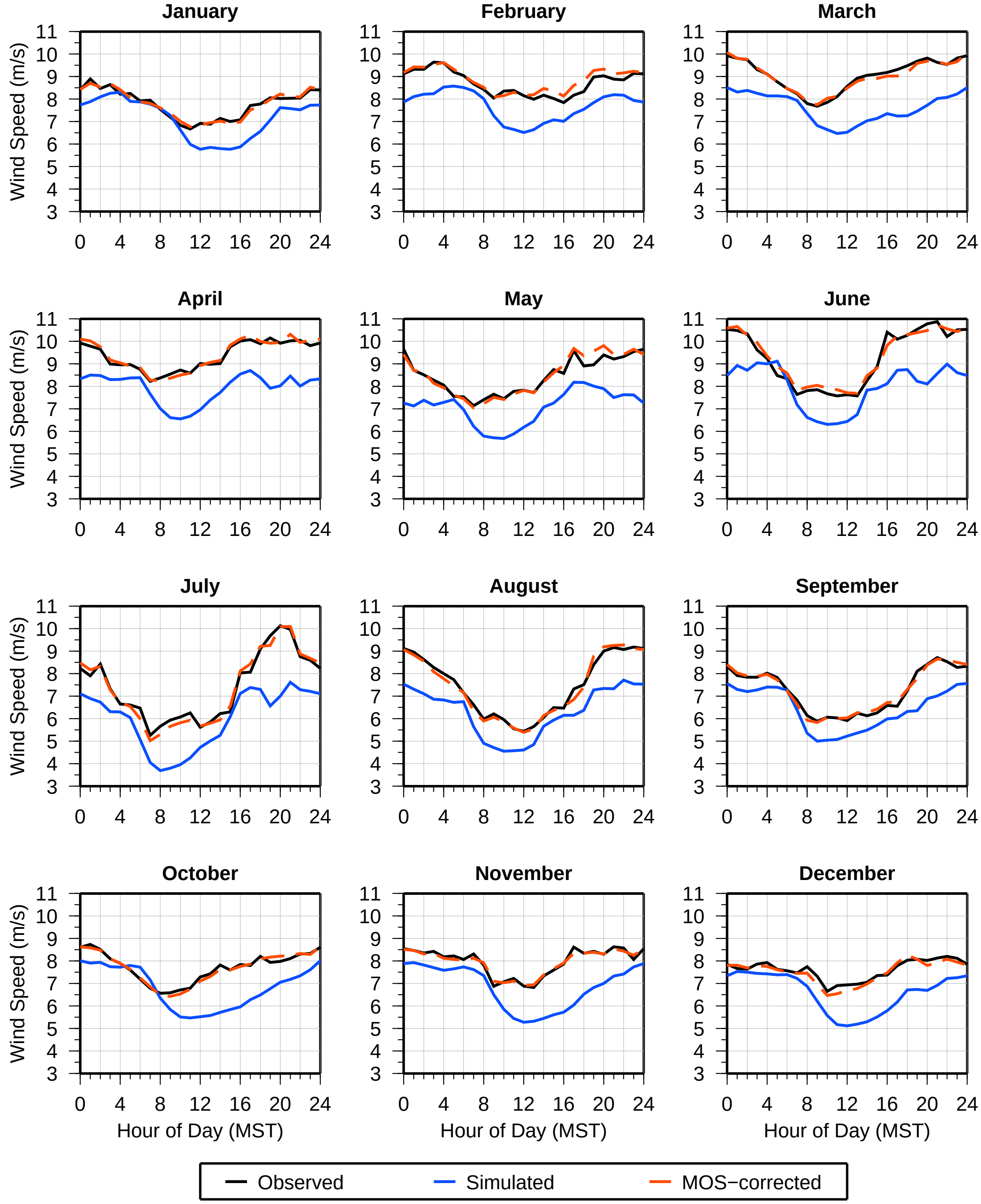

Figure 53: A comparison of the diurnal cycle of observed, simulated, and MOS-corrected $60\,m$ wind speed for each calendar month at Tower M2327. Hours missing greater than 50% of the available observations are not plotted. The horizontal axis is Mountain Standard Time (MST). Tabular formatted data available in Figures 54 and 55 (p. 96 and 97).

12.2.7 Tabular Data

Month	Observed	Simulated	Bias	MOS-corrected	Availability(%)
11/2010	8.70	7.16	-1.54	8.62	82.1
12/2010	6.99	6.11	-0.88	7.51	95.2
01/2011	7.43	6.23	-1.20	7.05	88.7
02/2011	9.17	8.02	-1.15	9.13	77.1
03/2011	9.33	7.38	-1.95	9.07	90.1
04/2011	9.37	7.76	-1.61	9.42	98.6
05/2011	8.80	7.42	-1.38	8.88	97.6
06/2011	10.04	8.27	-1.77	9.85	23.6
07/2011	–	–	–	–	0.0
08/2011	6.93	5.66	-1.27	6.51	26.1
09/2011	7.05	6.16	-0.90	6.89	99.9
10/2011	7.86	6.74	-1.12	7.78	92.7
11/2011	7.97	7.29	-0.68	8.32	94.0
12/2011	7.52	6.49	-1.04	7.40	85.1
01/2012	8.07	7.45	-0.62	8.11	99.2
02/2012	8.83	7.54	-1.29	8.77	75.9
03/2012	9.06	7.76	-1.29	9.19	94.2
04/2012	9.02	7.54	-1.48	9.12	94.6
05/2012	7.90	6.60	-1.30	7.94	100.0
06/2012	9.09	7.95	-1.14	9.25	100.0
07/2012	7.39	5.93	-1.45	7.32	99.9
08/2012	8.33	6.86	-1.47	7.98	100.0
09/2012	6.96	6.12	-0.84	6.97	100.0
10/2012	7.59	6.72	-0.87	7.50	88.0
11/2012	7.34	6.24	-1.10	7.14	91.4
12/2012	8.29	6.97	-1.32	7.88	98.5
01/2013	3.80	3.79	-0.00	5.50	0.1
02/2013	–	–	–	–	0.0
03/2013	–	–	–	–	0.0
04/2013	–	–	–	–	0.0
05/2013	–	–	–	–	0.0
06/2013	–	–	–	–	0.0
07/2013	–	–	–	–	0.0
08/2013	6.24	5.63	-0.61	6.77	71.4

Table 32: Monthly-mean 60 m wind speeds (m/s) at Tower M2327. Time series graph of data is available in Figure 47 (p. 87). (continued on next page)

Month	Observed	Simulated	Bias	MOS-corrected	Availability(%)
09/2013	7.64	6.92	-0.72	7.84	100.0
10/2013	7.74	6.87	-0.87	7.79	96.5
11/2013	7.86	6.56	-1.30	7.79	96.0
12/2013	7.50	6.74	-0.76	7.12	74.1
01/2014	7.75	7.55	-0.20	8.01	95.7
02/2014	8.01	7.38	-0.64	8.49	78.1
03/2014	8.74	7.64	-1.09	8.79	84.3
04/2014	9.65	8.42	-1.23	9.65	93.6
05/2014	11.10	9.23	-1.87	10.06	5.9
All	**8.14**	**7.00**	**-1.14**	**8.14**	**69.5**

Table 32: Monthly-mean $60\,m$ wind speeds (m/s) at Tower M2327. Time series graph of data is available in Figure 47 (p. 87). The average values shown at the bottom of the table, labeled 'All', are computed as the mean of monthly means.

Observed = mean of all available wind speed observations
Simulated = mean of simulated model output for times with observations
Bias = Simulated – Observed
MOS-corrected = mean of MOS-corrected output for times with observations

Observations

Hour of Day (MST)	Jan	Feb	Mar	Apr	May	Jun	Jly	Aug	Sep	Oct	Nov	Dec	Avg
0	8.41	9.12	9.93	9.93	9.65	10.53	8.23	9.13	8.33	8.61	8.54	7.85	8.92
1	8.90	9.32	9.81	9.79	8.72	10.48	7.90	8.96	7.92	8.74	8.47	7.66	8.81
2	8.47	9.32	9.74	9.66	8.52	10.34	8.43	8.64	7.85	8.51	8.36	7.64	8.68
3	8.64	9.65	9.31	9.00	8.28	9.62	7.33	8.28	7.85	8.09	8.43	7.87	8.50
4	8.22	9.61	9.12	8.96	8.06	9.23	6.65	8.00	8.02	7.90	8.19	7.93	8.34
5	8.25	9.20	8.77	8.98	7.55	8.48	6.61	7.74	7.83	7.60	8.23	7.63	8.12
6	7.92	9.04	8.47	8.76	7.53	8.34	6.47	7.15	7.29	7.19	8.07	7.57	7.86
7	7.95	8.67	8.24	8.23	7.14	7.65	5.25	6.62	6.82	6.79	8.31	7.48	7.56
8	7.55	8.43	7.80	8.37	7.41	7.81	5.66	5.98	6.15	6.56	7.82	7.75	7.36
9	7.19	8.05	7.68	8.54	7.66	7.86	5.94	6.21	5.89	6.59	6.87	7.32	7.17
10	6.83	8.35	7.85	8.73	7.45	7.68	6.08	5.96	6.06	6.72	7.08	6.65	7.12
11	6.67	8.38	8.11	8.59	7.78	7.58	6.26	5.56	6.03	6.79	7.23	6.91	7.17
12	6.92	8.15	8.57	9.01	7.83	7.63	5.61	5.44	5.92	7.29	6.88	6.94	7.24
13	6.88	8.00	8.93	8.98	7.73	7.58	5.85	5.65	6.25	7.43	6.83	6.97	7.31
14	7.14	8.18	9.06	9.02	8.26	8.26	6.22	6.05	6.13	7.83	7.33	7.05	7.57
15	7.00	8.02	9.11	9.76	8.75	8.88	6.30	6.50	6.26	7.60	7.60	7.35	7.77
16	7.07	7.84	9.18	10.01	8.57	10.41	8.04	6.47	6.59	7.85	7.87	7.37	7.99
17	7.70	8.11	9.22	10.04	9.74	10.29	7.90	7.16	6.66	7.86	8.59	7.80	8.34
18	7.80	8.31	9.38	9.89	9.00	10.44	8.97	7.55	7.19	8.32	8.25	8.04	8.47
19	8.00	8.87	9.68	10.15	9.08	10.50	9.75	8.34	8.13	8.06	8.38	8.08	8.76
20	8.00	9.07	9.72	9.91	9.44	10.88	10.25	8.97	8.41	8.12	8.27	7.98	8.86
21	8.09	8.80	9.65	9.99	9.25	11.00	9.86	9.19	8.76	8.23	8.55	8.07	8.93
22	8.11	8.74	9.58	10.02	9.29	10.37	8.86	9.02	8.59	8.41	8.52	8.12	8.86
23	8.47	9.05	9.78	9.83	9.46	10.65	8.76	9.13	8.33	8.42	8.03	8.08	8.85
Avg	7.76	8.67	9.05	9.35	8.43	9.27	7.39	7.39	7.22	7.73	7.95	7.59	8.14

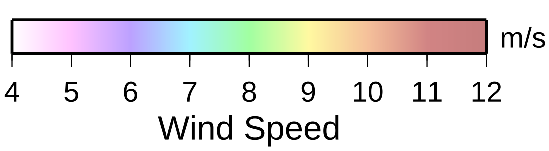

Figure 54: Hourly-mean values of observed 60 m wind speed at Tower M2327. Hours missing greater than 50% of the available observations are not plotted. The vertical axis is Mountain Standard Time (MST). Time series graphs of data are available in Figures 52 and 53 (p. 92 and 93).

MOS−Corrected

Hour of Day (MST)	Jan	Feb	Mar	Apr	May	Jun	Jly	Aug	Sep	Oct	Nov	Dec	Avg
0	8.43	9.17	10.06	10.11	9.42	10.59	8.48	9.08	8.41	8.63	8.51	7.81	8.95
1	8.71	9.43	9.81	10.02	8.70	10.66	8.17	8.83	8.04	8.59	8.47	7.81	8.84
2	8.53	9.42	9.77	9.76	8.65	10.27	8.33	8.55	7.90	8.48	8.32	7.69	8.71
3	8.68	9.53	9.38	9.17	8.15	9.95	7.28	8.09	7.88	8.10	8.33	7.79	8.49
4	8.42	9.63	9.10	9.05	7.94	9.35	6.71	7.78	7.98	7.90	8.12	7.76	8.32
5	8.06	9.32	8.77	8.90	7.62	8.88	6.55	7.46	7.73	7.63	8.08	7.61	8.07
6	7.88	9.05	8.47	8.83	7.45	8.59	6.01	7.16	7.25	7.24	8.02	7.52	7.84
7	7.81	8.74	8.28	8.28	7.04	7.82	5.03	6.34	6.64	6.86	8.13	7.45	7.50
8	7.61	8.53	7.89	8.26	7.22	7.98	5.30	5.90	5.93	6.47	7.92	7.46	7.29
9	7.37	8.09	7.75	8.36	7.52	8.05	5.66	6.06	5.84	6.43	7.10	6.96	7.12
10	7.02	8.15	8.03	8.50	7.42	7.93	5.82	5.87	6.05	6.53	7.04	6.47	7.07
11	6.76	8.30	8.12	8.59	7.67	7.86	5.92	5.59	6.01	6.75	7.11	6.55	7.11
12	6.86	8.15	8.49	8.93	7.82	7.72	5.67	5.40	6.03	7.11	6.91	6.68	7.19
13	6.95	8.20	8.79	9.07	7.72	7.70	5.80	5.54	6.27	7.31	6.94	6.78	7.31
14	7.02	8.47	8.92	9.16	8.20	8.48	5.95	6.14	6.27	7.62	7.38	6.99	7.57
15	6.92	8.36	8.92	9.84	8.61	8.81	6.56	6.38	6.43	7.59	7.66	7.25	7.78
16	6.98	8.13	9.03	10.11	8.93	9.82	8.12	6.55	6.72	7.75	7.91	7.47	8.03
17	7.50	8.53	8.89	10.34	9.79	10.21	8.24	6.98	6.77	7.90	8.38	7.86	8.35
18	7.66	8.70	9.12	10.09	9.37	10.47	8.87	7.53	7.32	8.14	8.37	8.20	8.53
19	7.92	9.10	9.63	9.96	9.59	10.36	9.28	8.76	7.88	8.18	8.43	8.07	8.77
20	8.14	9.24	9.73	9.93	9.75	10.80	9.95	9.13	8.45	8.21	8.34	7.84	8.91
21	8.04	9.04	9.70	10.23	9.37	10.92	10.02	9.28	8.67	8.33	8.57	7.95	8.97
22	8.06	8.95	9.72	9.85	9.35	10.79	8.92	9.29	8.59	8.40	8.45	8.12	8.90
23	8.44	9.07	9.85	9.95	9.49	10.69	8.93	9.04	8.51	8.33	8.26	8.00	8.90
Avg	7.74	8.80	9.03	9.40	8.45	9.36	7.32	7.35	7.23	7.69	7.95	7.51	8.14

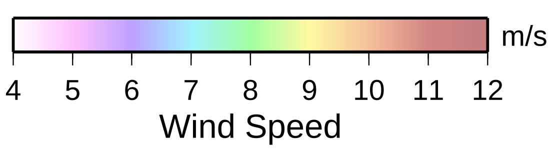

Figure 55: Hourly-mean values of MOS-corrected 60 m wind speed at Tower M2327. Hours missing greater than 50% of the available observations are not plotted. The vertical axis is Mountain Standard Time (MST). Time series graphs of data are available in Figures 52 and 53 (p. 92 and 93).

Wind Speed (m/s)	N	NNE	NE	ENE	E	ESE	SE	SSE	S	SSW	SW	WSW	W	WNW	NW	NNW	All
0 - 0.5	0.00	0.01	0.02	0.00	0.00	0.00	0.00	0.00	0.00	0.00	0.00	0.00	0.00	0.00	0.01	0.00	0.07
0.5 - 1.5	0.13	0.11	0.10	0.07	0.09	0.06	0.06	0.08	0.04	0.08	0.10	0.10	0.07	0.11	0.11	0.07	1.37
1.5 - 2.5	0.33	0.27	0.22	0.23	0.29	0.20	0.18	0.25	0.19	0.14	0.20	0.24	0.31	0.22	0.29	0.31	3.88
2.5 - 3.5	0.44	0.28	0.39	0.38	0.39	0.26	0.36	0.25	0.17	0.26	0.36	0.40	0.36	0.33	0.48	0.56	5.66
3.5 - 4.5	0.59	0.48	0.31	0.53	0.32	0.38	0.32	0.32	0.41	0.28	0.40	0.59	0.40	0.34	0.60	0.58	6.86
4.5 - 5.5	0.72	0.58	0.38	0.43	0.38	0.42	0.46	0.57	0.45	0.48	0.50	0.62	0.63	0.53	0.68	0.82	8.66
5.5 - 6.5	0.74	0.50	0.37	0.41	0.19	0.32	0.37	0.61	0.79	0.56	0.52	0.70	0.67	0.58	0.74	0.96	9.05
6.5 - 7.5	0.84	0.49	0.33	0.30	0.23	0.25	0.50	0.86	0.88	0.61	0.58	0.80	0.76	0.62	0.67	1.04	9.77
7.5 - 8.5	0.71	0.43	0.29	0.26	0.22	0.31	0.51	0.83	1.02	0.55	0.50	0.71	0.74	0.46	0.47	0.88	8.90
8.5 - 9.5	0.71	0.38	0.20	0.18	0.12	0.19	0.40	0.84	1.26	0.60	0.59	0.55	0.63	0.33	0.41	0.68	8.08
9.5 - 10.5	0.62	0.27	0.11	0.03	0.10	0.15	0.37	0.90	1.29	0.69	0.67	0.68	0.40	0.24	0.31	0.70	7.53
10.5 - 11.5	0.54	0.20	0.05	0.03	0.07	0.12	0.27	0.95	1.15	0.65	0.62	0.61	0.36	0.13	0.21	0.53	6.49
11.5 - 12.5	0.41	0.18	0.03	0.02	0.04	0.10	0.21	0.82	1.15	0.59	0.60	0.48	0.18	0.13	0.18	0.40	5.50
12.5 - 13.5	0.37	0.11	0.03	0.00	0.01	0.04	0.16	0.56	0.99	0.59	0.37	0.27	0.13	0.12	0.14	0.29	4.18
13.5 - 14.5	0.30	0.06	0.00	0.00	0.01	0.02	0.12	0.58	0.82	0.33	0.25	0.20	0.08	0.09	0.11	0.27	3.24
14.5 - 15.5	0.25	0.05	0.00	0.00	0.00	0.02	0.07	0.42	0.54	0.29	0.21	0.08	0.04	0.05	0.07	0.19	2.29
15.5 - 16.5	0.22	0.02	0.00	0.00	0.00	0.01	0.07	0.33	0.46	0.19	0.12	0.04	0.03	0.04	0.05	0.12	1.70
16.5 - 17.5	0.13	0.03	0.00	0.00	0.00	0.00	0.05	0.11	0.21	0.10	0.08	0.02	0.03	0.02	0.05	0.14	0.96
17.5 - 18.5	0.17	0.00	0.00	0.00	0.00	0.00	0.00	0.08	0.13	0.09	0.07	0.00	0.02	0.01	0.02	0.11	0.72
18.5 - 19.5	0.11	0.01	0.00	0.00	0.00	0.00	0.01	0.07	0.07	0.05	0.04	0.00	0.00	0.00	0.02	0.06	0.45
19.5 - 20.5	0.06	0.00	0.00	0.00	0.00	0.00	0.01	0.04	0.02	0.05	0.05	0.01	0.01	0.00	0.01	0.02	0.30
20.5 - 21.5	0.05	0.00	0.00	0.00	0.00	0.00	0.00	0.01	0.03	0.01	0.01	0.00	0.00	0.00	0.01	0.08	0.21
21.5 - 22.5	0.03	0.00	0.00	0.00	0.00	0.00	0.00	0.01	0.01	0.01	0.00	0.00	0.00	0.00	0.00	0.04	0.11
22.5 - 23.5	0.00	0.00	0.00	0.00	0.00	0.00	0.00	0.00	0.01	0.00	0.00	0.00	0.00	0.00	0.00	0.02	0.05
23.5 - 24.5	0.01	0.00	0.00	0.00	0.00	0.00	0.00	0.00	0.01	0.00	0.00	0.00	0.00	0.00	0.00	0.01	0.03
> 24.5	0.03	0.00	0.00	0.00	0.00	0.00	0.00	0.00	0.01	0.00	0.00	0.00	0.00	0.01	0.00	0.05	0.11

Table 33: Distribution of observed 60 m wind speed by direction at Tower M2327. Histogram of data is available in Figure 48 (p. 88).

Wind Speed (m/s)	N	NNE	NE	ENE	E	ESE	SE	SSE	S	SSW	SW	WSW	W	WNW	NW	NNW	All
0 - 0.5	0.00	0.00	0.01	0.02	0.02	0.09	0.14	0.06	0.01	0.00	0.00	0.00	0.00	0.00	0.00	0.00	0.35
0.5 - 1.5	0.01	0.03	0.04	0.06	0.11	0.20	0.23	0.23	0.09	0.05	0.00	0.03	0.01	0.01	0.01	0.01	1.13
1.5 - 2.5	0.15	0.21	0.33	0.36	0.40	0.40	0.34	0.41	0.38	0.30	0.16	0.12	0.10	0.09	0.14	0.14	4.01
2.5 - 3.5	0.39	0.52	0.49	0.35	0.35	0.41	0.32	0.38	0.49	0.46	0.32	0.25	0.29	0.25	0.33	0.32	5.91
3.5 - 4.5	0.54	0.60	0.49	0.37	0.27	0.46	0.39	0.53	0.52	0.52	0.44	0.43	0.43	0.44	0.39	0.53	7.35
4.5 - 5.5	0.79	0.76	0.36	0.32	0.30	0.40	0.54	0.66	0.55	0.59	0.58	0.67	0.62	0.50	0.66	0.76	9.06
5.5 - 6.5	0.88	0.56	0.34	0.24	0.20	0.29	0.46	0.71	0.59	0.58	0.71	0.77	0.71	0.56	0.70	0.82	9.13
6.5 - 7.5	0.78	0.42	0.28	0.15	0.17	0.19	0.35	0.91	0.85	0.55	0.69	0.87	0.81	0.81	0.70	0.90	9.42
7.5 - 8.5	0.62	0.45	0.14	0.13	0.11	0.17	0.30	0.77	0.93	0.58	0.55	0.88	0.82	0.61	0.62	0.79	8.49
8.5 - 9.5	0.47	0.41	0.13	0.08	0.11	0.12	0.27	0.74	1.08	0.71	0.60	0.83	0.72	0.44	0.58	0.54	7.82
9.5 - 10.5	0.46	0.22	0.11	0.05	0.11	0.15	0.23	0.90	1.25	0.66	0.49	0.84	0.58	0.41	0.41	0.51	7.39
10.5 - 11.5	0.50	0.22	0.09	0.06	0.08	0.09	0.22	0.78	1.10	0.58	0.48	0.67	0.38	0.33	0.33	0.46	6.36
11.5 - 12.5	0.60	0.24	0.04	0.02	0.02	0.04	0.23	0.67	1.06	0.47	0.35	0.56	0.38	0.22	0.16	0.40	5.48
12.5 - 13.5	0.48	0.16	0.05	0.03	0.00	0.02	0.17	0.54	0.77	0.37	0.22	0.40	0.33	0.12	0.13	0.34	4.13
13.5 - 14.5	0.34	0.07	0.02	0.01	0.01	0.02	0.11	0.41	0.71	0.34	0.14	0.27	0.25	0.08	0.13	0.33	3.24
14.5 - 15.5	0.27	0.05	0.02	0.00	0.00	0.02	0.08	0.32	0.46	0.22	0.11	0.11	0.16	0.05	0.12	0.29	2.29
15.5 - 16.5	0.21	0.02	0.00	0.00	0.01	0.01	0.05	0.22	0.25	0.16	0.09	0.12	0.14	0.04	0.10	0.27	1.70
16.5 - 17.5	0.12	0.02	0.00	0.00	0.00	0.01	0.04	0.11	0.14	0.11	0.05	0.02	0.05	0.00	0.06	0.21	0.96
17.5 - 18.5	0.14	0.01	0.00	0.00	0.00	0.01	0.01	0.12	0.12	0.06	0.05	0.01	0.02	0.00	0.05	0.11	0.72
18.5 - 19.5	0.09	0.02	0.00	0.00	0.00	0.00	0.01	0.05	0.05	0.04	0.04	0.00	0.04	0.01	0.00	0.10	0.45
19.5 - 20.5	0.06	0.00	0.00	0.00	0.00	0.00	0.00	0.04	0.03	0.03	0.03	0.00	0.00	0.00	0.01	0.08	0.30
20.5 - 21.5	0.04	0.00	0.00	0.00	0.00	0.00	0.00	0.01	0.03	0.03	0.03	0.00	0.01	0.00	0.00	0.04	0.21
21.5 - 22.5	0.03	0.00	0.00	0.00	0.00	0.00	0.00	0.01	0.02	0.02	0.01	0.00	0.00	0.00	0.00	0.02	0.11
22.5 - 23.5	0.00	0.00	0.00	0.00	0.00	0.00	0.00	0.00	0.00	0.00	0.00	0.00	0.00	0.00	0.00	0.03	0.05
23.5 - 24.5	0.00	0.00	0.00	0.00	0.00	0.00	0.00	0.00	0.01	0.01	0.00	0.00	0.00	0.00	0.01	0.00	0.03
> 24.5	0.00	0.00	0.00	0.00	0.00	0.00	0.00	0.00	0.03	0.01	0.00	0.00	0.00	0.02	0.01	0.02	0.11

Table 34: Distribution of MOS-corrected 60 m wind speed by direction at Tower M2327. All model values are computed only for times with valid observations. Histogram of data is available in Figure 48 (p. 88).

Sector	Mean Speed(m/s)	Weibull Scale(A)	Weibull Shape(k)	Frequency(%)
N	8.82	9.95	2.03	8.86
NNE	6.88	7.76	2.14	4.64
NE	5.70	6.43	2.16	2.98
ENE	5.29	5.97	2.43	3.00
E	5.32	6.01	2.05	2.55
ESE	6.39	7.22	2.11	2.99
SE	7.78	8.78	2.22	4.69
SSE	9.64	10.85	2.65	9.89
S	10.18	11.41	2.95	12.59
SSW	9.53	10.73	2.54	7.50
SW	8.89	10.04	2.35	7.13
WSW	7.85	8.84	2.48	7.37
W	7.27	8.20	2.41	6.09
WNW	6.98	7.88	2.12	4.55
NW	6.99	7.89	2.00	5.89
NNW	8.41	9.49	2.03	9.28
ALL	**8.14**	**9.19**	**2.14**	**100.00**

Table 35: Observed 60 m mean wind speed, Weibull parameters, and frequency at Tower M2327. Blank values correspond to times with less than 10 data points. Wind rose of data is available in Figure 49 (p. 89).

Sector	Mean Speed(m/s)	Weibull Scale(A)	Weibull Shape(k)	Frequency(%)
N	9.04	10.20	2.23	8.30
NNE	6.89	7.78	2.16	5.19
NE	5.52	6.23	1.95	3.05
ENE	5.00	5.63	1.86	2.34
E	5.08	5.70	1.74	2.38
ESE	5.17	5.77	1.60	3.23
SE	6.83	7.63	1.64	4.69
SSE	8.77	9.91	2.18	9.99
S	9.56	10.77	2.50	11.99
SSW	8.78	9.92	2.20	7.74
SW	8.31	9.38	2.33	6.38
WSW	8.55	9.60	2.83	8.21
W	8.47	9.54	2.58	7.13
WNW	7.68	8.65	2.51	5.18
NW	7.89	8.91	2.28	5.87
NNW	9.19	10.37	2.19	8.33
ALL	**8.14**	**9.19**	**2.13**	**100.00**

Table 36: MOS-corrected 60 m mean wind speed, Weibull parameters, and frequency at Tower M2327. All MOS-corrected model values are computed only for times with valid observations; blank values correspond to times with less than 10 data points. Wind rose of data is available in Figure 49 (p. 89).

REFERENCES

[1] K.J. Allwine and C.D. Whiteman. MELSAR: A mesoscale air quality model for complex terrain: Volume 1–overview, technical description and user's guide. Technical report, Pacific Northwest National Laboratory, 1985.

[2] O. Arino, P. Bicheron, F. Achard, J. Latham, R. Witt, and J.L. Weber. Globcover: The most detailed portrait of earth. *ESA Bulletin*, 136, 2008.

[3] D. P. Dee, S. M. Uppala, A. J. Simmons, P. Berrisford, P. Poli, S. Kobayashi, U. Andrae, M. A. Balmaseda, G. Balsamo, P. Bauer, P. Bechtold, A. C. M. Beljaars, L. van de Berg, J. Bidlot, N. Bormann, C. Delsol, R. Dragani, M. Fuentes, A. J. Geer, L. Haimberger, S. B. Healy, H. Hersbach, E. V. Hólm, L. Isaksen, P. Kållberg, M. Köhler, M. Matricardi, A. P. McNally, B. M. Monge-Sanz, J.-J. Morcrette, B.-K. Park, C. Peubey, P. de Rosnay, C. Tavolato, J.-N. Thépaut, and F. Vitart. The era-interim reanalysis: Configuration and performance of the data assimilation system. *Quart. J. Roy. Meteor. Soc.*, 137:553—-597, 2011.

[4] A. Jarvis et al. Hole-filled seamless SRTM data V4. International Centre for Tropical Agriculture (CIAT), available from http://srtm.csi.cgiar.org, 2008.

[5] E. Kalnay, M. Kanamitsu, R. Kistler, W. Collins, D. Deaven, L. Gandin, M. Iredell, S. Saha, G. White, J. Woollen, Y. Zhu, M. Chelliah, W. Ebisuzaki, W.Higgins, J. Janowiak, K. C. Mo, C. Ropelewski, J. Wang, A. Leetmaa, R. Reynolds, Roy Jenne, and Dennis Joseph. The NCEP/NCAR 40-year reanalysis project. *Bull. Amer. Meteor. Soc.*, 77:437–470, 1996.

[6] G.C. Larsen, Jørgen Højstrup, and H. A. Madsen. Wind fields in wakes. In *Proceedings EWEC 1996*, pages 764–768, Göteborg, Sweden, 1996.

[7] M.K. Liu and M.A. Yocke. Siting of wind turbine generators in complex terrain. *Journal of Energy*, 4:10–16, 1980.

[8] M.M. Rienecker, M.J. Suarez, R. Gelaro, R. Todling, J. Bacmeister, E. Liu, M.G. Bosilovich, S.D. Schubert, L. Takacs, G.K. Kim, S. Bloom, J. Chen, D. Collins, A. Conaty, and A. da Silva. Merra: Nasa's modern-era retrospective analysis for research and applications. *J. Climate*, 24:3624–3648, 2011.

[9] T. Sorensen, P. Nielsen, and M. L. Thøgersen. Recalibrating wind turbine wake model parameters - validating the wake model performance for large offshore wind farms. In *Proceedings EWEC 2006*, Athens, Greece, 2006.